Sum Rules for Electromagnetic Moments and Polarizabilities of Spin-1 Particles in Massive Yang-Mills QED

von

Franziska Hagelstein

Masterarbeit in Physik
vorgelegt dem Fachbereich Physik, Mathematik und Informatik (FB 08)
der Johannes Gutenberg-Universität Mainz
am 12. März 2014

1. Gutachter: Prof. Dr. Marc Vanderhaeghen
2. Gutachter: Prof. Dr. Stefan Weinzierl

Franziska Hagelstein
Institut für Kernphysik
Staudingerweg 7
Johannes Gutenberg-Universität Mainz
55128 Mainz
hagelste@uni-mainz.de

Betreuer:
Dr. Vladimir Pascalutsa
Institut für Kernphysik
PRISMA Cluster of Excellence
Johannes Gutenberg-Universität Mainz
55128 Mainz
vladipas@kph.uni-mainz.de

Abstract

In this thesis we study the Compton scattering on targets with spin 1, and establish a number of sum rules which relate the static electromagnetic properties of such targets to the integrals of total photoabsorption cross sections. These sum rules are model-independent relations based on very general principles, such as unitarity and causality. We nonetheless find it useful to test these sum rules in a field theory and this is the main purpose of this thesis.

We compute the Compton scattering amplitude to one loop order in a partially massive SU(2) Yang-Mills theory, which describes the electromagnetic interaction of a massive charged spin-1 particle, i.e., the spin-1 quantum electrodynamics. The expressions for all contributing diagrams are derived analytically. We check that the scalar Compton scattering amplitudes fulfill (subtracted) dispersion relations. We verify the relation between the imaginary part of the forward scattering amplitude and the total tree-level photoabsorption cross-section, as given by the optical theorem. We compute the one-loop corrections to the W-boson propagator and the γWW-vertex. From this we deduce the one-loop corrections to the electromagnetic moments of the spin-1 particle.

The contribution of polarizabilities to the sum rules is considered in detail. We identify the forward spin polarizability γ_0, the electric (α_{E1}) and magnetic (β_{M1}) dipole and the electric (α_{E2}) and magnetic (β_{M2}) quadrupole polarizabilities. We observe that in certain sum rules one has to introduce an infra-red cutoff equal to the photon energy ν. In this regard, certain one-loop polarizabilities are 'dynamical' and logarithmically divergent for ν going to 0.

Subsequently, we study the derivatives of the sum rules (the so-called δsum rules). We again find the need of an infra-red cutoff and a 'dynamical' δpolarizability γ_0'. From the δGDH sum rule we reproduce the one-loop part of the anomalous magnetic dipole moment.

Our results are expected to be applicable to all spin-1 targets, be they composite (e.g., deuteron) or fundamental (e.g., W-boson). In future these sum rules can be used to access various electromagnetic properties of spin-1 particles experimentally by measuring polarized photoabsorption cross sections.

CONTENTS

CHAPTER 1

INTRODUCTION AND MOTIVATION

The strong interaction forms protons and neutrons, as well as other hadrons, and binds them together into the atomic nuclei. We would like to understand how to describe the hadronic and nuclear structure based on the fundamental theory of the strong interaction, i.e. the quantum chromodynamics (QCD), but this is not an easy task. In fact, a Millennium Prize is promised to the one who first rigorously describes the proton mass ('mass gap') generation based on QCD. Although we are not going to provide a solution for this problem in this master thesis, our work does bare relevance to the physics of the strong interaction, as well to the Yang-Mills theories of which QCD is an example.

We will consider model-independent relations, called sum rules, which are based on very general principles such as unitarity, causality, Lorentz and gauge symmetries. These relations are akin to the Kramers-Kronig relation, albeit somewhat more sophisticated since they involve polarization of light and of matter particles. Similar principles are exploited in the ITEP sum rules [1], which connect hadronic vacuum polarization and the cross-section for hadronization in e^+e^- collisions. Such sum rules can be used for an indirect measurement of certain quantities that are hard to access otherwise. In this thesis we will obtain sum rules relating the electromagnetic properties of spin-1 particles to integrals of photoabsorption cross-sections over all energies. They can in future be used to access polarizabilities of spin-1 targets, such as the deuteron, through polarized cross-sections of photoabsorption.

1.1. Examples of Sum Rules

To illustrate how this works on a well-known example of spin-1/2 targets we briefly consider the case of the proton. In this case the most basic sum rule is the one of Gerasimov-Drell-Hearn (GDH), written down in 1966 by Gerasimov [2] and independently by Drell and Hearn [3]:

$$\frac{2\pi e^2}{M^2}\,\kappa^2 = \int_0^\infty \frac{d\nu}{\nu}\left[\sigma_{3/2}(\nu) - \sigma_{1/2}(\nu)\right]. \tag{1.1}$$

It expresses the target's anomalous magnetic moment κ in terms of its total helicity-difference photoabsorption cross-section integrated over the photon energy ν. Here and in what follows e and M denote the charge and the mass of the targeted particle.

Six years prior to that, Baldin has written an analog of the Kramers-Kronig relation for a single proton, which now bares his name, viz. the Baldin sum rule [4]:

$$4\pi^2(\alpha_{E1}+\beta_{M1}) = \int_0^\infty \frac{d\nu}{\nu^2}\left[\sigma_{1/2}(\nu)+\sigma_{3/2}(\nu)\right], \tag{1.2}$$

relating the sum of the static electric (α_{E1}) and magnetic (β_{M1}) polarizabilities to the unpolarized total photoabsorption cross-section.

A less famous, but no less useful sum rule is the so-called forward spin polarizability (FSP) sum rule [5]:

$$4\pi^2\gamma_0 = \int_0^\infty \frac{d\nu}{\nu^3}\left[\sigma_{1/2}(\nu)-\sigma_{3/2}(\nu)\right], \tag{1.3}$$

relating the forward spin polarizability γ_0 to the helicity-difference photoabsorption cross-section. Note the different energy weighting under the integral, as compared to the GDH sum rule.

The anomalous electromagnetic (e.m.) moments and the polarizabilities are static properties of a particle and characterize its inner structure, while the cross-sections are dynamic observables describing a scattering process. The utility of these and other sum rules lies in the link between measurable cross-sections and target properties and in the proton case a program exploiting this has been successfully carried out. The GDH-Collaboration between the accelerators MAMI and ELSA verified the GDH sum rule with circularly polarized real photons and longitudinally polarized nucleons [6]. They measured the running GDH integral:

$$I_{\text{run}}(E_{\text{run}}) = \int_0^{E_{\text{run}}} \frac{d\nu}{\nu}\left[\sigma_{3/2}(\nu)-\sigma_{1/2}(\nu)\right], \tag{1.4}$$

and obtained for the proton:

$$I_{\text{run}}(\infty) = 212 \pm 6_{\,\text{stat.}} \pm 16_{\,\text{syst.}}\ \mu\text{b}, \tag{1.5}$$

including an extrapolation to unmeasured high-energy regions. This result is in agreement with the GDH sum rule value for the proton of 205 μb, see fig. 1.1.

The evaluation of the Baldin sum rule yields for, respectively, the proton [7] and neutron [8]:

$$\alpha_{E1}^{(p)}+\beta_{M1}^{(p)} = 13.8 \pm 0.4 \times 10^{-4}\,\text{fm}^3, \tag{1.6a}$$
$$\alpha_{E1}^{(n)}+\beta_{M1}^{(n)} = 15.2 \pm 0.4 \times 10^{-4}\,\text{fm}^3. \tag{1.6b}$$

As for the spin polarizabilities, there are four of them at lowest order in the energy expansion, labelled as $\gamma_{Xl,Yl'}$, with Xl and Yl' being the multipolarity of the initial respectively final photon. Therefore, $\gamma_{E1,E1}$ and $\gamma_{M1,M1}$ describe dipole excitations, whereas $\gamma_{E1,M2}$ and $\gamma_{M1,E2}$ describe photon scattering off the target with a change of the photons angular momentum by one unit. However, only one linear combination of them,

$$\gamma_0 = -(\gamma_{E1,E1}+\gamma_{M1,M1}+\gamma_{E1,M2}+\gamma_{M1,E2}), \tag{1.7}$$

called the forward spin polarizability enters the FSP sum rule above. Utilizing exactly the same helicity-difference cross-section used to verify the GDH sum rule for the proton, one obtains the following value [9]:

$$\gamma_0^{(p)} = -0.90 \pm 0.08_{\text{stat.}} \pm 0.11_{\text{syst.}} \times 10^{-4}\,\text{fm}^4. \tag{1.8}$$

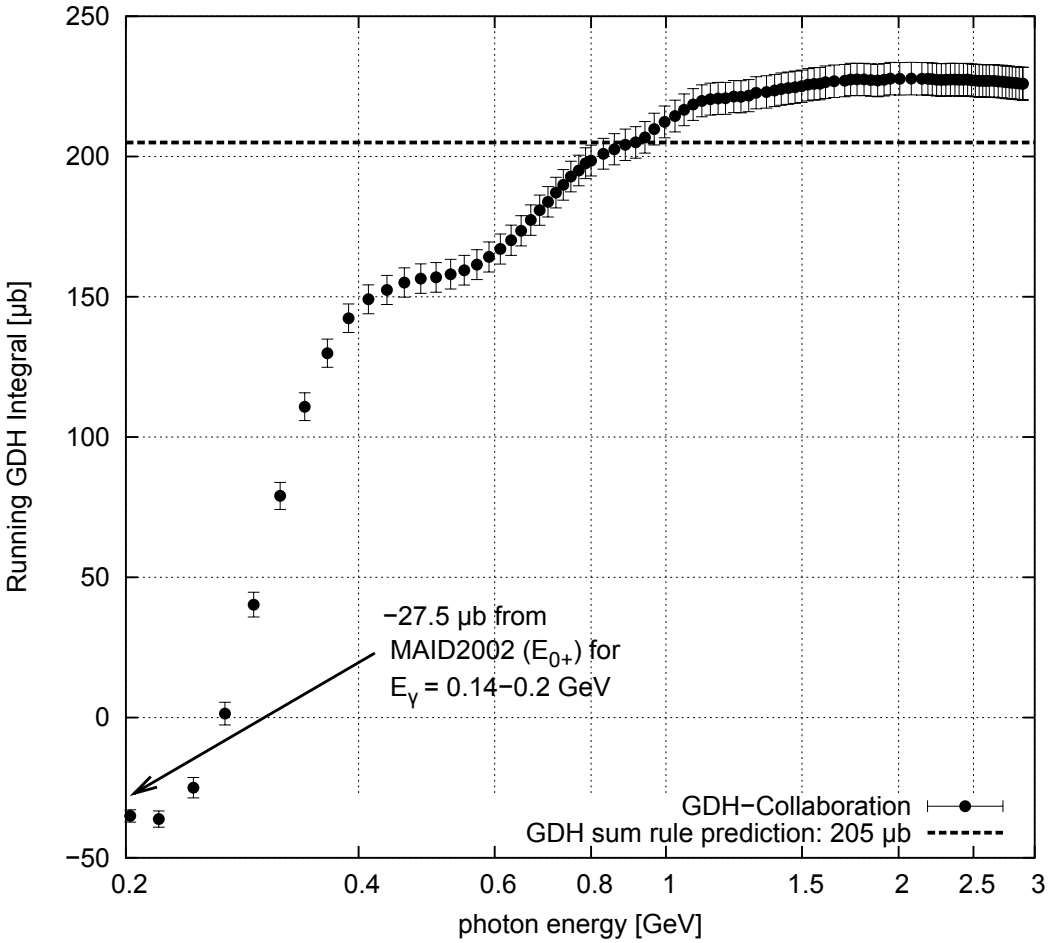

Figure 1.1.: Running GDH integral up to 2.9 GeV including the threshold contribution (taken from [6])

This provides a stringent constraint, and thus-far the only piece of reliable information, about the spin polarizabilities of the proton.

1.2. Aims and Outline

Thus, sum rules for spin-1/2 targets are well-established and are proving to be instrumental for our understanding of the nucleon. To do the same, say, for the deuteron, it is necessary to extent these sum rules to the spin-1 case. It is commonly assumed that the spin-1/2 sum rules can just be taken over to the spin-1 situation and this is for instance how the deuteron forward-spin polarizability $\gamma_0^{(D)}$ is determined nowadays [10, 11].

However, a particle with spin S has in general $2S + 1$ electromagnetic moments. Even a point-like (structureless) particle, with a point-like charge density, has $2S + 1$ electromagnetic moments. Hence, a spin-1/2 particle has two electromagnetic moments — the charge e and the magnetic dipole moment μ, while a spin-1 particle in addition has an electric quadrupole moment Q. It is therefore plausible that, compared to the spin-1/2 case, the additional electric quadrupole moment should enter and modify the sum rules. A similar argument exists for the (spin) polarizabilities. The main aim of

this thesis is precisely to access whether and how the electric quadrupole moment and possible additional spin-polarizability effects enter in the sum rules.

A large part of this thesis is also devoted to the verification of the newly (re)established sum rules in quantum field theory. For this purpose we consider a partially massive SU(2) Yang-Mills theory, which can be casted into quantum electrodynamics (QED) of a massive charged spin-1 particle. All the sum rules will be verified in this spin-1 QED at one-loop level.

The outline of the thesis is as follows. In chapter 2 we survey the general principles of light absorption and scattering on targets with spin. We discuss the optical theorem and dispersion relations as the basis for the general derivation of sum rules. In chapter 3 we demonstrate the basic concept of the thesis by working out the simpler spin-0 case. In chapter 4 we go to spin-1 targets and propose new sum rules and δsum rules. In chapter 5 we calculate the tree-level scattering cross-sections and the scattering amplitude at one-loop level in spin-1 QED. In chapter 6 all results are gathered to analyse the spin-1 sum rules. The concluding chapter 7 summarises our results and gives an outlook on possible future work. We summarize our proposed sum rules in appendix A and give the appearing tree-level cross-sections. In appendix B we present the analytical expression for the scalar forward Compton scattering amplitudes. The utilized Feynman Rules are given in appendix C. Appendix D resumes the calculation of one-loop integrals. In appendix E one can find the analytical expressions for the scattering amplitudes of all contributing diagrams.

1.3. Conventions

Here we enlist the conventions used in this thesis. Unless specified, all calculations are presented in natural units ($\hbar = c = 1$). The fine-structure constant is defined as $\alpha = e^2/4\pi$.

The Minkowski metric

$$g = \begin{pmatrix} 1 & 0 & 0 & 0 \\ 0 & -1 & 0 & 0 \\ 0 & 0 & -1 & 0 \\ 0 & 0 & 0 & -1 \end{pmatrix} \tag{1.9}$$

is introduced to define the four-vector scalar product:

$$a \cdot b = g_{\rho\sigma} a^\rho b^\sigma = a_\sigma b^\sigma = a_0 b_0 - \vec{a} \cdot \vec{b}. \tag{1.10}$$

where the Einstein summation convention is used to sum over repeated indices.

The polarization vectors of the incoming and forward scattered particles are written as follows [12]:

$$\chi_0 = \begin{pmatrix} \frac{|\vec{p}|}{M} \\ 0 \\ 0 \\ \frac{E}{M} \end{pmatrix}, \qquad \chi_\pm = \frac{1}{\sqrt{2}} \begin{pmatrix} 0 \\ -1 \\ \mp i \\ 0 \end{pmatrix}, \qquad \varepsilon_\pm = \frac{1}{\sqrt{2}} \begin{pmatrix} 0 \\ 1 \\ \pm i \\ 0 \end{pmatrix}, \tag{1.11a}$$

$$\chi_0^* = \begin{pmatrix} \frac{|\vec{p}|}{M} \\ 0 \\ 0 \\ \frac{E}{M} \end{pmatrix}, \qquad \chi_\pm^* = \frac{1}{\sqrt{2}} \begin{pmatrix} 0 \\ -1 \\ \pm i \\ 0 \end{pmatrix}, \qquad \varepsilon_\pm^* = \frac{1}{\sqrt{2}} \begin{pmatrix} 0 \\ 1 \\ \mp i \\ 0 \end{pmatrix}, \tag{1.11b}$$

where the photon is travelling along the z-axis and the W-boson is coming from the opposite direction.

It is helpful to introduce the following $(2S+1)\times(2S+1)$ matrices:

$$\left(\mathcal{C}_\sigma^{(S)}\right)_{\lambda'+S+1,\,\lambda+S+1} = \sqrt{S(S+1)}\,C(1\sigma, S\lambda;\, S\lambda'), \tag{1.12}$$

where

$$C(j_1 m_1, j_2 m_2; jm) \equiv \langle j_1 j_2 m_1 m_2 | j_1 j_2 jm\rangle \tag{1.13}$$

are the Clebsch-Gordan coefficients, and the indices run as $\sigma = \overline{-1,1}$ and $\lambda = \overline{-S,S}$. Then, one can verify that the matrices:

$$\mathcal{S}_1 = \left[\sqrt{2}\right]^{-1}(\mathcal{C}_{+1} - \mathcal{C}_{-1})\,, \tag{1.14a}$$

$$\mathcal{S}_2 = \left[i\sqrt{2}\right]^{-1}(\mathcal{C}_{+1} + \mathcal{C}_{-1})\,, \tag{1.14b}$$

$$\mathcal{S}_3 = \mathcal{C}_0, \tag{1.14c}$$

satisfy the SU(2) algebra $[\mathcal{S}_i,\, \mathcal{S}_j] = i\epsilon_{ijk}\mathcal{S}_k$, as well as the other properties of the spin operators for spin S: $\vec{\mathcal{S}}^2 = S(S+1)$, $(\mathcal{S}_3)_{\lambda'\lambda} = \lambda\,\delta_{\lambda'\lambda}$. For spin-1 we obtain the spin operators:

$$\mathcal{S}_1 = \frac{1}{\sqrt{2}}\begin{pmatrix} 0 & 1 & 0 \\ 1 & 0 & -1 \\ 0 & -1 & 0 \end{pmatrix}, \tag{1.15a}$$

$$\mathcal{S}_2 = \frac{i}{\sqrt{2}}\begin{pmatrix} 0 & -1 & 0 \\ 1 & 0 & -1 \\ 0 & 1 & 0 \end{pmatrix}, \tag{1.15b}$$

$$\mathcal{S}_3 = \begin{pmatrix} 1 & 0 & 0 \\ 0 & 0 & 0 \\ 0 & 0 & -1 \end{pmatrix}, \tag{1.15c}$$

which are connected to the spin-1 polarization vectors in the following way:

$$\chi_i^*\,\chi_j - \chi_j^*\,\chi_i = [\mathcal{S}_i,\, \mathcal{S}_j] = i\epsilon_{ijk}\mathcal{S}_k, \tag{1.16a}$$

$$\chi_i^*\,\chi_j + \chi_j^*\,\chi_i = 2\delta_{ij} - \{\mathcal{S}_i,\, \mathcal{S}_j\}, \tag{1.16b}$$

$$\chi_i^*\,\chi_j = \delta_{ij} - \mathcal{S}_j,\, \mathcal{S}_i. \tag{1.16c}$$

Used Software

To work out this thesis the following software was used: *Mathematica 8*, the symbolic manipulation system *TFORM* [13], the *LoopTools* package [14] for evaluation of scalar and tensor one-loop integrals and *JaxoDraw* [15] for drawing Feynman diagrams.

CHAPTER 2

GENERAL PRINCIPLES OF LIGHT ABSORPTION AND SCATTERING

In this section we recapitulate the general principles of light scattering on targets with spin 1. The Compton scattering process is surveyed by giving the kinematics and polarization vectors of the involved particles in different reference frames. We introduce the optical theorem and the dispersion theory — the cornerstones of the sum rules. In the end of the section we will outline the sum rule derivation for any spin.

2.1. Kinematics of Compton Scattering

We are going to focus on Compton scattering off massive spin-1 particle, such as the W-boson. Therefore, we will often refer to the target as the W-boson. Nevertheless, the following survey of the Compton scattering process is largely valid for any spin.

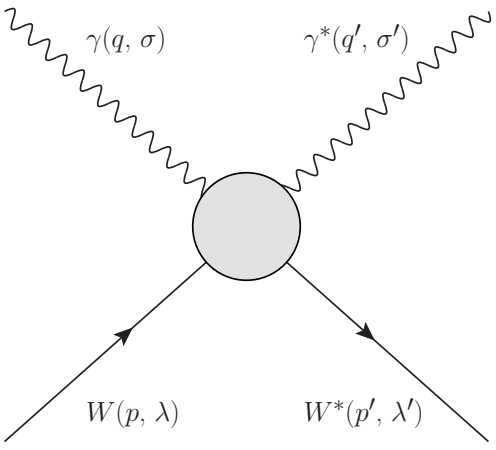

Figure 2.1.: Compton scattering off massive vector bosons

Figure 2.1 represents an elastic Compton scattering process between a photon γ with momentum q and helicity σ, and a W-boson with momentum p and helicity λ. The particles emerging from the scattering process are a photon $\gamma^*(q', \sigma')$ and a W-boson $W^*(p', \lambda')$. We are considering real Compton scattering, thus the incoming and outgoing particles fulfill the on-shell condition, meaning that for a particle with mass M and four-momentum p one has $p^2 = M^2$. For massive vector bosons and massless photons one has:

$$p^2 = M^2 = p'^2, \tag{2.1a}$$
$$q^2 = 0 = q'^2. \tag{2.1b}$$

2.1.1. Mandelstam Variables

It is useful to introduce the Mandelstam variables:

$$s = (p+q)^2 \ = (p'+q')^2, \tag{2.2a}$$
$$t = (p-p')^2 = (q'-q)^2, \tag{2.2b}$$
$$u = (p-q')^2 = (p'-q)^2. \tag{2.2c}$$

These variables are Lorentz scalars. They are particularly helpful with regard to 'crossing' symmetries. The sum of the Mandelstam variables of an interaction equals the sum of the masses of the involved particles, here:

$$s + t + u = p^2 + q^2 + p'^2 + q'^2 = 2M^2. \tag{2.3}$$

2.1.2. Center-of-Mass Frame

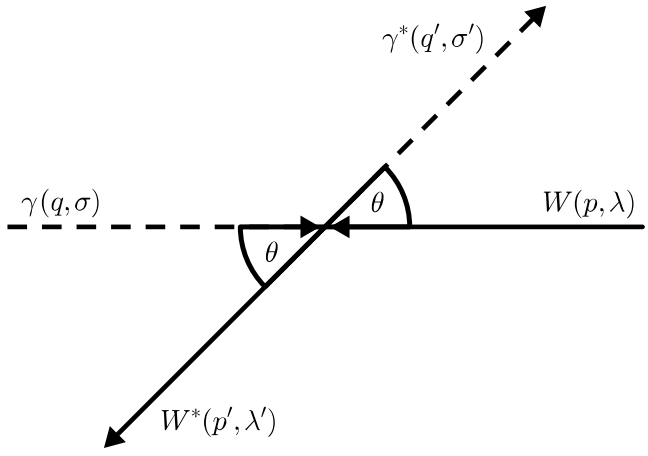

Figure 2.2.: Compton scattering in the center-of-mass frame

Figure 2.2 shows the Compton scattering process in the center-of-mass (cm) frame. The particles approach each other along the z-axis and then scatter over an angle θ.

The four-momenta of the particles in the cm-frame are listed below:

$$p = \begin{pmatrix} E_{\mathrm{cm}} \\ 0 \\ 0 \\ -\omega \end{pmatrix}, \qquad q = \begin{pmatrix} \omega \\ 0 \\ 0 \\ \omega \end{pmatrix}, \tag{2.4}$$

$$p' = R_y(\theta)\, p = \begin{pmatrix} E_{\mathrm{cm}} \\ -\omega \sin\theta \\ 0 \\ -\omega \cos\theta \end{pmatrix}, \qquad q' = R_y(\theta)\, q = \begin{pmatrix} \omega \\ \omega \sin\theta \\ 0 \\ \omega \cos\theta \end{pmatrix}.$$

The final momenta can be calculated by rotating the initial momenta, cf. fig. 2.2. Here the rotation matrix

$$R_y(\theta) = \begin{pmatrix} 1 & 0 & 0 & 0 \\ 0 & \cos\theta & 0 & \sin\theta \\ 0 & 0 & 1 & 0 \\ 0 & -\sin\theta & 0 & \cos\theta \end{pmatrix} \tag{2.5}$$

produces a rotation about the y-axis over the scattering angle θ.

In the following, the Compton scattering process will only be considered in the forward limit, i.e.: $t = 0$, or $\theta = 0$. Therefore, the final and initial momenta are equal in the cm-frame:

$$p = p' = \begin{pmatrix} E_{\mathrm{cm}} \\ 0 \\ 0 \\ -\omega \end{pmatrix}, \qquad q = q' = \begin{pmatrix} \omega \\ 0 \\ 0 \\ \omega \end{pmatrix}. \tag{2.6}$$

The photon energy can be written in terms of the Mandelstam invariant s and the mass of the W-boson M:

$$\omega = \frac{s - M^2}{2\sqrt{s}}. \tag{2.7}$$

2.1.3. Laboratory Frame

In the laboratory system the initial W-boson should be at rest. Therefore the four-momenta of the particles take on the following form:

$$p = \begin{pmatrix} M \\ 0 \\ 0 \\ 0 \end{pmatrix}, \quad q = \begin{pmatrix} \nu \\ 0 \\ 0 \\ \nu \end{pmatrix}, \quad p' = \begin{pmatrix} E \\ |\vec{p}|\sin\varphi \\ 0 \\ |\vec{p}|\cos\varphi \end{pmatrix}, \quad q' = \begin{pmatrix} \nu' \\ \nu'\sin\vartheta \\ 0 \\ \nu'\cos\vartheta \end{pmatrix}. \tag{2.8}$$

In the particular case of the forward limit and with the aid of the on-shell conditions one can simplify the four-momenta in the laboratory frame:

$$p = p' = \begin{pmatrix} M \\ 0 \\ 0 \\ 0 \end{pmatrix}, \qquad q = q' = \begin{pmatrix} \nu \\ 0 \\ 0 \\ \nu \end{pmatrix}. \tag{2.9}$$

Again, the photon energy can be written in terms of the Mandelstam invariant s and the mass of the W-boson M:

$$\nu = \frac{s - M^2}{2M}. \tag{2.10}$$

2.1.4. Helicities

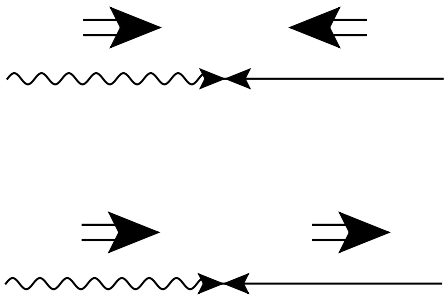

Figure 2.3.: Spin realizations of a double polarization experiment

Helicity is the projection of a particles spin $\vec{S}$ on its momentum $\vec{p}$:

$$h = \vec{S} \cdot \hat{p}, \tag{2.11}$$

where $\hat{p} = \vec{p}/|\vec{p}|$.

Figure 2.3 shows two possible realizations of a double polarization experiment in the cm-frame, where the photon and the target have inverse momenta. The helicity of the photon is in both cases fixed: $\gamma(S_z = 1, \sigma = 1)$, where S_z is the spin projection on the photon momentum $\hat{q} = \vec{e}_z$. The target is either polarized opposite to (upper drawing) or along (lower drawing) the photon momentum. The total helicity of the γW-system,

$$\Lambda = \sigma - \lambda, \tag{2.12}$$

is obtained by subtracting the photon's and target's helicity. We therefore have the following three situations in the spin-1 case:

- parallel polarization:
  $\gamma(S_z = \sigma = 1)$, $\mathrm{W}(S_z = 1, \lambda = -1) \longrightarrow \gamma\mathrm{W}(S_z = \Lambda = 1 + S)$,
- longitudinal polarization:
  $\gamma(S_z = \sigma = 1)$, $\mathrm{W}(S_z = 0, \lambda = 0) \longrightarrow \gamma\mathrm{W}(S_z = \Lambda = 1)$,
- antiparallel polarization:
  $\gamma(S_z = \sigma = 1)$, $\mathrm{W}(S_z = -1, \lambda = 1) \longrightarrow \gamma\mathrm{W}(S_z = \Lambda = 1 - S)$.

The double-polarized total photoabsorption cross-sections will be labelled as σ_Λ, with Λ the total helicity.

2.1.5. Polarization Vectors

In scattering amplitudes the external particles are described by polarization vectors, which characterize the spin orientation. A massive particle of spin S admits $2S + 1$ different spin orientations. The helicity of a massless particles with spin S is Lorentz-invariant and can only be $\pm S$, due to the fact that massless particles travel at the speed of light.

The photons are chosen to be right-handed ($\sigma = +1$) or left-handed ($\sigma = -1$) circularly polarized. The W-bosons are either longitudinal ($\lambda = 0$) or transverse ($\lambda = \pm 1$).

The polarization vectors of the incoming particles in the cm-frame are written as follows [12]:

$$\chi_0 = \begin{pmatrix} -\frac{\omega}{M} \\ 0 \\ 0 \\ \frac{E_{\text{cm}}}{M} \end{pmatrix}, \qquad \chi_\pm = \frac{1}{\sqrt{2}} \begin{pmatrix} 0 \\ -1 \\ \mp i \\ 0 \end{pmatrix}, \qquad \varepsilon_\pm = \frac{1}{\sqrt{2}} \begin{pmatrix} 0 \\ 1 \\ \pm i \\ 0 \end{pmatrix}. \tag{2.13}$$

The corresponding momenta are defined in eq. (2.6), where the photon is traveling along the z-axis and the W-boson is coming from the opposite direction. Light is transversely polarized, meaning the photon polarization vector is perpendicular to the direction of motion.

The polarization vectors of the outgoing particles are calculated by rotating and complex-conjugating the initial polarization vectors:

$$\chi_0^* = \begin{pmatrix} -\frac{\omega}{M} \\ \frac{E_{\text{cm}}}{M} \sin\theta \\ 0 \\ \frac{E_{\text{cm}}}{M} \cos\theta \end{pmatrix}, \quad \chi_\pm^* = \frac{1}{\sqrt{2}} \begin{pmatrix} 0 \\ -\cos\theta \\ \pm i \\ \sin\theta \end{pmatrix}, \quad \varepsilon_\pm^* = \frac{1}{\sqrt{2}} \begin{pmatrix} 0 \\ \cos\theta \\ \mp i \\ -\sin\theta \end{pmatrix}. \tag{2.14}$$

In our particular case of forward scattering ($\theta = 0$) the polarization vectors of the outgoing particles read as follows:

$$\chi_0^* = \begin{pmatrix} -\frac{\omega}{M} \\ 0 \\ 0 \\ \frac{E_{\text{cm}}}{M} \end{pmatrix}, \qquad \chi_\pm^* = \frac{1}{\sqrt{2}} \begin{pmatrix} 0 \\ -1 \\ \pm i \\ 0 \end{pmatrix}, \qquad \varepsilon_\pm^* = \frac{1}{\sqrt{2}} \begin{pmatrix} 0 \\ 1 \\ \mp i \\ 0 \end{pmatrix}. \tag{2.15}$$

In the laboratory frame we use the same polarization vectors and substitute $\omega = 0$ and $E_{\text{cm}} = M$.

The polarization vectors are orthonormal:

$$\epsilon_\mu^*(\sigma') \cdot \epsilon^\mu(\sigma) = -\delta_{\sigma\sigma'}, \tag{2.16a}$$

$$\chi_\mu^*(\lambda') \cdot \chi^\mu(\lambda) = -\delta_{\lambda\lambda'}, \tag{2.16b}$$

and fulfill completeness relations:

$$\sum_{\sigma=1,2} \epsilon_i^*(\sigma, q)\, \epsilon_j(\sigma, q) = \delta_{ij} - \hat{q}_i \hat{q}_j, \tag{2.17a}$$

$$\sum_{\lambda=1,2,3} \chi_\mu^*(\lambda, p)\, \chi_\nu(\lambda, p) = -g_{\mu\nu} + \frac{p_\mu p_\nu}{M^2}. \tag{2.17b}$$

A helpful substitution rule is:

$$\sum_{\sigma=1,2} \epsilon_\mu^*(\sigma)\, \epsilon_\nu(\sigma) \longrightarrow -g_{\mu\nu}, \tag{2.18}$$

which is valid provided the polarization vectors are contracted with a gauge-invariant amplitude, e.g.:

$$\sum_{\sigma=1,2} \epsilon_\mu^*(\sigma) \epsilon_\nu(\sigma) \mathcal{A}^{*\mu} \mathcal{A}^\nu = -g_{\mu\nu} \mathcal{A}^{*\mu} \mathcal{A}^\nu, \quad q \cdot \mathcal{A} = 0. \tag{2.19}$$

The polarization vectors obey the following transversality conditions:

$$p \cdot \chi(p) = 0, \qquad p' \cdot \chi^*(p') = 0, \qquad q \cdot \varepsilon(q) = 0, \qquad q' \cdot \varepsilon^*(q') = 0, \tag{2.20}$$

where the momenta are assumed to be on-shell. In other words, the four-dimensional scalar product of the four-momentum and the polarization vector of a particle vanishes if the particle is on-shell. These relations follow from the Lorentz condition $\partial_\mu A^\mu = 0$ and respectively $\partial_\mu W^\mu = 0$, as can be seen by inserting the plane-wave expressions: $A^\mu(x) \sim \epsilon^\mu e^{-iq\cdot x}$ and $W^\mu \sim \chi^\mu e^{-ip\cdot x}$. In the forward kinematics we furthermore have:

$$p \cdot \varepsilon = p' \cdot \varepsilon = p \cdot \varepsilon^* = p' \cdot \varepsilon^* = 0. \tag{2.21}$$

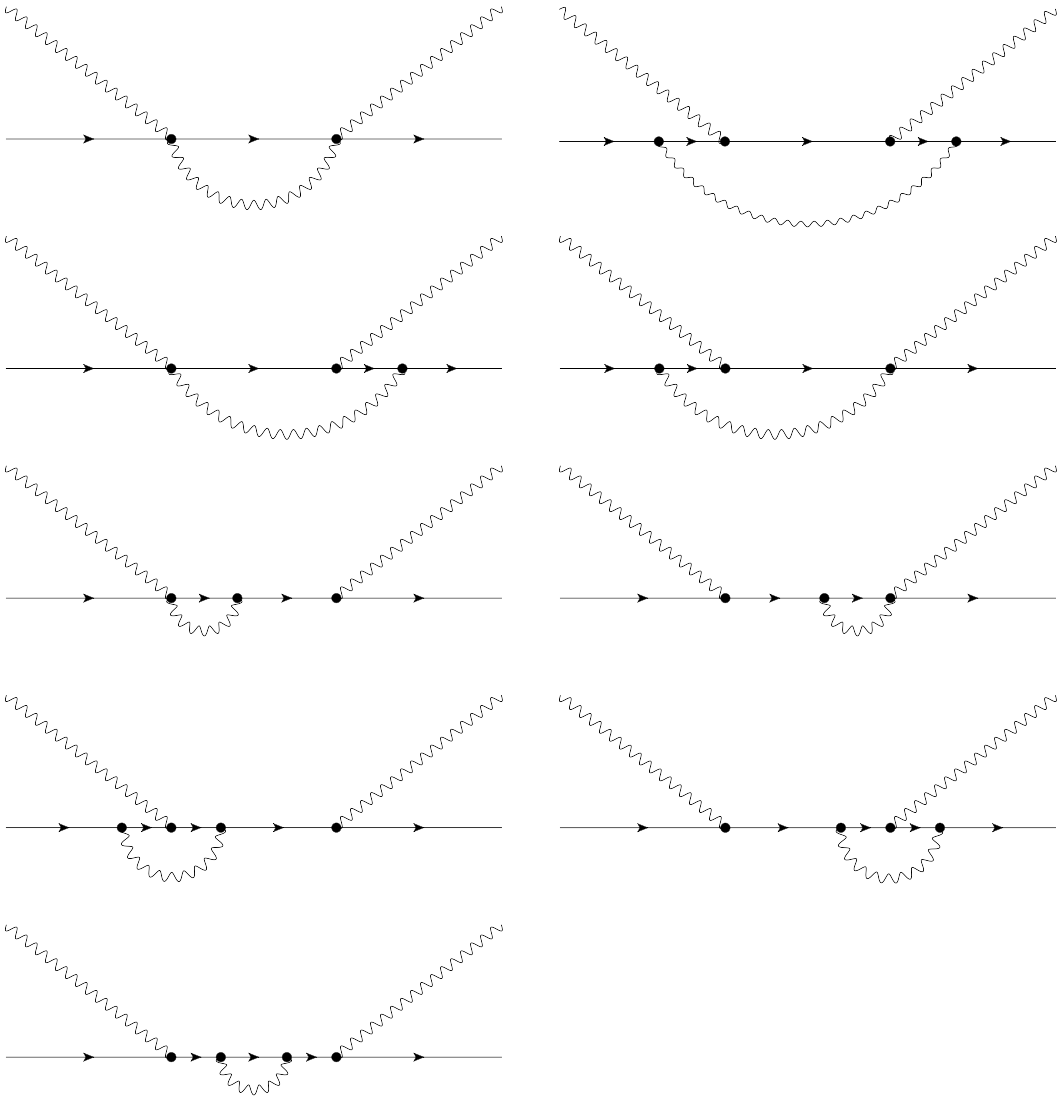

Figure 2.4.: Diagrams which give imaginary contributions to the scattering amplitude

2.2. Optical Theorem

[1] In a scattering process, the overlap of 'in'- and possible 'out'-going states can be described by the scattering matrix S, first introduced in [17, 18]. The scattering matrix in the Heisenberg picture corresponds to the time-evolution operator in the limit of large temporal spacings ($T \to \infty$), meaning the scattering matrix transforms asymptotic initial into final particle states (well-separated, non-interacting, free particles):

$$ {}_{out}\langle \boldsymbol{p}_1'\boldsymbol{p}_2' \cdots | \boldsymbol{p}_1\boldsymbol{p}_2\rangle_{in} = \lim_{T\to\infty} \langle \underbrace{\boldsymbol{p}_1'\boldsymbol{p}_2' \cdots}_{T} | \underbrace{\boldsymbol{p}_1\boldsymbol{p}_2}_{T} \rangle = \langle \boldsymbol{p}_1'\boldsymbol{p}_2' \cdots | S | \boldsymbol{p}_1\boldsymbol{p}_2\rangle. \tag{2.22} $$

The S-matrix is usually written as

$$ S = \mathbb{1} + iT, \tag{2.23} $$

i.e., the sum of a unit matrix and a scattering amplitude T, which vanishes if the particles do not interact (leaving $S = \mathbb{1}$). Using the unitarity of S we obtain a relation for the T-matrix:

$$ SS^\dagger = \mathbb{1} \quad \longrightarrow \quad i\left(T - T^\dagger\right) = -T^\dagger T. \tag{2.24} $$

The T matrix is connected to the scattering amplitude in the following way:

$$ \langle \boldsymbol{p}_1'\boldsymbol{p}_2' \cdots | T | \boldsymbol{p}_1\boldsymbol{p}_2\rangle = (2\pi)^4\, \delta^{(4)}\left(p_1 + p_2 - p_1' - p_2' - \cdots\right) \mathcal{A}\left(p_1, p_2 \to p_1', p_2', \cdots\right). \tag{2.25} $$

Building the matrix element of eq. (2.24) between two-particle states:

$$ i \left\langle \boldsymbol{p}_1'\boldsymbol{p}_2' \left| T - T^\dagger \right| \boldsymbol{p}_1\boldsymbol{p}_2 \right\rangle = - \left\langle \boldsymbol{p}_1'\boldsymbol{p}_2' \left| T^\dagger T \right| \boldsymbol{p}_1\boldsymbol{p}_2 \right\rangle, \tag{2.26} $$

and utilizing eq. (2.25), the left-hand side becomes:

$$ (2\pi)^4\, \delta^{(4)}(p_1 + p_2 - p_1' - p_2')\, i \left[\mathcal{A}\left(p_1, p_2 \to p_1', p_2'\right) - \mathcal{A}^*\left(p_1', p_2' \to p_1, p_2\right)\right]. \tag{2.27} $$

On the right-hand side we insert a complete set of intermediate states:

$$ \begin{aligned} &- \sum_n \left[\prod_{i=1}^n \int \frac{d^3k_i}{(2\pi)^3} \frac{1}{2E_i}\right] \left\langle \boldsymbol{p}_1'\boldsymbol{p}_2' \left| T^\dagger \right| \boldsymbol{k}_1 \cdots \boldsymbol{k}_n \right\rangle \langle \boldsymbol{k}_1 \cdots \boldsymbol{k}_n | T | \boldsymbol{p}_1\boldsymbol{p}_2\rangle \\ &= - \sum_n \left[\prod_{i=1}^n \int \frac{d^3k_i}{(2\pi)^3} \frac{1}{2E_i}\right] (2\pi)^4\, \delta^{(4)}\left(p_1' + p_2' - \textstyle\sum_i k_i\right) \mathcal{A}^*\left(p_1', p_2' \to \{k_i\}\right) \\ &\quad \times (2\pi)^4\, \delta^{(4)}\left(p_1 + p_2 - \textstyle\sum_i k_i\right) \mathcal{A}\big(p_1, p_2 \to \{k_i\}\big). \end{aligned} \tag{2.28} $$

In the forward limit, where $p_1' = p_1$ and $p_2' = p_2$, we then have:

$$ \begin{aligned} &2\ \mathrm{Im}\, \mathcal{A}(p_1, p_2 \to p_1, p_2) \\ &= \sum_n \left[\prod_{i=1}^n \int \frac{d^3k_i}{(2\pi)^3} \frac{1}{2E_i}\right] (2\pi)^4\, \delta^{(4)}\left(p_1 + p_2 - \textstyle\sum_i k_i\right) \left|\mathcal{A}\big(p_1, p_2 \to \{k_i\}\big)\right|^2. \end{aligned} \tag{2.29} $$

On the right-hand side we can identify a cross-section [cf. eq. (2.37) below]. Hence, we arrive to a relation between the imaginary part of a forward scattering amplitude and the total scattering cross-section, i.e. the optical theorem:

$$ \mathrm{Im}\, \mathcal{A}\left(p_1, p_2 \to p_1, p_2\right) = 2M\nu\, \sigma_{tot}(\nu)\, (p_1, p_2 \to \text{anything}). \tag{2.30} $$

The origin of the kinematic factor $2M\nu$, with ν being the lab frame photon energy, is shortly described in section 2.3.

[1] In preparation of this section we i.a. used [16].

Absorptive Parts of the Scattering Amplitude

If it is possible to cut a one-loop diagram and all the cut propagators in the loop can simultaneously go on-shell, then the diagram has an imaginary contribution. Hence, it is not difficult to see if a one-loop Feynman diagram gives an imaginary contribution to the amplitude or not. For our process of interest, i.e. forward Compton scattering, the nine diagrams in fig. 2.4 do so. The first four diagrams belong to the group of one-particle-irreducible (1PI) diagrams, whereas the others are one-particle-reducible (1PR) diagrams comprising vertex and self-energy corrections.

The scattering amplitude becomes in general complex above a certain energy threshold ν_0 corresponding to a particle production process. In our treatment of the Compton scattering process off W-bosons we have pairs of photons and W-bosons going on-shell in the intermediate state, see fig. 2.4. Therefore the initial particles always provide the needed amount of energy for the intermediate particles to go on-shell and hence the threshold is at zero energy.

2.3. Cross-sections

[2] In the cm-frame the total cross-section for Compton scattering is defined as follows:

$$\frac{d\sigma}{d\Omega_{\mathrm{cm}}} = \frac{1}{64\pi^2 s}|T|^2. \tag{2.31}$$

This formula should be briefly motivated. The cross-section of a scattering process $1+2 \longrightarrow 3+4+\cdots+n$ is defined as:

$$\sigma = \frac{\mathcal{S}}{4|\vec{p}_1|_{\mathrm{cm}}\sqrt{s}}\times \tag{2.32}$$
$$\int |T|^2 (2\pi)^4 \delta^{(4)}\left(p_1+p_2-p_3-\cdots-p_n\right) \prod_{j=3}^{n} 2\pi\delta\left(p_j^2-m_j^2\right)\Theta\left(p_j^0\right)\frac{d^4p_j}{(2\pi)^4},$$

with the symmetry factor $\mathcal{S}$. This factor should correct double-counting of identical outgoing particles and is defined as:

$$\mathcal{S} = \prod_i n_i!, \tag{2.33}$$

where n_i is the number of outgoing particles of type i.

The factor $4|\vec{p}_1|_{\mathrm{cm}}\sqrt{s}$ corresponds to $4M\nu$ in our lab frame notation, see section 2.1.2. We will not establish this kinematic factor, but we want to mention that the cross-section is related to the transition probability W per unit volume and time in the following way:

$$\frac{dW}{dV\,dt} = \text{incident flux} \times \text{target density} \times d\sigma, \tag{2.34}$$

where the incident flux is proportional to $2|\vec{p}_1|_{\mathrm{lab}}$ and the target density is proportional to $2M$. For the complete derivation we refer to [21].

The integration over the phase space of outgoing particles is restricted to allowed processes by the Dirac delta functions and the Heaviside step functions. They reflect

[2] In preparation of this section we i.a. used [19, 20].

the overall energy and momentum conservation and the requirement that the outgoing particles have to be on-shell and need to have positive energy. For a delta function of a continuously differentiable function g it is true that:

$$\delta(g(x)) = \sum_i \frac{\delta(x - x_i)}{|g'(x_i)|} \quad \text{with} \quad g(x_i) = 0, \tag{2.35}$$

hence the delta functions in the phase space factor can be expanded:

$$\begin{aligned} &\delta\left(p_j^2 - m_j^2\right) \\ &= \delta\left(\left(p_j^0\right)^2 - \vec{p}_j{}^2 - m_j^2\right) \\ &= \frac{1}{2\sqrt{\vec{p}_j{}^2 + m_j^2}} \left[\delta\left(p_j^0 + \sqrt{\vec{p}_j{}^2 + m_j^2}\right) + \delta\left(p_j^0 - \sqrt{\vec{p}_j{}^2 + m_j^2}\right)\right]. \end{aligned} \tag{2.36}$$

Performing the integration over the energies p_j^0 and taking advantage of the previously rewritten delta functions and the theta functions leads to:

$$\begin{aligned} \sigma = &\frac{\mathcal{S}}{4|\vec{p}_1|_{\text{cm}}\sqrt{s}} \times \\ &\int |T|^2 (2\pi)^4 \delta^{(4)}(p_1 + p_2 - p_3 - \cdots - p_n) \prod_{j=3}^{n} \frac{1}{2\sqrt{\vec{p}_j{}^2 + m_j^2}} \frac{d^3\vec{p}_j}{(2\pi)^3}. \end{aligned} \tag{2.37}$$

For further simplifications we will restrict to scattering processes of the type $1 + 2 \longrightarrow 3 + 4$. The phase space measure is Lorentz-invariant and we are free to choose any reference frame. It is convenient to study the kinematics of such a scattering process in the cm-frame, where $\vec{p}_1 = -\vec{p}_2$ and $\vec{p}_3 = -\vec{p}_4$ (from now on we will drop the subscript cm). The particle energies are $E_j = \sqrt{\vec{p}_j{}^2 + m_j^2}$ and the center-of-mass energy squared is $s = (E_1 + E_2)^2$. Putting these equations together we can express $|\vec{p}_1|$ and $|\vec{p}_3|$ in terms of s:

$$|\vec{p}_1| = \frac{1}{2\sqrt{s}} \sqrt{s^2 - 2\left(m_1^2 + m_2^2\right) s + \left(m_1^2 - m_2^2\right)^2}, \tag{2.38a}$$

$$|\vec{p}_3| = \frac{1}{2\sqrt{s}} \sqrt{s^2 - 2\left(m_3^2 + m_4^2\right) s + \left(m_3^2 - m_4^2\right)^2}. \tag{2.38b}$$

For the integration over the momenta spherical coordinates are useful:

$$\begin{aligned} \sigma = &\frac{\mathcal{S}}{4|\vec{p}_1|\sqrt{s}} \times \\ &\int |T|^2 \frac{1}{(2\pi)^2} \delta(E_3 + E_4 - \sqrt{s}) \frac{1}{2\sqrt{\vec{p}_3{}^2 + m_3^2}} \frac{1}{2\sqrt{\vec{p}_3{}^2 + m_4^2}} |\vec{p}_3|^2 d|\vec{p}_3| d\Omega, \end{aligned} \tag{2.39}$$

with $d\Omega = \sin\theta d\theta d\varphi$ and θ being the scattering angle between $\vec{p}_1$ and $\vec{p}_3$. In this the spatial part of the four-dimensional delta function $\delta^{(3)}(\vec{p}_3 + \vec{p}_4)$ was already separated and annihilated with the p_4-integration. The leftover delta function can be rewritten corresponding to eq. (2.35) and with the aid of eq. (2.38b):

$$\begin{aligned}\delta(E_3 - E_4 - \sqrt{s}) = &\left[\frac{|\vec{p}_3|}{E_3} + \frac{|\vec{p}_3|}{E_4}\right]^{-1} \delta\left(|\vec{p}_3| - \frac{1}{2\sqrt{s}}\sqrt{s^2 - 2\left(m_3^2 + m_4^2\right)s + \left(m_3^2 - m_4^2\right)^2}\right) \\ = &\frac{E_3 E_4}{|\vec{p}_3|\sqrt{s}}\,\delta\left(|\vec{p}_3| - \frac{1}{2\sqrt{s}}\sqrt{s^2 - 2\left(m_3^2 + m_4^2\right)s + \left(m_3^2 - m_4^2\right)^2}\right). \quad (2.40)\end{aligned}$$

After some cancellations we are left over with:

$$\frac{d\sigma}{d\Omega} = \frac{\mathcal{S}}{64\pi^2 s}\frac{|\vec{p}_3|}{|\vec{p}_1|}\,|T|^2\,. \quad (2.41)$$

The integration over φ gives a factor of 2π. For the θ-integration it is convenient to make the following substitution:

$$\int_0^\pi \sin\theta d\theta = \int_{-1}^1 d\cos\theta. \quad (2.42)$$

Sometimes the differential solid angle is also replaced by the differential of the Mandelstam variable t, which can be expressed as:

$$t = (p_1 - p_3)^2 = m_1^2 + m_3^2 - 2E_1E_3 + 2|\vec{p}_1||\vec{p}_3|\cos\theta, \quad (2.43)$$

thus

$$\begin{aligned} dt =& 2|\vec{p}_1||\vec{p}_3|d\cos\theta \quad (2.44)\\ =& 2|\vec{p}_1||\vec{p}_3|\frac{d\Omega}{2\pi}.\end{aligned}$$

Now we will skip to our Compton scattering process $\mathrm{W} + \gamma \longrightarrow \mathrm{W}^* + \gamma^*$. In this case the symmetry factor $\mathcal{S} = 1$ is trivial and for the particle masses we have $m_1 = m_3 = M$ respectively $m_2 = m_4 = 0$ and as a result $|\vec{p}_1| = |\vec{p}_3|$, hence the cross-section formula reduces to eq. (2.31).

2.4. Dispersion Relations

A consequence of causality is that the forward scattering amplitudes $f(\nu)$ are analytic (holomorphic) functions in the entire upper half of the complex energy plane. They can be analytically continued into the lower half of the complex plane by applying the Schwarz reflection principle, which as a matter of fact holds for all the elementary functions.

Schwarz reflection principle: [22]

If a function $f(z)$ is

1. analytic over some region, including a point on the real axis
2. real for real z,

then $f^*(z) = f(z^*)$.

The property of the amplitudes to be analytic is directly connected to the underlying physical system being linear, time-translation invariant and bound to the micro-causality condition.

The starting point in deriving the dispersion relation is the Cauchy representation:

$$f(\nu) = \frac{1}{2\pi i} \oint_{\mathcal{C}} \frac{d\nu'}{\nu' - \nu} f(\nu'), \tag{2.45}$$

with $\mathcal{C}$ being a contour enclosing the domain of analyticity and ν located within the region bounded by $\mathcal{C}$.

As described in the previous section, the scattering amplitudes as functions of the (real) photon energy ν become imaginary after exceeding a threshold energy ν_0, which corresponds to the energy needed to create the lightest 'on-shell' intermediate state. Crossing the real axis, the real parts of $f(\nu)$ are continuous, whereas the imaginary parts of $f(\nu)$ are discontinuous and flip the sign, leading to a branch cut. This behaviour follows from the Schwarz reflection principle: $f(\nu - i\epsilon) = f^*(\nu + i\epsilon)$ with $\epsilon \to 0^+$.

Hence, $f(\nu)$ is analytic in the entire complex plane except for the branch cuts and poles located on the real axis. In the Cauchy representation (2.45) one therefore has to choose $\mathcal{C}$ to avoid the branch cuts. Choosing $\mathcal{C}$ as depicted in fig. 2.5, and neglecting the integrals over the big semicircles, we write the rest as the integrals along $\mathcal{C}_1, \cdots, \mathcal{C}_4$:

$$\begin{aligned}
\int_{\mathcal{C}_1} \frac{d\nu'}{\nu' - \nu_+} f(\nu') &= \int_{\nu_0 + i\epsilon}^{\infty + i\epsilon} \frac{d\nu'}{\nu' - \nu_+} f(\nu') && \text{(2.46a)} \\
&= \int_{\nu_0}^{\infty} \frac{d\nu'}{\nu' + i\epsilon - \nu_+} f(\nu' + i\epsilon), \\
\int_{\mathcal{C}_2} \frac{d\nu'}{\nu' - \nu_+} f(\nu') &= \int_{-\infty + i\epsilon}^{-\nu_0 + i\epsilon} \frac{d\nu'}{\nu' - \nu_+} f(\nu') && \text{(2.46b)} \\
&= -\int_{\nu_0}^{\infty} \frac{d\nu'}{\nu' - i\epsilon + \nu_+} f(-\nu' + i\epsilon), \\
\int_{\mathcal{C}_3} \frac{d\nu'}{\nu' - \nu_+} f(\nu') &= \int_{-\nu_0 - i\epsilon}^{-\infty - i\epsilon} \frac{d\nu'}{\nu' - \nu_+} f(\nu') && \text{(2.46c)} \\
&= \int_{\nu_0}^{\infty} \frac{d\nu'}{\nu' + i\epsilon + \nu_+} f(-\nu' - i\epsilon) \\
&= \int_{\nu_0}^{\infty} \frac{d\nu'}{\nu' + i\epsilon + \nu_+} f^*(-\nu' + i\epsilon), \\
\int_{\mathcal{C}_4} \frac{d\nu'}{\nu' - \nu_+} f(\nu') &= \int_{\infty - i\epsilon}^{\nu_0 - i\epsilon} \frac{d\nu'}{\nu' - \nu_+} f(\nu') && \text{(2.46d)} \\
&= -\int_{\nu_0}^{\infty} \frac{d\nu'}{\nu' - i\epsilon - \nu_+} f(\nu' - i\epsilon) \\
&= -\int_{\nu_0}^{\infty} \frac{d\nu'}{\nu' - i\epsilon - \nu_+} f^*(\nu' + i\epsilon).
\end{aligned}$$

where $\nu_+ = \nu + i\eta$, with real ν and η, is a point inside $\mathcal{C}$.

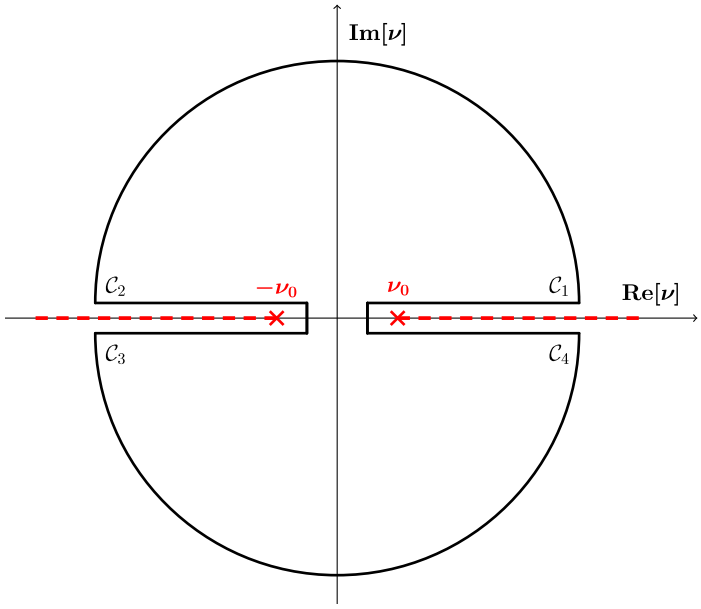

Figure 2.5.: Branch cuts and the contours in the complex ν plane.

Combining the integrals of the left respectively right plane and performing the limit $\epsilon \to 0$ gives:

$$\int_{\mathcal{C}_1+\mathcal{C}_4} \frac{d\nu'}{\nu'-\nu_+} f(\nu') = \int_{\nu_0}^{\infty} d\nu' \, \frac{f(\nu') - f^*(\nu')}{\nu'-\nu_+} = 2i \int_{\nu_0}^{\infty} d\nu' \, \frac{\operatorname{Im} f(\nu')}{\nu'-\nu_+}, \tag{2.47a}$$

$$\int_{\mathcal{C}_2+\mathcal{C}_3} \frac{d\nu'}{\nu'-\nu_+} f(\nu') = \int_{\nu_0}^{\infty} d\nu' \, \frac{f^*(-\nu') - f(-\nu')}{\nu'+\nu_+} = -2i \int_{\nu_0}^{\infty} d\nu' \, \frac{\operatorname{Im} f(-\nu')}{\nu'+\nu_+}. \tag{2.47b}$$

Due to the Schwarz reflection principle, $\operatorname{Im} f(\nu)$ is an odd and $\operatorname{Re} f(\nu)$ is an even function of ν. From a physical point of view $\operatorname{Re} f(\nu)$ is required to be even due to the 'crossing' symmetry of the Compton scattering amplitude.

Making use of these symmetries we obtain:

$$f(\nu_+) = \frac{1}{2\pi i} \oint_{\mathcal{C}} \frac{d\nu'}{\nu'-\nu_+} f(\nu') = \frac{2}{\pi} \int_{\nu_0}^{\infty} d\nu' \, \frac{\nu'}{\nu'^2 - \nu_+^2} \operatorname{Im} f(\nu'). \tag{2.48}$$

Taking the limit to the real axis $\eta \to 0^+$, we finally obtain the dispersion relation:

$$\operatorname{Re} f(\nu) = \frac{2}{\pi} \int_{\nu_0}^{\infty} d\nu' \, \frac{\nu'}{\nu'^2 - \nu^2} \operatorname{Im} f(\nu'). \tag{2.49}$$

Recall that in the beginning we neglected the integral over the big semicircles, therefore assuming that:

$$f(\nu) \xrightarrow{\nu\to\infty} 0. \tag{2.50}$$

This assumption is called a 'no-subtraction hypothesis' and, as we will discover further on, it is not always fulfilled. One can have, for example:

$$f(\nu) \xrightarrow{\nu\to\infty} \text{const}, \tag{2.51}$$

and then the integration over the semicircles contributes a non-vanishing constant value. In this case, however one may formulate a dispersion relation for $f(\nu)/\nu^2$, and hence obtain a perfectly well-defined 'subtracted' dispersion relation for the amplitude f.

2.5. Derivation of Sum Rules

The forward scattering amplitude for Compton scattering on a target with spin S in general consists of $2S+1$ scalar amplitudes $f_0, \ldots, f_{2S}$:

$$T_\lambda(\nu) = \frac{e^2}{M} \sum_{n=0}^{2S} f_n(\nu) \left(\frac{\lambda\nu}{SM}\right)^n, \tag{2.52}$$

where M is the mass and e is the charge of the target. This formula for the (double-polarized) Compton amplitude is valid e.g. for circularly polarized photons with helicity fixed to $\sigma = \sigma' = +1$ and targets with conserved helicity $\lambda = \lambda'$.

The scalar amplitudes $f_n(\nu)$ are functions of the photon energy ν. They are analytic in the entire complex plane (except for the real axis) on grounds of the causality of the scattering process. Therefore these amplitudes fulfill a dispersion relation derived in the previous section:

$$\mathrm{Re}\, f_n(\nu) = \frac{2}{\pi} \int_0^\infty d\nu' \, \frac{\nu'}{\nu'^2 - \nu^2} \, \mathrm{Im}\, f_n(\nu'). \tag{2.53}$$

To derive sum rules one has to make use of the optical theorem, which relates the imaginary part of the forward scattering amplitude to the cross-section:

$$\mathrm{Im}\, T_\lambda(\nu) = 2M\nu \, \sigma_\Lambda(\nu), \tag{2.54}$$

with $\Lambda = 1 - \lambda$. Inserting the general expression (2.52) for the forward scattering amplitude into the optical theorem, one obtains $2S+1$ equations (one for each possible value of λ):

$$\frac{e^2}{M} \sum_{n=0}^{2S} \mathrm{Im}\, f_n(\nu) \left(\frac{\lambda\nu}{SM}\right)^n = 2M\nu \, \sigma_\Lambda(\nu). \tag{2.55}$$

By solving this set of equations, one can extract an expression for the imaginary part of each scalar amplitude in terms of the helicity-dependent cross-sections. Thus, the dispersion relations together with the optical theorem lead to the sought sum rules which relate the real parts of the scalar amplitudes to energy-weighted integrals over cross-sections.

To illustrate the whole derivation procedure we focus here on the spin-$1/2$ sum rules, of which the GDH sum rule is the most known example.

First, one considers the forward Compton scattering amplitude. Adopting the Coulomb gauge $[\epsilon^0 = 0, \, \epsilon = (0, \vec{\epsilon})]$ one obtains the general expression:

$$T(\nu, \theta = 0) = \vec{\epsilon}^{\,*} \cdot \vec{\epsilon} \; F_0(\nu) + i \, \nu \, \vec{\sigma} \cdot (\vec{\epsilon}^{\,*} \times \vec{\epsilon}) \; F_1(\nu), \tag{2.56}$$

with the spin operator $\vec{\sigma}$. The amplitude T is to be invariant under photon 'crossing' ($\epsilon \leftrightarrow \epsilon^*$ and $\nu \leftrightarrow -\nu$), implying that the scalar amplitudes F_0 and F_1 are even functions of ν. The general expression (2.56) of the scattering amplitude also reflects parity conservation of the electromagnetic interaction, since it is invariant under a helicity flip ($\epsilon \leftrightarrow \epsilon^*$ and $\vec{\sigma} \leftrightarrow -\vec{\sigma}$).

For the even functions F_0 and F_1 one can write a dispersion relation of the type (2.53). Furthermore, the scalar amplitudes occur in the optical theorem, which in this case reads as follows:

$$\mathrm{Im}\, F_0(\nu) = \frac{\nu}{8\pi} \left[\sigma_{1/2}(\nu) + \sigma_{3/2}(\nu)\right], \tag{2.57a}$$

$$\mathrm{Im}\, F_1(\nu) = \frac{1}{8\pi}\left[\sigma_{1/2}(\nu) - \sigma_{3/2}(\nu)\right]. \tag{2.57b}$$

Combining the optical theorem and the dispersion relations one obtains:

$$\mathrm{Re}\, F_0(\nu) = \frac{1}{4\pi^2}\int_0^\infty d\nu' \, \frac{\nu'^2}{\nu'^2 - \nu^2}\left[\sigma_{1/2}(\nu') + \sigma_{3/2}(\nu')\right], \tag{2.58a}$$

$$\mathrm{Re}\, F_1(\nu) = \frac{1}{4\pi^2}\int_0^\infty d\nu' \, \frac{\nu'}{\nu'^2 - \nu^2}\left[\sigma_{1/2}(\nu') - \sigma_{3/2}(\nu')\right]. \tag{2.58b}$$

Now one can make a low-energy expansion on both sides of the equations. On the left-hand side, one is then making use of the low-energy theorems for the Compton scattering amplitudes $f_0(\nu)$ found by Thirring [23], and $f_1(\nu)$ found by Low [24], Gell-Mann and Goldberger [25], while on the right-hand side one simply expands in ν around 0. Up to $\mathcal{O}(\nu^4)$ one obtains:

$$-\frac{e^2}{4\pi M} + (\alpha_{E1} + \beta_{M1})\,\nu^2 = \frac{1}{4\pi^2}\int_0^\infty d\nu' \, \left(1 + \frac{\nu^2}{\nu'^2}\right)\left[\sigma_{1/2}(\nu') + \sigma_{3/2}(\nu')\right], \tag{2.59a}$$

$$-\frac{e^2\kappa^2}{8\pi M^2} + \gamma_0\,\nu^2 = \frac{1}{4\pi^2}\int_0^\infty d\nu' \, \left(\frac{1}{\nu'} + \frac{\nu^2}{\nu'^3}\right)\left[\sigma_{1/2}(\nu') - \sigma_{3/2}(\nu')\right]. \tag{2.59b}$$

The low-energy part of the real scattering amplitude depends on the electromagnetic moments as well as on the static electric (α_{E1}), magnetic (β_{M1}) and spin-dependent (γ_0) dipole polarizabilities.

In a last step one can read of several sum rules arising from the individual orders in ν: the GDH sum rule (1.1), the helicity-independent Baldin sum rule (1.2) and the FSP sum rule (1.3).

CHAPTER 3

SUM RULE VERIFICATION IN SCALAR QED

In this chapter we demonstrate how the sum rules can be checked in a field theory. For this we take the simpler case of scalar (spin-0) QED. We will calculate the forward Compton scattering off scalar particles, the corresponding total photoabsorption cross-section, and will verify the sum rules which related them.

3.1. Scalar Compton Scattering Amplitude

In scalar QED we have only two kinds of vertices. Spin-1 QED will beside involve an additional vertex for the bosonic self-interaction. The Feynman rules for scalar QED are given in the appendix C.

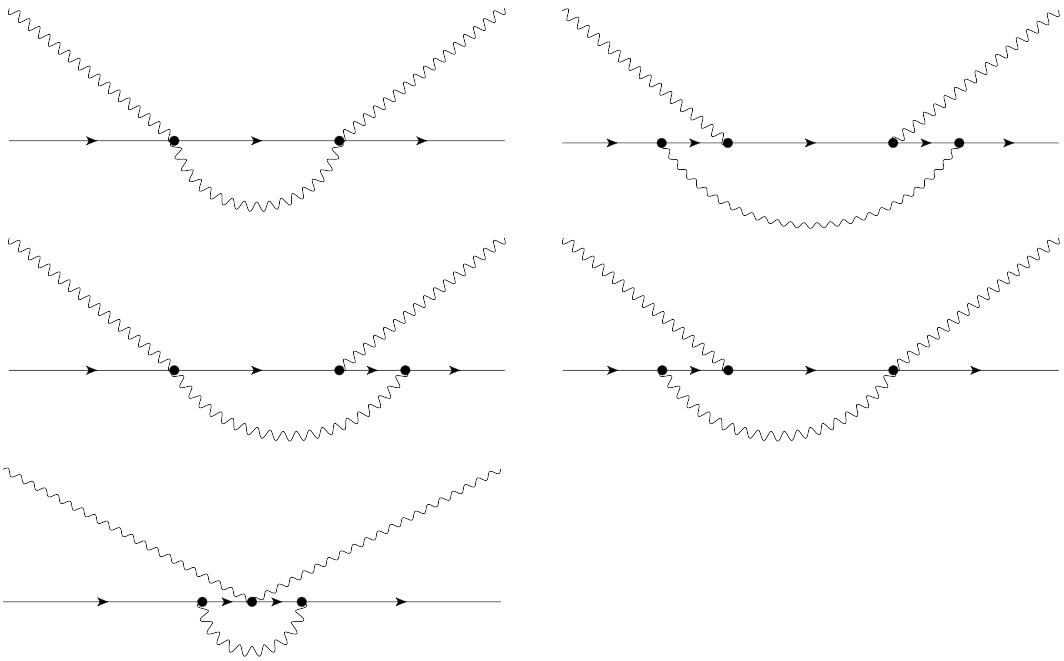

Figure 3.1.: s-channel 1PI diagrams 1-5 [labelled in reading direction]

We begin with considering the forward scattering amplitude f at one-loop level. All of the one-particle-reducible (1PR) diagrams vanish for real photons due to the transversality (2.20) and eq. (2.21). Hence, we only need to compute the one-particle-irreducible (1PI) diagrams. We can distinguish five different types of 1PI diagrams shown in Fig. 3.1. The first four of these diagrams contribute together with their 'crossed' counterparts.

Our calculation yields the following result for the forward Compton scattering amplitude in scalar QED:

$$\begin{aligned}\bar{f}(\nu) = f(\nu) - f(0) = (4\pi\alpha)^2 \Bigg\{ & \frac{M^2\pi^2 + 6\nu^2}{12\pi^2\nu^2} + \frac{2\nu^2}{\pi^2\left(M^2 - 4\nu^2\right)} \ln\frac{2\nu}{M} \\ & - \frac{M\left\{(M+\nu)\,\mathrm{Li}_2\left[1+\frac{2\nu}{M}\right] + (M-\nu)\,\mathrm{Li}_2\left[1-\frac{2\nu}{M}\right]\right\}}{4\pi^2\nu^2} \\ & + i\,\frac{(M+\nu)^2}{2\pi\nu(M+2\nu)} - i\,\frac{M(M+\nu)}{2\pi\nu^2}\ln\left[1+\frac{2\nu}{M}\right]\Bigg\},\end{aligned} \tag{3.1}$$

where we have introduced dilogarithms Li_2, cf. appendix B. Expanding around $\nu = 0$,

$$\begin{aligned}\bar{f}(\nu) = (4\pi\alpha)^2 \Bigg\{ & \frac{i}{3M\pi}\,\nu + \frac{1 - 12i\pi + 24\ln\frac{2\nu}{M}}{18M^2\pi^2}\,\nu^2 + \frac{7i}{5M^3\pi}\,\nu^3 \\ & + \frac{4(14 - 165i\pi + 330\ln\frac{2\nu}{M})}{225M^4\pi^2}\,\nu^4 + \frac{128i}{21M^5\pi}\,\nu^5 \\ & + \frac{2(17 - 308i\pi + 616\ln\frac{2\nu}{M})}{49M^6\pi^2}\,\nu^6\Bigg\},\end{aligned} \tag{3.2}$$

we convince ourselves that $\mathrm{Re}\, f(\nu)$ is even in ν. The imaginary part arises from the diagrams 1 to 4 in figure 3.1. They give the following contributions:

- 1PI diagram type 1:

$$\mathrm{Im}\, f(\nu) = 4\pi\alpha^2 \frac{2\nu}{M+2\nu}, \tag{3.3a}$$

- 1PI diagram type 2:

$$\mathrm{Im}\, f(\nu) = 4\pi\alpha^2 \left\{ \frac{2M}{\nu} + \frac{M+\nu}{M+2\nu} - \left(\frac{M^2}{\nu^2}\left(1+\frac{\nu}{M}\right) + \frac{M}{2\nu}\right)\ln\left[1+\frac{2\nu}{M}\right]\right\}, \tag{3.3b}$$

- 1PI diagram type 3+4:

$$\mathrm{Im}\, f(\nu) = -4\pi\alpha^2 \left\{ \frac{M+\nu}{M+2\nu} - \frac{M}{2\nu}\ln\left[1+\frac{2\nu}{M}\right]\right\}. \tag{3.3c}$$

All together the imaginary contribution to the scattering amplitude is:

$$\mathrm{Im}\, f(\nu) = 4\pi\alpha^2 \left\{ \frac{2\nu}{M+2\nu} + \frac{2M}{\nu} - \frac{M^2}{\nu^2}\left(1+\frac{\nu}{M}\right)\ln\left[1+\frac{2\nu}{M}\right]\right\}. \tag{3.4}$$

3.2. Unpolarized Cross-Section

The unpolarized total cross-section can be calculated from the tree-level scattering amplitude:

$$T_{\sigma\sigma'} = \left(\quad + \quad + \quad \right) \tag{3.5}$$
$$= e^2(\epsilon^*_{\sigma'})_\mu(\epsilon_\sigma)_\nu \Big[(2p'+q')^\mu \frac{1}{s-M^2}(2p+q)^\nu + (2p-q')^\mu \frac{1}{u-M^2}(2p'-q)^\nu + 2\,g^{\mu\nu} \Big]$$
$$= e^2(\epsilon^*_{\sigma'})_\mu(\epsilon_\sigma)_\nu \left(\frac{4\,p'^\mu p^\nu}{2M\nu} - \frac{4\,p'^\nu p^\mu}{2M\nu'} + 2\,g^{\mu\nu} \right).$$

In the lab frame the target is initially at rest, hence:

$$p \cdot \varepsilon(q) = p \cdot \varepsilon^*(q') = 0. \tag{3.6}$$

The scattering amplitude is then simply given by:

$$T_{\sigma\sigma'} = 2\,e^2 \epsilon^*_{\sigma'} \cdot \epsilon_\sigma = -e^2 \left(\cos\theta + \sigma\sigma' \right), \tag{3.7}$$

with the scattering angle θ.
The total unpolarized cross-section is defined as:

$$\frac{d\sigma}{dt} = \frac{1}{16\pi(s-M^2)^2} \frac{1}{2} \sum_{\sigma\sigma'} |T_{\sigma\sigma'}|^2, \tag{3.8}$$

together with

$$\frac{1}{2} \sum_{\sigma\sigma'} |T_{\sigma\sigma'}|^2 = 2\,e^4 \left(1 + \cos^2\theta \right), \tag{3.9}$$

and

$$dt = \frac{(s-M^2)^2}{2s} d\cos\theta. \tag{3.10}$$

One thus finds:

$$\sigma(\nu) = \frac{2\pi\alpha^2}{\nu^2} \left(\frac{2(M+\nu)^2}{M^2+2M\nu} - \left(1 + \frac{M}{\nu} \right) \ln \left[1 + \frac{2\nu}{M} \right] \right). \tag{3.11}$$

In the Thomson limit ($\nu \to 0$) one obtains:

$$\sigma(0) = \frac{8\pi\alpha^2}{3M^2}, \tag{3.12}$$

what is the familiar Thomson cross-section.

3.3. Verification of Sum Rules and the Infra-red Cutoff

A comparison between eq. (3.4) and eq. (3.11) shows that the imaginary part of the forward Compton scattering amplitude is related to the unpolarized tree-level cross-section in the following way:

$$\mathrm{Im}\, f(\nu) = 2M\nu\, \sigma^{(0)}(\nu). \tag{3.13}$$

Therefore, the optical theorem for scalar Compton scattering is verified in our calculation.

Given the scattering amplitude (3.1) one can also test whether the amplitude fulfills the (subtracted) dispersion relation:

$$\mathrm{Re}\,\bar{f}(\nu) = \frac{2}{\pi}\int_0^\infty d\nu'\ \mathrm{Im}\,f(\nu')\,\frac{1}{\nu'^2-\nu^2}\frac{\nu^2}{\nu'}. \tag{3.14}$$

Substituting eq. (3.13), we obtain the sum rule for the forward Compton scattering amplitude:

$$\frac{\mathrm{Re}\,\bar{f}(\nu)}{2M} = \frac{2\,\nu^2}{\pi}\int_0^\infty d\nu'\,\frac{\sigma^{(0)}(\nu')}{\nu'^2-\nu^2}. \tag{3.15}$$

We have verified that our amplitude in eq. (3.1) satisfied the above sum rule with the cross-section given by eq. (3.11).

It is interesting to consider the low-energy expansion of this sum rule. Expanding the right-hand side (rhs) in ν,

$$\frac{2\,\nu^2}{\pi}\int_0^\infty d\nu'\,\frac{\sigma^{(0)}(\nu')}{\nu'^2-\nu^2} = \frac{2}{\pi}\sum_{n=1}^\infty \nu^{2n}\int_0^\infty d\nu'\,\frac{\sigma^{(0)}(\nu')}{\nu'^{2n}}, \tag{3.16}$$

we see that each coefficient in this expansion is divergent in the infra-red, even though the full expression is finite. This is because in QED the production threshold is at $\nu_0 = 0$, since the photon is massless. The same result is obtained when we expand the left-hand side (lhs), cf. eq. (3.2), each coefficient in the low-energy expansion is logarithmically divergent as ν goes to 0. We observe that in order to make the low-energy expansion of the rhs to be quantitatively consistent with the expansion of the lhs, we need to introduce an infra-red cutoff equal to ν, i.e.:

$$\mathrm{Re}\,\bar{f}(\nu) = \frac{4M}{\pi}\sum_{n=1}^\infty \nu^{2n}\int_\nu^\infty d\nu'\,\frac{\sigma^{(0)}(\nu')-\sigma^{(0)}(0)}{\nu'^{2n}}\,. \tag{3.17}$$

Now we can formulate the Baldin sum rule. At the leading order in the energy expansion, the amplitude $\bar{f}$ is still generally expressed in terms of the sum of the electric and magnetic polarizabilities:

$$\bar{f}(\nu) = 8\pi M(\alpha_{E1}+\beta_{M1})\,\nu^2 + \mathcal{O}(\nu^4), \tag{3.18}$$

only in this case they ought to be 'dynamical', i.e., carry a residual dependence on the energy. The Baldin sum rule for the 'dynamical polarizabilities' then becomes:

$$\alpha_{E1}(\nu)+\beta_{M1}(\nu) = \frac{1}{2\pi^2}\int_\nu^\infty d\nu'\,\frac{\sigma^{(0)}(\nu')-\sigma^{(0)}(0)}{\nu'^2}. \tag{3.19}$$

Both sides of the sum rule give now the same result for the one-loop polarizabilities in scalar QED:

$$\alpha_{E1}(\nu)+\beta_{M1}(\nu) = \frac{\alpha^2}{9\pi M^3}\left(1+24\ln\frac{2\nu}{M}\right). \tag{3.20}$$

Thus, the main new outcome of our analysis is that in QED the sum rules need to be treated with an infra-red cutoff equal to the photon energy ν.

CHAPTER 4

SUM RULES FOR SPIN-1 TARGETS

For the derivation of the spin-1 sum rules including all electromagnetic moments we proceed as described in chapter 2. First, we consider the forward Compton scattering amplitude $T_{\lambda'\sigma',\lambda\sigma}(\nu)$, which depends on the photon energy ν and the helicities of the target (λ) and the photon (σ). We will consider the amplitudes with conserved helicities, $\lambda' = \lambda$, $\sigma' = \sigma$, as well as the helicity-flip amplitude.

The double-polarized amplitude can generally be decomposed as shown in eq. (2.52). In the case of interest ($S = 1$) the helicity-conserving amplitude has the following form:

$$T_{\lambda+,\lambda+}(\nu) = \frac{e^2}{M} \sum_{n=0}^{2} f_n(\nu) \left(\frac{\lambda\nu}{M}\right)^n = \sum_{n=0}^{2} F_n(\nu)(\lambda\nu)^n, \tag{4.1}$$

with the three scalar amplitudes f_n or F_n.

In addition, there is a helicity-flip amplitude:

$$T_{+-,-+}(\nu) = T_{-+,+-}(\nu) \equiv G(\nu), \tag{4.2}$$

which gives rise to one scalar amplitude G. This is the amplitude where the helicities of both, the photon and the target, are flipped in the scattering process. Such amplitude is absent for spin-0 and spin-$1/2$ targets, but is non-trivial in the spin-1 case.

All the aforementioned scalar amplitudes are even in ν and therefore fulfill the dispersion relation (2.53). These dispersion relations can symbolically be presented in an expansion of the following form:

$$\mathrm{Re}\, f_n(\nu) = \frac{2}{\pi} \int_0^\infty d\nu' \, \frac{\mathrm{Im}\, f_n(\nu')}{\nu'} \sum_{k=0}^{\infty} \left(\frac{\nu}{\nu'}\right)^{2k}. \tag{4.3}$$

In the spin-1 case the optical theorem for the helicity-conserving amplitude gives a set of three equations. From the combination of these equations one can extract an identity for each scalar amplitude F_0, F_1, F_2:

$$\mathrm{Im}\, F_0(\nu) = 2M\nu\, \sigma_1(\nu), \tag{4.4a}$$
$$\mathrm{Im}\, F_1(\nu) = M\big[\sigma_0(\nu) - \sigma_2(\nu)\big], \tag{4.4b}$$
$$\mathrm{Im}\, F_2(\nu) = M/\nu\big[\sigma_0(\nu) + \sigma_2(\nu) - 2\,\sigma_1(\nu)\big]. \tag{4.4c}$$

For an unpolarized target with:

$$T_{\text{unpol.}} = \frac{1}{3}\sum_{\lambda} T_{\lambda} = \frac{e^2}{M}\left[f_0(\nu) + \frac{2\nu^2}{3M^2} f_2(\nu)\right] = F_0(\nu) + \frac{2\nu^2}{3} F_2(\nu) = F(\nu), \tag{4.5}$$

the optical theorem involves the unpolarized cross-section:

$$\text{Im}\, T_{\text{unpol.}} = \text{Im}\, F(\nu) = \frac{2M\nu}{3}\Big[\sigma_2(\nu) + \sigma_1(\nu) + \sigma_0(\nu)\Big] = 2M\nu\, \sigma(\nu). \tag{4.6}$$

The optical theorem for the helicity-flip amplitude yields:

$$\text{Im}\; T_{+-,-+}(\nu) = \text{Im}\; G(\nu) = 2M\nu \left[\, \sigma_{2\perp}(\nu) - \sigma_{2||}(\nu) \,\right], \tag{4.7}$$

where $\sigma_{2\perp}$ and $\sigma_{2||}$ are the double-polarized total cross-sections for photons linearly polarized perpendicular or parallel with respect to the linear polarization of the target.

4.1. Low-Energy Theorems

[1] Our next step will be a derivation of the low-energy theorems by the effective-Lagrangian method. As the result, we will see how the low-energy expansion of the Compton amplitudes is expressed in terms of the inner-structure information, such as the e.m. moments and polarizabilities of the target.

4.1.1. Electromagnetic Moments

A multipole expansion of e.m.-current density of a spin-1 particle reveals the charge, the magnetic dipole moment and the electric quadrupole moment. The classical definition of the electric quadrupole moment Q is:

$$Q = \int d^3x\, (3z^2 - \vec{x}^{\,2})\, \rho(\vec{x}), \tag{4.8}$$

with $\rho(\vec{x})$ being the charge distribution. If the charge distribution of a particle is not spherically symmetric, this leads to a non-vanishing quadrupole moment.

The magnetic dipole moment is related to particle's spin S by:

$$\vec{\mu} = g\frac{e}{2M}\vec{S}, \tag{4.9}$$

with the Landé g-factor. In an external magnetic field with magnetic flux density $\vec{B}$ the potential energy of a particle is:

$$E_{\text{pot}} = -\vec{\mu}\cdot\vec{B}. \tag{4.10}$$

A particle of arbitrary spin S has in general $2S+1$ electromagnetic moments. The natural values for the electromagnetic moments of any particle with spin S are the values for the leading order electromagnetic moments of an elementary spin-S particle. The natural values for spin-1 particles with unit electric charge are [31]:

$$\mu = \frac{e}{M}, \qquad Q = -\frac{e}{M^2}. \tag{4.11}$$

[1] In preparation of this section we i.a. used [26–30].

It is conventional to define the anomalous e.m. moments as the deviation of the e.m. moments from their natural values. Herein the anomalous e.m. moments are defined as follows:

$$\kappa = \frac{M}{e}\mu - 1, \tag{4.12a}$$

$$\mathcal{Q} = \frac{1}{2}\left(\frac{M^2}{e}Q + 1\right). \tag{4.12b}$$

For point-like particles, as the W-boson, the anomalous moments $\kappa, \mathcal{Q}$ by definition vanish at the classical (tree) level. They obtain non-vanishing values at the quantum level. Substituting eq. (4.9) into eq. (4.12a), we obtain the relation between κ and the gyromagnetic ratio g for spin 1,[2]

$$\kappa = \frac{g}{2} - 1, \tag{4.13}$$

from which one can see that $g = 2$ at the tree level.

To define the interaction among massive spin-1 particles, described by complex vector fields $W_\mu(x)$, and the electromagnetic field $A_\mu(x)$ we choose the following effective Lagrangian density:

$$\begin{aligned}\mathcal{L} = &-\frac{1}{4}F_{\mu\nu}F^{\mu\nu} - \frac{1}{2}W^*_{\mu\nu}W^{\mu\nu} + M^2 W^*_\mu W^\mu \\ &- ie\, W^*_{\mu\nu}A^\mu W^\nu + ie\, A_\mu W^*_\nu W^{\mu\nu} + e^2A^2\, W^*_\mu W^\mu - e^2 A_\nu W^*_\mu A^\mu W^\nu \\ &+ ie\,\ell_1 W^*_\mu W_\nu\, F^{\mu\nu} + \frac{ie\,\ell_2}{2M^2}\left[(D^*_\mu W^*_\nu)W^\alpha \partial_\alpha F^{\mu\nu} - W^*_\alpha (D_\mu W_\nu)\partial^\alpha F^{\mu\nu}\right],\end{aligned} \tag{4.14}$$

with $D_\mu = \partial_\mu + ieA_\mu$ and $W_{\mu\nu} = \partial_\mu W_\nu - \partial_\nu W_\mu$. This Lagrangian is invariant with respect to the U(1) gauge transformations:

$$A_\mu \to A_\mu + \partial_\mu \phi, \quad W^\mu \to W^\mu e^{-ie\phi} \tag{4.15}$$

The electromagnetic moments are given in terms of the parameters ℓ_i as follows:

$$\mu = (1 + \ell_1)\,\frac{e}{2M}\,, \qquad Q = (\ell_2 - \ell_1)\,\frac{e}{M^2}\,. \tag{4.16}$$

There are two types of interaction vertices emerging from this Lagrangian: a 3-point vertex (γWW) and a 4-point vertex ($\gamma\gamma$WW). The corresponding Feynman rules for the effective Lagrangian are listed in the appendix C, see eqs. (C.5 – C.8). The resulting tree-level forward Compton scattering amplitude is then found to be:

$$\begin{aligned}\frac{T}{2M} = &+\frac{e^2}{M}\,\varepsilon^*\cdot\varepsilon\;\chi^*\cdot\chi \\ &+\frac{e^2\nu}{4M^2}(1-\ell_1)^2\;[\varepsilon^*\cdot\chi^*\;\varepsilon\cdot\chi - \varepsilon^*\cdot\chi\;\varepsilon\cdot\chi^*] \\ &-\frac{e^2}{2M^3}\,\ell_2\,(1-\ell_1)\,\varepsilon^*\cdot\varepsilon\;\chi^*\cdot q\;\chi\cdot q - \frac{e^2\nu^2}{4M^3}\,\ell_2\,(1-\ell_1)[\varepsilon^*\cdot\chi^*\;\varepsilon\cdot\chi + \varepsilon^*\cdot\chi\;\varepsilon\cdot\chi^*] \\ &+\frac{e^2\nu^3}{16M^4}\,\ell_2^2\,[\varepsilon^*\cdot\chi^*\;\varepsilon\cdot\chi - \varepsilon^*\cdot\chi\;\varepsilon\cdot\chi^*],\end{aligned} \tag{4.17}$$

[2] Note that κ is sometimes defined as $\kappa = (g-2)S$, which is two times bigger than our definition.

where the lab frame has been tacitly assumed.

For the helicity-conserving scattering amplitude one can replace the scalar products of polarization vectors and photon momenta in the following way:

$$\epsilon^* \cdot \epsilon \, \chi^* \cdot \chi = 1, \tag{4.18a}$$
$$\epsilon^* \cdot \chi^* \, \epsilon \cdot \chi - \epsilon^* \cdot \chi \, \epsilon \cdot \chi^* = -\lambda, \tag{4.18b}$$
$$\epsilon^* \cdot \chi^* \, \epsilon \cdot \chi + \epsilon^* \cdot \chi \, \epsilon \cdot \chi^* = \lambda^2, \tag{4.18c}$$
$$\epsilon^* \cdot \epsilon \, \chi^* \cdot q \, \chi \cdot q = -\nu^2(1-\lambda^2), \tag{4.18d}$$

where the photon helicity was fixed to $\sigma = \sigma' = +1$.
For the helicity-flip amplitude $T_{+-,-+}$ only one combination of vectors gives a contribution:

$$\epsilon^* \cdot \chi^* \, \epsilon \cdot \chi + \epsilon^* \cdot \chi \, \epsilon \cdot \chi^* = 2. \tag{4.19}$$

In the next step, we use eq. (4.1) to obtain the low-energy expansion of the scalar amplitudes:

$$f_0(\nu) = 1 + \frac{\nu^2}{2M^2} \, \ell_2(1-\ell_1), \tag{4.20a}$$
$$f_1(\nu) = -\frac{1}{4}(1-\ell_1)^2 - \frac{\nu^2}{16M^2} \, \ell_2^2, \tag{4.20b}$$
$$f_2(\nu) = -\frac{3}{4} \, \ell_2(1-\ell_1), \tag{4.20c}$$
$$f(\nu) = 1, \tag{4.20d}$$
$$G(\nu) = -\frac{e^2\nu^2}{2M^3} \, \ell_2 \, (1-\ell_1), \tag{4.20e}$$

or, written in terms of the anomalous e.m. moments:

$$\kappa = \frac{1}{2}(\ell_1 - 1), \tag{4.21}$$
$$\mathcal{Q} = \frac{1}{2}(\ell_2 - \ell_1 + 1), \tag{4.22}$$

we have:

$$f_0(\nu) = 1 - \frac{2\,\nu^2}{M^2}\kappa\,(\kappa + \mathcal{Q}), \tag{4.23a}$$
$$f_1(\nu) = -\kappa^2 - \frac{\nu^2}{4M^2}(\kappa + \mathcal{Q})^2, \tag{4.23b}$$
$$f_2(\nu) = +3\,\kappa\,(\kappa + \mathcal{Q}), \tag{4.23c}$$
$$f(\nu) = 1, \tag{4.23d}$$
$$G(\nu) = \frac{2\,e^2\nu^2}{M^3}\kappa\,(\kappa + \mathcal{Q}). \tag{4.23e}$$

If we choose the natural values for our model parameters ($\ell_1 = 1$, $\ell_2 = 0$) the scalar amplitudes become $f_0 = 1$, $f_1 = 0 = f_2 = G$.

4.1.2. Polarizabilities

[3] When a composite particle is immersed in an electric $\vec{E}$ or magnetic $\vec{B}$ field, its charged constituents are displaced, forming electric and magnetic dipoles, proportional to the strength of the field:

$$\vec{d}_{\text{ind.}} = 4\pi\,\alpha_{E1}\,\vec{E}, \tag{4.24a}$$

$$\vec{\mu}_{\text{ind.}} = 4\pi\,\beta_{M1}\,\vec{B}. \tag{4.24b}$$

The proportionality coefficients are called the dipole polarizabilities α_{E1} and β_{M1}. They reflect the mobility of the constituents. In this way polarizabilities shed light on the masses, charges and interactions of the target's constituents.
For elementary particles the polarizabilities vanish at the classical level. For the proton and the neutron we saw that $\alpha_{E1} > \beta_{M1} > 0$, so the nucleons are essentially induced electric dipoles and are paramagnetic.

As an effective Lagrangian including polarizabilities we choose:

$$\begin{aligned}
\mathcal{L}_{\text{Pol.}} = &-\frac{\pi a_1}{M^2} F^{\eta\rho}F_{\rho\zeta}[(D_\eta W_\tau)^*(D^\zeta W^\tau) + (D^\zeta W^\tau)^*(D_\eta W_\tau)] \\
&-\frac{\pi b_1}{M^2} \widetilde{F}^{\eta\rho}\widetilde{F}_{\rho\zeta}[(D_\eta W_\tau)^*(D^\zeta W^\tau) + (D^\zeta W^\tau)^*(D_\eta W_\tau)] \\
&+\frac{\pi a_2}{M^2}|F_{\mu\nu}W^{\mu\nu}|^2 + \frac{\pi b_2}{M^2}|\widetilde{F}_{\mu\nu}W^{\mu\nu}|^2 \\
&+\frac{2\pi a_2}{3M^2} F^{\eta\rho}F_{\rho\zeta}[(D_\eta W_\tau)^*(D^\zeta W^\tau) + (D^\zeta W^\tau)^*(D_\eta W_\tau)] \\
&+\frac{2\pi b_2}{3M^2} \widetilde{F}^{\eta\rho}\widetilde{F}_{\rho\zeta}[(D_\eta W_\tau)^*(D^\zeta W^\tau) + (D^\zeta W^\tau)^*(D_\eta W_\tau)] \\
&-\frac{4\pi\gamma_E}{M^3}\partial_\lambda F^{\sigma\tau}F^{\eta\rho}[(D_\tau W_\sigma)^*(D^\lambda D_\rho W_\eta) + (D^\lambda D_\rho W_\eta)^*(D_\tau W_\sigma)] \\
&-\frac{4\pi\gamma_B}{M^3}\partial_\lambda \widetilde{F}^{\sigma\tau}\widetilde{F}^{\eta\rho}[(D_\tau W_\sigma)^*(D^\lambda D_\rho W_\eta) + (D^\lambda D_\rho W_\eta)^*(D_\tau W_\sigma)].
\end{aligned} \tag{4.25}$$

The Lagrangian describes these multipole interactions:

$$\begin{aligned}
\mathcal{L}_{\text{Pol.}} = -H = &2\pi(a_1\vec{E}^2 + b_1\vec{B}^2 + a_2 E^i E^j X_{ij} + b_2 B^i B^j X_{ij} \\
&+ 2\gamma_E \dot{E}^i E^j X_{ij} + 2\gamma_B \dot{B}^i B^j X_{ij}),
\end{aligned} \tag{4.26}$$

with $X_{ij} = \frac{4}{3}\delta_{ij} - \{\mathcal{S}_i, \mathcal{S}_j\}$ and the spin operators $\mathcal{S}$. From this we can identify the forward spin polarizability:

$$\gamma_0 = \frac{\gamma_E + \gamma_B}{2M}, \tag{4.27}$$

the sum of electric and magnetic dipole polarizabilities:

$$\alpha_{E1} + \beta_{M1} = \frac{a_1 + b_1}{2M}, \tag{4.28}$$

and the electric and magnetic tensor polarizabilities:

$$\alpha_{E2} = \frac{a_2}{2M}, \tag{4.29a}$$

$$\beta_{M2} = \frac{b_2}{2M}. \tag{4.29b}$$

[3] In preparation of this section we i.a. used [32].

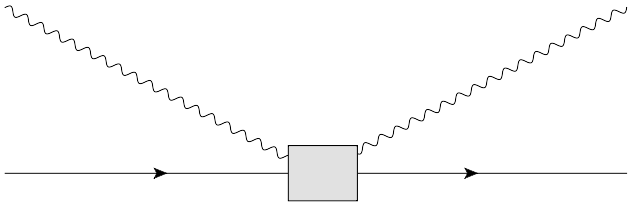

Figure 4.1.: Polarizability vertex diagram

From the polarizability Lagrangian we derive a two-photon two-boson vertex with the vertex function:

$$\begin{aligned}
\Gamma^{\mu\nu\alpha\beta}_{\text{Pol.}}(p,q;p,q) = &+ \frac{2\pi}{M^2}\Big(a_1 - \frac{2}{3}\,a_2\Big) g^{\alpha\beta}\Big[2\,(p\cdot q)^2\, g^{\mu\nu} - 2\,(p\cdot q)\,(p^\mu q^\nu + p^\nu q^\mu) \\
&\quad + q^2\,(p^\mu p^\nu + p^\nu p^\mu)\Big] \\
&+ \frac{2\pi}{M^2}\Big(b_1 - \frac{2}{3}\,b_2\Big) g^{\alpha\beta} p_\sigma p^\eta q_\tau q^\rho (\epsilon^{\sigma\tau\mu}\epsilon_{\eta\rho\nu} + \epsilon^{\sigma\tau\nu}\epsilon_{\eta\rho\mu}) \\
&+ \frac{4\pi a_2}{M^2}\Big[(p\cdot q)^2\big(g^{\alpha\mu}g^{\beta\nu} + g^{\alpha\nu}g^{\beta\mu}\big) + 2\,q^\alpha q^\beta p^\mu p^\nu \\
&\quad - (p\cdot q)\,\big(q^\alpha p^\mu g^{\beta\nu} + q^\alpha p^\nu g^{\beta\mu} + q^\beta p^\mu g^{\alpha\nu} + q^\beta p^\nu g^{\alpha\mu}\big)\Big] \\
&+ \frac{4\pi b_2}{M^2}\, p_\sigma p_\eta q_\tau q_\rho\, (\epsilon^{\alpha\sigma\tau\mu}\epsilon^{\beta\eta\rho\nu} + \epsilon^{\alpha\sigma\tau\nu}\epsilon^{\beta\eta\rho\mu}) \\
&- \frac{4\pi\gamma_E}{M^3}\Big[2\,(p\cdot q)^3\big(g^{\alpha\mu}g^{\beta\nu} - g^{\alpha\nu}g^{\beta\mu}\big) \\
&\quad - 2\,(p\cdot q)^2\big(q^\alpha p^\mu g^{\beta\nu} - q^\alpha p^\nu g^{\beta\mu} - q^\beta p^\mu g^{\alpha\nu} + q^\beta p^\nu g^{\alpha\mu}\big)\Big] \\
&+ \frac{8\pi\gamma_B}{M^3}\,(p\cdot q)\, p_\sigma p_\eta q_\tau q_\rho\, (\epsilon^{\alpha\sigma\tau\nu}\epsilon^{\beta\eta\rho\mu} - \epsilon^{\alpha\sigma\tau\mu}\epsilon^{\beta\eta\rho\nu}),
\end{aligned} \tag{4.30}$$

where the forward limit was assumed (with $p = p'$ and $q = q'$).

The low-energy contribution of the polarizabilities to the scattering amplitudes can be extracted from the trivial Feynman diagram, see fig. 4.1, build from the just mentioned vertex:

$$F_0(\nu) = \frac{2\pi}{M}\left(a_1 + b_1 - \frac{2}{3}\,(a_2 + b_2)\right)\,\nu^2, \tag{4.31a}$$

$$F_1(\nu) = \frac{4\pi}{M}(\gamma_E + \gamma_B)\,\nu^2, \tag{4.31b}$$

$$F_2(\nu) = \frac{2\pi}{M}(a_2 + b_2), \tag{4.31c}$$

$$F(\nu) = \frac{2\pi}{M}(a_1 + b_1)\,\nu^2, \tag{4.31d}$$

$$G(\nu) = \frac{2\pi}{M}(a_2 - b_2)\,\nu^2. \tag{4.31e}$$

From the Lagrangian, which has to be of mass dimension four, we can read of the dimensions of our polarizabilities: $[a_1] = [a_2] = [b_1] = [b_2] = [\text{MeV}]^{-2}$ and $[\gamma_E] = [\gamma_B] = [\text{MeV}]^{-3}$.

4.2. Sum Rules

We now have all the ingredients to write down the sum rules. To this end we substitute the optical theorem and the low-energy expansions in the dispersion relations, and finally obtain the following sum rules for the spin-1 case.
From f_0:

$$-\frac{e^2}{M^3}\,\kappa\,(\kappa+\mathcal{Q})+\frac{\pi}{M}\left(a_1+b_1-\frac{2}{3}\,(a_2+b_2)\right)=\frac{1}{\pi}\int_0^\infty\frac{d\nu}{\nu^2}\,\sigma_1(\nu). \tag{4.32}$$

From f_1:

- GDH sum rule

$$\frac{e^2}{M^2}\,\kappa^2=\frac{1}{\pi}\int_0^\infty\frac{d\nu}{\nu}\,\big[\sigma_2(\nu)-\sigma_0(\nu)\big], \tag{4.33}$$

- FSP sum rule

$$\frac{e^2}{4M^4}\,(\kappa+\mathcal{Q})^2-\frac{4\pi}{M}(\gamma_E+\gamma_B)=\frac{1}{\pi}\int_0^\infty\frac{d\nu}{\nu^3}\,\big[\sigma_2(\nu)-\sigma_0(\nu)\big]. \tag{4.34}$$

From f_2:

$$\frac{3e^2}{M^3}\,\kappa\,(\kappa+\mathcal{Q})+\frac{2\pi}{M}(a_2+b_2)=\frac{1}{\pi}\int_0^\infty\frac{d\nu}{\nu^2}\,\big[\sigma_0(\nu)+\sigma_2(\nu)-2\,\sigma_1(\nu)\big]. \tag{4.35}$$

From f:

- Baldin sum rule

$$\frac{3\pi}{M}(a_1+b_1)=\frac{1}{\pi}\int_0^\infty\frac{d\nu}{\nu^2}\big[\sigma_2(\nu)+\sigma_1(\nu)+\sigma_0(\nu)\big] \tag{4.36}$$

From G:

- QSR sum rule

$$\frac{e^2}{M^3}\,\kappa\,(\kappa+\mathcal{Q})+\frac{\pi}{M}(a_2-b_2)=\frac{1}{\pi}\int_0^\infty\frac{d\nu}{\nu^2}\,\big[\sigma_{2\perp}(\nu)-\sigma_{2\parallel}(\nu)\big] \tag{4.37}$$

The derived GDH sum rule is in agreement with the familiar formulation for arbitrary spin S:

$$\frac{e^2}{SM^2}\,\kappa^2=\frac{1}{\pi}\int_0^\infty\frac{d\nu}{\nu}\Delta\sigma(\nu), \tag{4.38}$$

with $\Delta\sigma(\nu)=\sigma_P(\nu)-\sigma_A(\nu)$, where $\sigma_{P/A}(\nu)$ are the photoabsorption cross-sections with photon and target spins parallel/antiparallel. The appearance of the factor $1/S$ in the low-energy theorem arises due to the decomposition of the scattering amplitude according to eq. (2.52). Note that the optical theorem for the F_1 amplitude is basically the same for the spin-$1/2$ and spin-1 cases, as spin and helicity cancel in the prefactor of F_1.

The FSP sum rule is, as anticipated, modified by the anomalous electric quadrupole moment $\mathcal{Q}$. Moreover the helicity-flip amplitude generates a new sum rule, which we referred to as the quadrupole sum rule (QSR).

4.3. δSum Rules

The idea of δsum rules was first presented in [33]. The advantage of, for instance, the δGDH sum rule is the linear relation between the anomalous magnetic dipole moment κ and a cross-section derivative.

Adding a Corben-Schwinger interaction term [34, 35]:

$$\mathcal{L} = 2ie\kappa_0 W_\mu W^*_\nu F^{\mu\nu} \tag{4.39}$$

to our Lagrangian, the anomalous magnetic dipole moment becomes:

$$\kappa = \kappa_0 + \delta\kappa, \tag{4.40}$$

where $\delta\kappa$ represents the loop corrections. Because of the additional coupling, the loop corrections $\delta\kappa$ and the cross-sections $\sigma_\Lambda(\nu, \kappa_0)$ now depend on κ_0.

In the limit $\kappa_0 \to 0$ the GDH sum rule

$$\frac{e^2}{M^2}\kappa^2 = \frac{e^2}{M^2}(\kappa_0 + \delta\kappa)^2 = \frac{1}{\pi}\int_0^\infty \frac{d\nu}{\nu}\,\Delta\sigma(\nu, \kappa_0) \tag{4.41}$$

holds. The δGDH can be obtained by differentiating with respect to κ_0 at $\kappa_0 = 0$. On the left-hand side we have, at lowest order of perturbation theory (*):

$$\frac{\partial}{\partial\kappa_0}\kappa^2\Big|_{\kappa_0=0} = 2(\kappa_0 + \delta\kappa)\left(1 + \frac{\partial}{\partial\kappa_0}\delta\kappa\right)\Big|_{\kappa_0=0} \overset{(*)}{=} 2\,\kappa, \tag{4.42}$$

which is linear in κ. The δGDH reads:

$$\frac{2e^2}{M^2}\kappa = \frac{1}{\pi}\int_0^\infty \frac{d\nu}{\nu}\,\Delta\sigma_{\kappa_0}(\nu), \tag{4.43}$$

with

$$\sigma_{\kappa_0}(\nu) = \frac{\partial}{\partial\kappa_0}\sigma(\nu, \kappa_0)\Big|_{\kappa_0=0}. \tag{4.44}$$

For the other spin-1 sum rules the derivatives of the low-energy theorems contain:

$$\frac{\partial}{\partial\kappa_0}\kappa(\kappa + \mathcal{Q})\Big|_{\kappa_0=0} = \frac{\partial}{\partial\kappa_0}\kappa^2 + \left(1 + \frac{\partial}{\partial\kappa_0}\delta\kappa\right)\mathcal{Q} + \kappa\frac{\partial}{\partial\kappa_0}\mathcal{Q}\Big|_{\kappa_0=0} \overset{(*)}{=} 2\kappa + \mathcal{Q}, \tag{4.45a}$$

$$\frac{\partial}{\partial\kappa_0}(\kappa + \mathcal{Q})^2\Big|_{\kappa_0=0} = 2(\kappa + \mathcal{Q})\left(1 + \frac{\partial}{\partial\kappa_0}\delta\kappa + \frac{\partial}{\partial\kappa_0}\mathcal{Q}\right)\Big|_{\kappa_0=0} \overset{(*)}{=} 2(\kappa + \mathcal{Q}), \tag{4.45b}$$

and are accordingly also linear in the anomalous e.m. moments. In addition the other δsum rule values contain derivatives of the polarizabilities:

$$c' = \frac{\partial}{\partial\kappa_0}c\Big|_{\kappa_0=0}. \tag{4.46}$$

The spin-1 δsum rules are given below.

- δF_0 sum rule

$$-\frac{e^2}{M^3}(2\kappa + \mathcal{Q}) + \frac{\pi}{M}\left[a'_1 + b'_1 - \frac{2}{3}(a'_2 + b'_2)\right] = \frac{1}{\pi}\int_0^\infty \frac{d\nu}{\nu^2}\,\sigma_{1,\kappa_0}(\nu), \tag{4.47}$$

- δGDH sum rule

$$\frac{2\,e^2}{M^2}\kappa = \frac{1}{\pi}\int_0^\infty \frac{d\nu}{\nu}\,\Delta\sigma_{\kappa_0}(\nu), \tag{4.48}$$

- δFSP sum rule

$$\frac{e^2}{2M^4}(\kappa+\mathcal{Q}) - \frac{4\pi}{M}(\gamma'_E+\gamma'_B) = \frac{1}{\pi}\int_0^\infty \frac{d\nu}{\nu^3}\,\Delta\sigma_{\kappa_0}(\nu), \tag{4.49}$$

- δF_2 sum rule

$$\frac{3e^2}{M^3}(2\kappa+\mathcal{Q}) + \frac{2\pi}{M}(a'_2+b'_2) = \frac{1}{\pi}\int_0^\infty \frac{d\nu}{\nu^2}\,\sigma_{Q,\kappa_0}(\nu), \tag{4.50}$$
$$\text{with}\quad \sigma_Q(\nu) = \sigma_0(\nu)+\sigma_2(\nu)-2\,\sigma_1(\nu),$$

- δBaldin sum rule

$$\frac{3\pi}{M}(a'_1+b'_1) = \frac{1}{\pi}\int_0^\infty \frac{d\nu}{\nu^2}\sigma_{\kappa_0}(\nu), \tag{4.51}$$

- δQSR sum rule

$$\frac{e^2}{M^3}(2\kappa+\mathcal{Q}) + \frac{\pi}{M}(a'_2-b'_2) = \frac{1}{\pi}\int_0^\infty \frac{d\nu}{\nu^2}\left[\sigma_{2\perp,\kappa_0}(\nu)-\sigma_{2\parallel,\kappa_0}(\nu)\right]. \tag{4.52}$$

CHAPTER 5

QED WITH MASSIVE VECTOR BOSONS

This section is dedicated to the calculation of the forward Compton scattering amplitude at one-loop level and the tree-level Compton scattering cross-sections. The results will serve as a basis for the verification of the proposed sum rules in the framework of spin-1 QED.

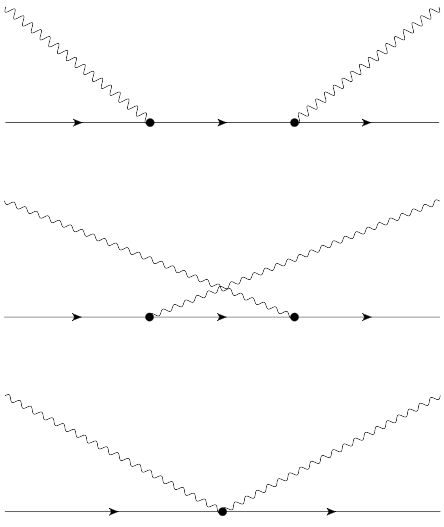

(a) s-channel contribution

(b) u-channel contribution

(c) seagull-channel contribution

Figure 5.1.: Tree-level diagrams

Spin-1 QED

According to the Standard Model with infinitely-heavy Z and Higgs bosons, the spin-1 QED can be described by the following Lagrangian:

$$\begin{aligned}\mathcal{L} = &-\frac{1}{4}F_{\mu\nu}F^{\mu\nu} - \frac{1}{2}W^*_{\mu\nu}W^{\mu\nu} + M^2 W^*_\mu W^\mu \\ &+ ie\, W^*_{\mu\nu}A^\mu W^\nu - ie\, A_\mu W^*_\nu W^{\mu\nu} - e^2 A^2\, W^*_\mu\, W^\mu + e^2 A_\nu W^*_\mu A^\mu W^\nu \\ &+ ie\, W^*_\mu W_\nu\, F^{\mu\nu} + \frac{1}{2}e^2\left(|W\cdot W|^2 - |W|^4\right),\end{aligned} \tag{5.1}$$

with $D_\mu = \partial_\mu - ieA_\mu$ and $W_{\mu\nu} = \partial_\mu W_\nu - \partial_\nu W_\mu$. The Lagrangian describes an electroweak theory with a weak mixing angle of $\theta_W = 90°$ and no Higgs. In this (partially) massive Yang-Mills theory the Z-boson acquires an infinite mass ($M_Z = {}^{M_W}/_{\cos\theta_W}$) and decouples.

There are three different interaction vertices in this case: a 3-point vertex (γWW), a 4-point vertex ($\gamma\gamma$WW) and a bosonic self-interaction vertex (WWWW). The corresponding Feynman rules for this spin-1 QED are listed in the appendix C, see eqs. (C.5 – C.9) with $\ell_1 = 1$ and $\ell_2 = 0$.

In the natural limit ($\ell_1 = 1$, $\ell_2 = 0$), the effective Lagrangian (4.14) used to calculate the low-energy expansion generates the same 3- and 4-point vertices as the Yang-Mills Lagrangian.

5.1. Tree-Level Diagrams

At tree-level we find three different diagrams, see fig. 5.1: a seagull diagram, a s-channel diagram, where the final state photon is emitted after the absorption of the incident photon, and an u-channel diagram, where first a photon is emitted and after that a photon is absorbed. The s- and u-channel diagrams differ by their time ordering. The u-channel diagrams we also refer to as 'crossed' diagrams.

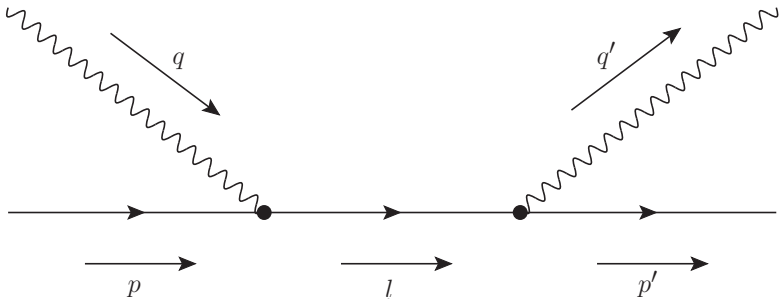

Figure 5.2.: Feynman diagram for s-channel Compton scattering at tree-level

For the scattering amplitude of the tree-level s-channel diagram, see fig. (5.2), one obtains:

$$\begin{aligned}\mathcal{A} = \frac{1}{i(2\pi)^4}\frac{1}{\delta^{(4)}(p+q-p'-q')}\times \\ \int \frac{1}{i(2\pi)^4}\, i\,(2\pi)^4\,\delta^{(4)}(p+q-l)\, i\,(2\pi)^4\,\delta^{(4)}(l-p'-q')\times \\ \underbrace{\chi^*_\alpha\,\varepsilon^*_\mu\,\Gamma^{\alpha\rho\mu}(l,p')\,\Delta_{\rho\sigma}(l)\,\Gamma^{\sigma\beta\nu}(p,l)\,\varepsilon_\nu\,\chi_\beta}_{=\mathcal{A}'}\, d^4l \\ = \chi^*_\alpha\,\varepsilon^*_\mu\,\Gamma^{\alpha\rho\mu}(p+q,p')\,\Delta_{\rho\sigma}(p+q)\,\Gamma^{\sigma\beta\nu}(p,p+q)\,\varepsilon_\nu\,\chi_\beta.\end{aligned} \tag{5.2}$$

The other diagrams can be described in the following way:

- s-channel:

$$\mathcal{A}' = \chi^*_\alpha\,\varepsilon^*_\mu\,\Gamma^{\alpha\rho\mu}(l_1,p')\,\Delta_{\rho\sigma}(l_1)\,\Gamma^{\sigma\beta\nu}(p,l_1)\,\varepsilon_\nu\,\chi_\beta \qquad \text{with} \qquad l_1 = p+q, \tag{5.3a}$$

- u-channel:

$$\mathcal{A}' = \chi^*_\alpha\, \varepsilon^*_\mu\, \Gamma^{\alpha\rho\nu}(l_2, p')\, \Delta_{\rho\sigma}(l_2)\, \Gamma^{\sigma\beta\mu}(p, l_2)\, \varepsilon_\nu\, \chi_\beta \qquad \text{with} \qquad l_2 = p - q', \tag{5.3b}$$

- seagull-channel:

$$\mathcal{A}' = \chi^*_\alpha\, \varepsilon^*_\mu\, \Gamma^{\alpha\beta\mu\nu}\, \varepsilon_\nu\, \chi_\beta. \tag{5.3c}$$

From this we can calculate the forward scattering amplitudes in spin-1 QED:

- s-channel:

$$\frac{e^2}{2M\nu}\left(-4\,\epsilon^*\cdot\epsilon\;\chi\cdot q\;\chi^*\cdot q + 2\,M\nu\,\epsilon^*\cdot\chi^*\;\epsilon\cdot\chi\right), \tag{5.4a}$$

- u-channel:

$$\frac{e^2}{2\,M\nu}\left(4\,\epsilon^*\cdot\epsilon\;\chi\cdot q\;\chi^*\cdot q + 2\,M\nu\,\epsilon^*\cdot\chi\;\epsilon\cdot\chi^*\right), \tag{5.4b}$$

- seagull-channel:

$$e^2\left(2\,\epsilon^*\cdot\epsilon\;\chi^*\cdot\chi - [\epsilon^*\cdot\chi^*\;\epsilon\cdot\chi + \epsilon^*\cdot\chi\;\epsilon\cdot\chi^*]\right). \tag{5.4c}$$

By the s- and u-channel expressions the photon 'crossing' is nice to observe. Replacing $\epsilon \leftrightarrow \epsilon^*$ and $\nu \leftrightarrow -\nu$ (or equivalently $s \leftrightarrow u$), s- an u-channel merge into one another.

Taken together, the resulting scattering amplitude is:

$$T = 2\,e^2\epsilon^*\cdot\epsilon\chi^*\cdot\chi, \tag{5.5}$$

what corresponds to the natural limit of eq. (4.17).

The contraction of the 'amputated' scattering amplitude with the photon momentum vanishes, as is expected from the Ward identity (see section 5.5.1). This serves as a proof of gauge invariance and shows us that we are having a current-conserving set of diagrams. Below we make explicit some steps in this proof:

q'_μ  $^\mu$ (5.6)

$$= q'_\mu\,\chi^*_\alpha\left(\Gamma^{\alpha\rho\mu}(l_1,p')\,\Delta_{\rho\sigma}(l_1)\,\Gamma^{\sigma\beta\nu}(p,l_1) + \Gamma^{\alpha\rho\nu}(l_2,p')\,\Delta_{\rho\sigma}(l_2)\,\Gamma^{\sigma\beta\mu}(p,l_2) + \Gamma^{\alpha\beta\mu\nu}\right)\varepsilon_\nu\,\chi_\beta$$

$$= e\Big(\underbrace{q'_\mu\,\Gamma^{\alpha\rho\mu}(l_1,p')}_{=[\Delta^{-1}(l_1)-\Delta^{-1}(p')]^{\alpha\rho}}\Delta_{\rho\sigma}(l_1)\,\Gamma^{\sigma\beta\nu}(p,l_1) + \Gamma^{\alpha\rho\nu}(l_2,p')\,\Delta_{\rho\sigma}(l_2)\underbrace{q'_\mu\,\Gamma^{\sigma\beta\mu}(p,l_2)}_{=[\Delta^{-1}(p)-\Delta^{-1}(l_2)]^{\sigma\beta}}$$
$$+\frac{1}{e}\,q'_\mu\,\Gamma^{\alpha\beta\mu\nu}\Big)\,\chi^*_\alpha\,\varepsilon_\nu\,\chi_\beta$$

$$= \{p \text{ and } p' \text{ are on-shell}\}$$

$$= e\Big(\big[\Delta^{-1}(l_1) - \cancel{\Delta^{-1}(p')}\big]^{\alpha\rho}\,\Delta_{\rho\sigma}(l_1)\,\Gamma^{\sigma\beta\nu}(p,l_1)$$
$$+\Gamma^{\alpha\rho\nu}(l_2,p')\,\Delta_{\rho\sigma}(l_2)\,\big[\cancel{\Delta^{-1}(p)} - \Delta^{-1}(l_2)\big]^{\sigma\beta} + \frac{1}{e}\,q'_\mu\,\Gamma^{\alpha\beta\mu\nu}\Big)\,\chi^*_\alpha\,\varepsilon_\nu\,\chi_\beta$$

$$= e\left(\delta^\alpha_\sigma\,\Gamma^{\sigma\beta\nu}(p,l_1) - \Gamma^{\alpha\rho\nu}(l_2,p')\,\delta^\beta_\rho + \frac{1}{e}\,q'_\mu\,\Gamma^{\alpha\beta\mu\nu}\right)\chi^*_\alpha\,\varepsilon_\nu\,\chi_\beta$$

$$= \left(e\,\Gamma^{\alpha\beta\nu}(p,l_1) - e\,\Gamma^{\alpha\beta\nu}(l_2,p') + q'_\mu\,\Gamma^{\alpha\beta\mu\nu}\right)\chi^*_\alpha\,\varepsilon_\nu\,\chi_\beta$$

$$= 0.$$

5.2. Cross-sections

In this section we calculate the tree-level cross-sections in spin-1 QED. All cross-sections are proportional to e^4, and we omit this factor for brevity.

The cross-section of a scattering process is dependent on the polarization of the initial particles. Therefore we differ between helicity-dependent cross-sections, linearly polarized cross-sections and the unpolarized cross-section.

5.2.1. Helicity-Dependent Cross-sections

In the cm-frame the total (target) helicity-dependent cross-sections is defined as follows:

$$\sigma_\Lambda = \sigma_{1-\lambda} = \frac{1}{32\pi s}\int_{-1}^{1} d\cos\theta \sum_{\lambda'\sigma'} |T_{\lambda'\sigma',\lambda+}|^2. \tag{5.7}$$

For the three possible target helicities we obtain (omitting e^4):

$$\begin{aligned}
\sigma_2(\nu) &= \frac{9M^5 + 36M^4\nu + 23M^3\nu^2 - 42M^2\nu^3 - 12M\nu^4 + 24\nu^5}{12\pi M^2\nu^2(M+2\nu)^3} && \text{(5.8a)}\\
&\quad - \frac{3(M-\nu)}{8\pi\nu^3}\ln\left[1+\frac{2\nu}{M}\right],\\
\sigma_1(\nu) &= -\frac{9M^3 + 30M^2\nu + 19M\nu^2 - 6\nu^3}{12\pi M\nu^2(M+2\nu)^2} + \frac{3M+\nu}{8\pi\nu^3}\ln\left[1+\frac{2\nu}{M}\right], && \text{(5.8b)}\\
\sigma_0(\nu) &= \frac{9M^3 + 30M^2\nu + 29M\nu^2 + 6\nu^3}{12\pi M^2\nu^2(M+2\nu)} && \text{(5.8c)}\\
&\quad - \frac{3M^2 + 7M\nu + 4\nu^2}{8\pi M\nu^3}\ln\left[1+\frac{2\nu}{M}\right].
\end{aligned}$$

5.2.2. Unpolarized Cross-Section

The unpolarized cross-section is the average of the above defined helicity-dependent cross-sections:

$$\begin{aligned}
\sigma(\nu) &= \frac{1}{3}\left[\sigma_2(\nu) + \sigma_1(\nu) + \sigma_0(\nu)\right] && \text{(5.9)}\\
&= \frac{9M^5 + 54M^4\nu + 129M^3\nu^2 + 168M^2\nu^3 + 140M\nu^4 + 48\nu^5}{36\pi M^2\nu^2(M+2\nu)^3}\\
&\quad + \frac{\left(3M^2 + 3M\nu + 4\nu^2\right)}{24\pi M\nu^3}\ln\left[1+\frac{2\nu}{M}\right].
\end{aligned}$$

5.2.3. Linearly Polarized Cross-sections

For the QSR sum rule linearly polarized cross-sections have to be calculated.

To establish these cross-sections we choose the polarization vectors of the photon and the target to be either orthogonal,

$$\varepsilon = (0,\, \cos\phi, \sin\phi,\, 0), \tag{5.10a}$$
$$\chi = (0,\, -\sin\phi, \cos\phi,\, 0), \tag{5.10b}$$

or parallel, $\varepsilon = \chi = (0, \cos\phi, \sin\phi, 0)$. ϕ is the polarization angle, over which one has to average. As far as the cross-section difference is concerned, only the following structures can yield a non-vanishing contribution:

$$(\varepsilon \cdot \chi)^2 \to -1, \tag{5.11a}$$

$$\varepsilon \cdot \chi \; n' \cdot \chi \; n' \cdot \varepsilon \to \sin^2\theta \, \cos^2\phi, \tag{5.11b}$$

$$(n' \cdot \chi)^2 (n' \cdot \varepsilon)^2 \to \cos^2\phi \, \cos 2\phi, \tag{5.11c}$$

where $n' = (1, \sin\theta, 0, \cos\theta)$ is the direction of the scattered photon.

Performing the calculation for the linearly double-polarized cross-sections, we finally obtain:

$$\sigma_{2\perp}(\nu) - \sigma_{2||}(\nu) = \frac{3M^3 + 15M^2\nu + 22M\nu^2 + 6\nu^3}{6\pi\nu^2(M+2\nu)^3} - \frac{M \ln\left[1 + \frac{2\nu}{M}\right]}{4\pi\nu^3}. \tag{5.12}$$

5.3. One-Loop Diagrams

Here we specify all topologically inequivalent diagrams, which contribute to the Compton scattering process at one-loop level. In the appendix E we give more detailed information on the individual contributions: their descriptions in terms of propagators and vertex functions, the involved loop integrals and of course their scalar amplitudes.

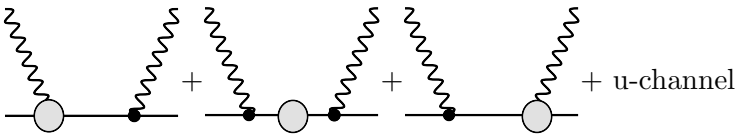

Figure 5.3.: 1PR diagrams

One can distinguish between one-particle-reducible (1PR) and one-particle-irreducible (1PI) diagrams. A diagram is called 1PI if there is no place to cut a single internal line and split the diagram into two parts, meaning if there still remains a connection between the external lines no matter where you cut any internal line. The 1PR diagrams contain vertex and propagator corrections which can be treated separately.

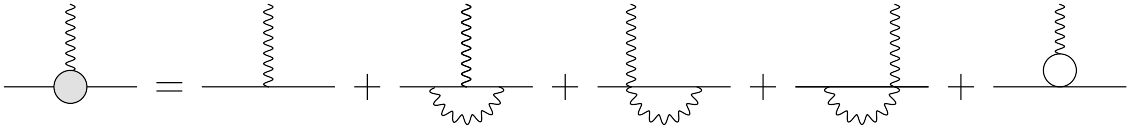

Figure 5.4.: 3-point vertex modification

The 3-point vertex corrections are shown in fig. 5.4. We refer to them respectively as: vertex correction, left-sided or right-sided contact correction and tadpole-vertex correction.

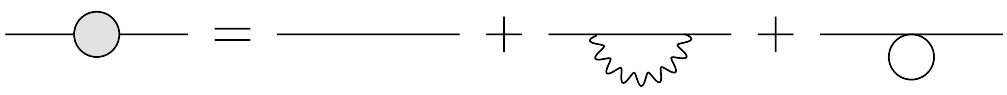

Figure 5.5.: Propagator modification

The modifications to the propagator are shown in fig. 5.5. There are two of them: the usual self-energy correction and a tadpole loop. We do not need to consider the contact photon loop, because this correction vanishes.

Corrections to the external lines need not be considered, because their only effect would be to renormalize the W-boson mass and field.

Just as in the scalar case we can build the five 1PI diagrams shown in fig. 3.1, as well as the corresponding 'crossed' diagrams. In the spin-1 QED case one additionally has to consider the three tadpole diagrams, see fig. 5.6.

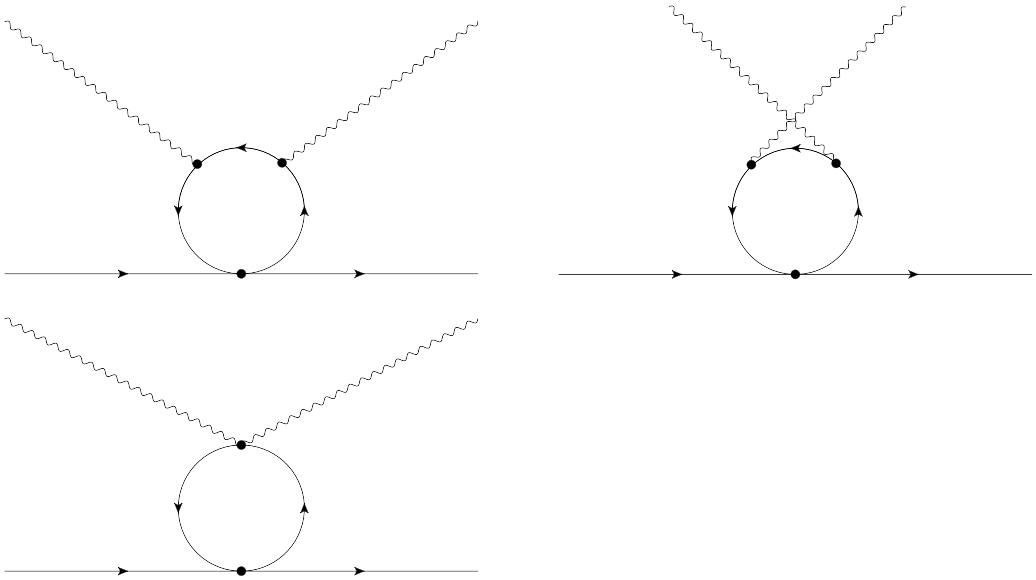

Figure 5.6.: Tadpole diagrams: s-channel, u-channel and seagull-contribution

5.4. Anomalous Electromagnetic Moments

The anomalous e.m. moments at one-loop level are given by the vertex modifications. We will now reproduce the anomalous magnetic dipole moment and the anomalous electric quadrupole moment as given in [36,37]. The complement for the electron is known as the Schwinger correction $(g-2)/2 = \alpha/2\pi$ [38], which originates from the vertex correction to the γee-vertex.

The electromagnetic interaction current in general consists of $2S+1$ independent covariant vertex functions $F_k(Q^2)$. From the effective Lagrangian 4.14 describing a spin-1 particle with arbitrary magnetic dipole and electric quadrupole moment we get:

$$\begin{aligned} j^\mu(\vec{q}) &= \chi^*_\alpha \widetilde{\Gamma}^{\alpha\beta\mu}\chi_\beta \\ &= -e\left[\chi^*\cdot\chi P^\mu F_1(Q^2) + (\chi^*\cdot q\chi^\mu - \chi\cdot q\chi^{*\mu})F_2(Q^2) - \frac{\chi^*\cdot q\,\chi\cdot qP^\mu}{2M^2}F_3(Q^2)\right]. \end{aligned} \tag{5.13}$$

Similarly the charge density and the 'magnetic density' can be expressed in terms of $2S+1$ multipole form factors $[G_{E0}(Q^2), G_{M1}(Q^2), \cdots]$, which are related to the electromagnetic moments:

$$e_0 = e\,G_{E0}(0), \tag{5.14a}$$
$$\mu = \frac{e}{2M} G_{M1}(0), \tag{5.14b}$$
$$Q = \frac{e}{M^2} G_{E2}(0). \tag{5.14c}$$

The multipole decomposition [31] reads:

$$j^0(\vec{q}) = e\left[G_{E0}(Q^2)\sqrt{4\pi}Y_{00}(\theta) - \frac{2}{3}\tau G_{E2}(Q^2)\sqrt{\frac{4\pi}{5}}Y_{20}(\theta) + \cdots\right], \tag{5.15a}$$
$$\vec{\Delta}\left(\vec{j}(\vec{q}) \times \vec{q}\right) = 2ie\sqrt{\tau}\left[G_{M1}(Q^2)\sqrt{\frac{4\pi}{3}}Y_{00}(\theta) + \cdots\right], \tag{5.15b}$$

with $\tau = Q^2/4M^2$.

Adopting the Breit frame, in which the photon transfers no energy ($q_0 = 0$), and inserting the spherical harmonics, a comparison between eqs. (5.15) and eq. (5.13) gives relations among multipole form factors and covariant vertex functions:

$$G_{E0}(Q^2) = \sqrt{1+\tau}F_1(Q^2) + 2/3\,\tau\, G_{E2}(Q^2), \tag{5.16a}$$
$$G_{M1}(Q^2) = \sqrt{1+\tau}F_2(Q^2), \tag{5.16b}$$
$$G_{E2}(Q^2) = \sqrt{1+\tau}\left[F_1(Q^2) - F_2(Q^2) + (1+\tau)F_3(Q^2)\right]. \tag{5.16c}$$

In the on-shell case these relations reduce to

$$G_{E0}(0) = F_1(0), \tag{5.17a}$$
$$G_{M1}(0) = F_2(0), \tag{5.17b}$$
$$G_{E2}(0) = F_1(0) - F_2(0) + F_3(0). \tag{5.17c}$$

The γWW vertex with all particles being on-shell reads as follows:

$$\Gamma^{\alpha\beta\mu} = -e\left[g^{\alpha\beta}P^\mu + (q^\alpha g^{\beta\mu} - q^\beta g^{\alpha\mu})(1+\ell_1) - \frac{l_2}{2M^2}q^\alpha q^\beta P^\mu\right]. \tag{5.18}$$

Thus at tree-level we can read of:

$$F_1(0) = 1, \tag{5.19a}$$
$$F_2(0) = 1 + \ell_1, \tag{5.19b}$$
$$F_3(0) = \ell_2, \tag{5.19c}$$

what corresponds to the following electromagnetic moments:

$$e_0 = e, \tag{5.20a}$$
$$\mu = \frac{e}{2M}(1+\ell_1) = \frac{e}{M}, \tag{5.20b}$$
$$Q = \frac{e}{M^2}(\ell_2 - \ell_1) = -\frac{e}{M^2}, \tag{5.20c}$$

where in the last step we have plugged in our model parameters in agreement with spin-1 QED ($\ell_1 = 1, \ell_2 = 0$) and achieved conformity with the natural values from eqs. (4.11).

At loop level in spin-1 QED the vertex has to be modified according to section 5.3:

$$\Gamma^{\alpha\beta\mu}_{(\text{loop})} = \frac{e^3}{(4\pi)^2}\left[\left(\frac{2}{3}+2L+4\ln w\right)g^{\alpha\beta}P^\mu + (8+4L+8\ln w)\left(q^\alpha g^{\beta\mu}-q^\beta g^{\alpha\mu}\right)+\frac{4}{9}\frac{q^\alpha q^\beta P^\mu}{2M^2}\right], \tag{5.21}$$

where L contains the ultra-violet divergence and is given explicitly by eq. (D.19). The term $\ln w$ denotes the infra-red divergence which is expected to be cancelling out in observables against the soft bremsstrahlung corrections. After the charge renormalisation, we can read off the $\mathcal{O}(\alpha)$ contributions to the covariant vertex functions:

$$F_1(0) = 0, \tag{5.22a}$$
$$F_2(0) = -\frac{5\alpha}{3\pi}, \tag{5.22b}$$
$$F_3(0) = \frac{\alpha}{9\pi}, \tag{5.22c}$$

what leads to the electromagnetic moments:

$$e_0 = e, \tag{5.23a}$$
$$\mu = \frac{e}{2M}(1+\ell_1) = \frac{e}{2M}\left(2-\frac{5\alpha}{3\pi}\right), \tag{5.23b}$$
$$Q = \frac{e}{M^2}(\ell_2-\ell_1) = -\frac{e}{M^2}\left(1-\frac{\alpha}{9\pi}-\frac{5\alpha}{3\pi}\right) = -\frac{e}{M^2}\left(1-\frac{16\alpha}{9\pi}\right), \tag{5.23c}$$

and the anomalous e.m. moments at one-loop level:

$$\kappa = \frac{M}{e}\mu - 1 = \frac{1}{2}(\ell_1-1) = -\frac{5\alpha}{6\pi}, \tag{5.24a}$$
$$\mathcal{Q} = \frac{M^2}{2e}Q + \frac{1}{2} = \frac{1}{2}(\ell_2-\ell_1+1) = \frac{8\alpha}{9\pi}. \tag{5.24b}$$

Inserting the fine-structure constant [39]

$$\alpha = 7.297\,352\,5698(24)\times 10^{-3} \approx \frac{1}{137}, \tag{5.25}$$

the QED one-loop corrections to the electromagnetic moments are:

$$\kappa \approx -1.936\times 10^{-3}, \tag{5.26a}$$
$$\mathcal{Q} \approx 2.065\times 10^{-3}. \tag{5.26b}$$

5.5. Ward-Takahashi Identity

In this section we test the consistency of the defined vertex functions and propagators by reproducing the appertaining Ward-Takahashi identities. For this purpose we give a short clarification of the Ward-Takahashi identities and the Ward identity.

Consider a QED process described by the scattering amplitude $\mathcal{A}(k) = \epsilon_\mu(k)\mathcal{A}^\mu(k)$. As one can see from the decomposition of the amplitude this process involves an external photon $\gamma(k)$. We introduce $\mathcal{A}_0$ as the analogously to $\mathcal{A}$ constructed amplitude but

without the mentioned photon. To recover $\mathcal{A}$ from $\mathcal{A}_0$ one has add up all diagrams contained in $\mathcal{A}_0$ every time modified by a photon at each possible insertion point.

$$\sum_{\text{insertion points}} k_\mu \left(\mu \; k \; \begin{array}{c} (p_1' \dots p_n') \\ \\ (p_1 \dots p_n) \end{array} \right) = e \sum_i \left(\begin{array}{c} (p_1' \dots (p_i' - k) \cdots) \\ \\ (p_1 \dots p_n) \end{array} - \begin{array}{c} (p_1' \dots p_n') \\ \\ (p_1 \dots (p_i + k) \cdots) \end{array} \right).$$

The Ward-Takahashi identity is illustrated in the above diagrammatic equation for a process with $2n$ external massive particles and an arbitrary number of external photons. The blobs in the Feynman diagrams should denote any particular diagram out of $\mathcal{A}_0$. On the left-hand side we sum over all possible insertion points, whereby only insertions at lines between external points give a non-vanishing contribution.

Let us calculate the Ward-Takahashi identities for the 3-point vertex:

$$\begin{aligned}
& p_\beta \Gamma^{\alpha\beta\mu} \\
&= -e\, p_\beta \left(g^{\alpha\beta} P^\mu - p'^\beta g^{\alpha\mu} - p^\alpha g^{\beta\mu} - q^\beta g^{\alpha\mu} + q^\alpha g^{\beta\mu} \right) \\
&= -e \left(p^\alpha P^\mu - p \cdot p' g^{\alpha\mu} - p^\alpha p^\mu - p \cdot q\, g^{\alpha\mu} + q^\alpha p^\mu \right) \\
&= -e \left(p^\alpha \left(p + p' \right)^\mu + (q - p)^\alpha p^\mu - p \cdot \left(p' + q \right) g^{\alpha\mu} \right) \\
&= -e \left(p^\alpha \left(\not{p} + p' \right)^\mu + (q - \not{p})^\alpha p^\mu - \left(p' - q \right) \cdot \left(p' + q \right) g^{\alpha\mu} \right) \\
&= -e \left(p^\alpha p'^\mu + q^\alpha p^\mu - p'^2 g^{\alpha\mu} + q^2 g^{\alpha\mu} \right) \\
&= -e \left(\left(p' - q \right)^\alpha p'^\mu + q^\alpha \left(p' - q \right)^\mu - p'^2 g^{\alpha\mu} + q^2 g^{\alpha\mu} \right) \\
&= -e \left(\left(p' - \not{q} \right)^\alpha p'^\mu + q^\alpha \left(\not{p}' - q \right)^\mu - p'^2 g^{\alpha\mu} + q^2 g^{\alpha\mu} \right) \\
&= -e \left(-p'^2 g^{\alpha\mu} + p'^\alpha p'^\mu + q^2 g^{\alpha\mu} - q^\alpha q^\mu \right) \\
&= e \left[\Delta^{-1}(q) - \Delta^{-1}(p') \right]^{\alpha\mu},
\end{aligned} \tag{5.27}$$

where we have introduced the inverse (massive) propagator

$$\left[\Delta^{-1}(l) \right]^{\rho\sigma} = (-l^2 + M^2) g^{\rho\sigma} + l^\rho l^\sigma. \tag{5.28}$$

The contraction of the 3-point vertex with p'_α and q_μ works analogously. Therefore only the results are printed:

$$p'_\alpha \Gamma^{\alpha\beta\mu} = e \left[\Delta^{-1}(q) - \Delta^{-1}(p) \right]^{\beta\mu}, \tag{5.29a}$$

$$p_\beta \Gamma^{\alpha\beta\mu} = e \left[\Delta^{-1}(q) - \Delta^{-1}(p') \right]^{\alpha\mu}, \tag{5.29b}$$

$$q_\mu \Gamma^{\alpha\beta\mu} = e \left[\Delta^{-1}(p') - \Delta^{-1}(p) \right]^{\alpha\beta}. \tag{5.29c}$$

One can also find a relation between the 3-point vertex function and the 4-point vertex function:

$$
\begin{aligned}
& e\left(\Gamma^{\alpha\beta\mu}(p,l)-\Gamma^{\alpha\beta\mu}(p',l')\right) \qquad (5.30)\\
&= -e^2\left(g^{\alpha\beta}P^{\mu}-l^{\beta}g^{\alpha\mu}-p^{\alpha}g^{\beta\mu}-\bar{q}^{\beta}g^{\alpha\mu}+\bar{q}^{\alpha}g^{\beta\mu}\right)\\
&\quad +e^2\left(g^{\alpha\beta}P'^{\mu}-l'^{\beta}g^{\alpha\mu}-p'^{\alpha}g^{\beta\mu}-\bar{q}^{\beta}g^{\alpha\mu}+\bar{q}^{\alpha}g^{\beta\mu}\right)\\
&= -e^2\left(g^{\alpha\beta}\left(P-P'\right)^{\mu}+\left(l'-l\right)^{\beta}g^{\alpha\mu}+\left(p'-p\right)^{\alpha}g^{\beta\mu}\right)\\
&= -e^2\left(g^{\alpha\beta}\left(p+l-p'-l'\right)^{\mu}+\underbrace{\left(l'-l\right)}_{=q}{}^{\beta}g^{\alpha\mu}+\underbrace{\left(p'-p\right)}_{=q}{}^{\alpha}g^{\beta\mu}\right)\\
&= e^2\left(2g^{\alpha\beta}q^{\mu}-g^{\alpha\mu}q^{\beta}-q^{\alpha}g^{\beta\mu}\right)\\
&= e^2q_{\nu}\left(2g^{\alpha\beta}g^{\mu\nu}-g^{\alpha\mu}g^{\beta\nu}-g^{\alpha\nu}g^{\beta\mu}\right)\\
&= q_{\nu}\Gamma^{\alpha\beta\mu\nu}.
\end{aligned}
$$

It is easy to contract the propagator with its inverse propagator:

$$
\begin{aligned}
& \Delta_{\rho\eta}(l)\left[\Delta^{-1}(l)\right]^{\eta\sigma} \qquad (5.31)\\
&= -\frac{1}{l^2-M^2}\left(g_{\rho\eta}-\frac{l_{\rho}l_{\eta}}{M^2}\right)\left[\left(-l^2+M^2\right)g^{\eta\sigma}+l^{\eta}l^{\sigma}\right]\\
&= -\frac{1}{l^2-M^2}\left[g_{\rho\eta}\left(\left(-l^2+M^2\right)g^{\eta\sigma}+l^{\eta}l^{\sigma}\right)-\frac{l_{\rho}l_{\eta}}{M^2}\left(\left(-l^2+M^2\right)g^{\eta\sigma}+l^{\eta}l^{\sigma}\right)\right]\\
&= -\frac{1}{l^2-M^2}\left[\left(-l^2+M^2\right)\delta_{\rho}^{\sigma}+l_{\rho}l^{\sigma}-\frac{l_{\rho}l^{\sigma}}{M^2}\left(-l^2+M^2\right)-\frac{l_{\rho}l^{\sigma}l^2}{M^2}\right]\\
&= -\frac{1}{l^2-M^2}\left[\left(-l^2+M^2\right)\delta_{\rho}^{\sigma}+l_{\rho}l^{\sigma}\left(1-\frac{\left(-l^2+M^2\right)}{M^2}-\frac{l^2}{M^2}\right)\right]\\
&= \delta_{\rho}^{\sigma},
\end{aligned}
$$

and obtain the following expression:

$$\Delta_{\rho\eta}(l)\left[\Delta^{-1}(l)\right]^{\eta\sigma}=\delta_{\rho}^{\sigma}, \qquad (5.32)$$

which verifies that these propagators are defined in a matching way.

5.5.1. Ward Identity

The Ward identity is a consequence of the more general Ward-Takahashi identity. For a physical process $\mathcal{A}(k)=\epsilon_{\mu}(k)\mathcal{A}^{\mu}(k)$ with all external particles on-shell one has:

$$k_{\mu}\mathcal{A}^{\mu}(k)=0. \qquad (5.33)$$

Here again $\mathcal{A}(k)$ describes a full process at a given order, meaning the Ward identity in general is not valid for single diagrams.

The validity of the Ward identity reflects the gauge symmetry of QED and the resulting current conservation $\delta_{\mu}j^{\mu}=0$. We have already proved the Ward identity for the Compton scattering process at tree-level, see eq. (5.6), and in the following we will see that a similar calculation can be made for the subset of one-loop tadpole diagrams. Here

one has to keep in mind that there is an integration over the internal momenta, which is abstracted below for reasons of simplicity:

$$
\begin{aligned}
& q_\nu \Big(\quad + \quad + \quad \Big)^\nu \qquad (5.34)\\
&= \chi^*_\alpha \, \varepsilon^*_\mu \, \Big(\Gamma^{\alpha\beta\rho\sigma} \, \Delta_{\rho\eta}(l_3) \, \Gamma^{\zeta\eta\mu}(l_3, l_2) \, \Delta_{\zeta\xi}(l_2) \, \Gamma^{\tau\xi\nu}(l_2, l_1) \, \Delta_{\sigma\tau}(l_1) \\
&\quad + \Gamma^{\alpha\beta\rho\sigma} \, \Delta_{\rho\eta}(l_6) \, \Gamma^{\zeta\eta\nu}(l_6, l_5) \, \Delta_{\zeta\xi}(l_5) \, \Gamma^{\tau\xi\mu}(l_5, l_4) \, \Delta_{\sigma\tau}(l_4) \\
&\quad + \Gamma^{\alpha\beta\rho\sigma} \, \Delta_{\rho\eta}(l_8) \, \Delta_{\sigma\tau}(l_7) \, \Gamma^{\tau\eta\mu\nu} \Big) \; q_\nu \, \chi_\beta \\
&= \Bigg(\Gamma^{\alpha\beta\rho\sigma} \, \Delta_{\rho\eta}(l_3) \, \Gamma^{\zeta\eta\mu}(l_3, l_2) \, \Delta_{\zeta\xi}(l_2) \underbrace{q_\nu \, \Gamma^{\tau\xi\nu}(l_2, l_1)}_{= e \, [\Delta^{-1}(l_1) - \Delta^{-1}(l_2)]^{\tau\xi}} \Delta_{\sigma\tau}(l_1) \\
&\quad + \Gamma^{\alpha\beta\rho\sigma} \, \Delta_{\rho\eta}(l_6) \underbrace{q_\nu \, \Gamma^{\zeta\eta\nu}(l_6, l_5)}_{= e \, [\Delta^{-1}(l_5) - \Delta^{-1}(l_6)]^{\zeta\eta}} \Delta_{\zeta\xi}(l_5) \, \Gamma^{\tau\xi\mu}(l_5, l_4) \, \Delta_{\sigma\tau}(l_4) \\
&\quad + \Gamma^{\alpha\beta\rho\sigma} \, \Delta_{\rho\eta}(l_8) \, \Delta_{\sigma\tau}(l_7) \, q_\nu \, \Gamma^{\tau\eta\mu\nu} \Big) \; \chi^*_\alpha \, \varepsilon^*_\mu \, \chi_\beta \\
&= e \, \Big(\Gamma^{\alpha\beta\rho\sigma} \, \Delta_{\rho\eta}(l_3) \, \Gamma^{\zeta\eta\mu}(l_3, l_2) \, \Delta_{\zeta\xi}(l_2) \, [\Delta^{-1}(l_1) - \Delta^{-1}(l_2)]^{\tau\xi} \, \Delta_{\sigma\tau}(l_1) \\
&\quad + \Gamma^{\alpha\beta\rho\sigma} \, \Delta_{\rho\eta}(l_6) \, [\Delta^{-1}(l_5) - \Delta^{-1}(l_6)]^{\zeta\eta} \, \Delta_{\zeta\xi}(l_5) \, \Gamma^{\tau\xi\mu}(l_5, l_4) \, \Delta_{\sigma\tau}(l_4) \\
&\quad + \frac{1}{e} \, \Gamma^{\alpha\beta\rho\sigma} \, \Delta_{\rho\eta}(l_8) \, \Delta_{\sigma\tau}(l_7) \, q_\nu \, \Gamma^{\tau\eta\mu\nu} \Big) \; \chi^*_\alpha \, \varepsilon^*_\mu \, \chi_\beta \\
&= e \, \Big(\Gamma^{\alpha\beta\rho\sigma} \, \Delta_{\rho\eta}(l_3) \, \Gamma^{\tau\eta\mu}(l_3, l_2) \, \Delta_{\sigma\tau}(l_2) \\
&\quad - \Gamma^{\alpha\beta\rho\sigma} \, \Delta_{\rho\eta}(l_3) \, \Gamma^{\tau\eta\mu}(l_3, l_2) \, \Delta_{\sigma\tau}(l_1) \\
&\quad + \Gamma^{\alpha\beta\rho\sigma} \, \Delta_{\rho\eta}(l_6) \, \Gamma^{\tau\eta\mu}(l_5, l_4) \, \Delta_{\sigma\tau}(l_4) \\
&\quad - \Gamma^{\alpha\beta\rho\sigma} \, \Delta_{\rho\eta}(l_5) \, \Gamma^{\tau\eta\mu}(l_5, l_4) \, \Delta_{\sigma\tau}(l_4) \\
&\quad + \frac{1}{e} \, \Gamma^{\alpha\beta\rho\sigma} \, \Delta_{\rho\eta}(l_8) \, \Delta_{\sigma\tau}(l_7) \, q_\nu \, \Gamma^{\tau\eta\mu\nu} \Big) \; \chi^*_\alpha \, \varepsilon^*_\mu \, \chi_\beta \\
&= e \, \Big(\Gamma^{\alpha\beta\rho\sigma} \, \Delta_{\rho\eta}(l_3) \, \Gamma^{\tau\eta\mu}(l_3, l_3 - q') \, \Delta_{\sigma\tau}(l_3 - q') \\
&\quad - \Gamma^{\alpha\beta\rho\sigma} \, \Delta_{\rho\eta}(l_3) \, \Gamma^{\tau\eta\mu}(l_3, l_2) \, \Delta_{\sigma\tau}(l_1) \\
&\quad + \Gamma^{\alpha\beta\rho\sigma} \, \Delta_{\rho\eta}(l_6) \, \Gamma^{\tau\eta\mu}(l_5, l_4) \, \Delta_{\sigma\tau}(l_4) \\
&\quad - \Gamma^{\alpha\beta\rho\sigma} \, \Delta_{\rho\eta}(l_5) \, \Gamma^{\tau\eta\mu}(l_5, l_5 - q') \, \Delta_{\sigma\tau}(l_5 - q') \\
&\quad + \frac{1}{e} \, \Gamma^{\alpha\beta\rho\sigma} \, \Delta_{\rho\eta}(l_8) \, \Delta_{\sigma\tau}(l_7) \, q_\nu \, \Gamma^{\tau\eta\mu\nu} \Big) \; \chi^*_\alpha \, \varepsilon^*_\mu \, \chi_\beta \\
&= \{\text{the first and the forth summand cancel each other}\} \\
&= e \, \Big(- \Gamma^{\alpha\beta\rho\sigma} \, \Delta_{\rho\eta}(l_3) \, \Gamma^{\tau\eta\mu}(l_3, l_3 - q') \, \Delta_{\sigma\tau}(l_3 + p' - p) \\
&\quad + \Gamma^{\alpha\beta\rho\sigma} \, \Delta_{\rho\eta}(l_6) \, \Gamma^{\tau\eta\mu}(l_6 + q, l_6 + p' - p) \, \Delta_{\sigma\tau}(l_6 + p' - p) \\
&\quad + \frac{1}{e} \, \Gamma^{\alpha\beta\rho\sigma} \, \Delta_{\rho\eta}(l_8) \, \Delta_{\sigma\tau}(l_8 + p' - p) \, q_\nu \, \Gamma^{\tau\eta\mu\nu} \Big) \; \chi^*_\alpha \, \varepsilon^*_\mu \, \chi_\beta \\
&= \{\text{rename the integration variables}\}
\end{aligned}
$$

$$
\begin{aligned}
&= \Bigg(\Gamma^{\alpha\beta\rho\sigma}\,\Delta_{\rho\eta}(l)\,\underbrace{e\,\Big(\Gamma^{\tau\eta\mu}(l+q,l+p'-p)-\Gamma^{\tau\eta\mu}(l,l-q')\Big)}_{=-q_\nu\Gamma^{\tau\eta\mu\nu}}\,\Delta_{\sigma\tau}(l+p'-p) \\
&\quad + \Gamma^{\alpha\beta\rho\sigma}\,\Delta_{\rho\eta}(l)\,\Delta_{\sigma\tau}(l+p'-p)\,q_\nu\,\Gamma^{\tau\eta\mu\nu}\Bigg)\;\chi^*_\alpha\,\varepsilon^*_\mu\,\chi_\beta \\
&= 0.
\end{aligned}
$$

Along the same way one obtains:

$$
q'_\mu \left(\quad + \quad + \quad \right)^\mu = 0, \tag{5.35}
$$

what is reasonable by symmetry.
The off-shell vertex modifications are related to the self-energy:

$$
q_\nu \left(\quad + \quad + \quad \right)^\nu \tag{5.36}
$$

$$
\begin{aligned}
&= \chi^*_\alpha \Big(\Gamma^{\alpha\rho\sigma}(p'-k,p')\,\Delta_{\rho\eta}(p'-k)\,D_{\sigma\tau}(k)\,\Gamma^{\eta\beta\tau\nu} \\
&\quad + \Gamma^{\alpha\zeta\sigma\nu}\,\Delta_{\zeta\xi}(p-k)\,D_{\sigma\tau}(k)\,\Gamma^{\xi\beta\tau}(p,p-k) \\
&\quad + \Gamma^{\alpha\rho\sigma}(p'-k,p')\,\Delta_{\rho\eta}(p'-k)\,D_{\sigma\tau}(k)\,\Gamma^{\eta\zeta\nu}(p-k,p'-k)\times \\
&\qquad \Delta_{\zeta\xi}(p-k)\,\Gamma^{\xi\beta\tau}(p,p-k)\Big)\;q_\nu\,\chi_\beta \\
&= \Bigg(\Gamma^{\alpha\rho\sigma}(p'-k,p')\,\Delta_{\rho\eta}(p'-k)\,D_{\sigma\tau}(k)\,\underbrace{q_\nu\,\Gamma^{\eta\beta\tau\nu}}_{=e\left(\Gamma^{\eta\beta\tau}(p,p-k)-\Gamma^{\eta\beta\tau}(p',p'-k)\right)} \\
&\quad + \underbrace{q_\nu\,\Gamma^{\alpha\zeta\sigma\nu}}_{=e\left(\Gamma^{\alpha\zeta\sigma}(p-k,p)-\Gamma^{\alpha\zeta\sigma}(p'-k,p')\right)}\,\Delta_{\zeta\xi}(p-k)\,D_{\sigma\tau}(k)\,\Gamma^{\xi\beta\tau}(p,p-k) \\
&\quad + \Gamma^{\alpha\rho\sigma}(p'-k,p')\,\Delta_{\rho\eta}(p'-k)\,D_{\sigma\tau}(k)\,\underbrace{q_\nu\,\Gamma^{\eta\zeta\nu}(p-k,p'-k)}_{=e[\Delta^{-1}(p'-k)-\Delta^{-1}(p-k)]^{\eta\zeta}}\times \\
&\qquad \Delta_{\zeta\xi}(p-k)\,\Gamma^{\xi\beta\tau}(p,p-k)\Bigg)\,\chi^*_\alpha\chi_\beta \\
&= e\Big(\Gamma^{\alpha\rho\sigma}(p'-k,p')\,\Delta_{\rho\eta}(p'-k)\,D_{\sigma\tau}(k)\,\Big(\Gamma^{\eta\beta\tau}(p,p-k)-\Gamma^{\eta\beta\tau}(p',p'-k)\Big) \\
&\quad + \Big(\Gamma^{\alpha\zeta\sigma}(p-k,p)-\Gamma^{\alpha\zeta\sigma}(p'-k,p')\Big)\,\Delta_{\zeta\xi}(p-k)\,D_{\sigma\tau}(k)\,\Gamma^{\xi\beta\tau}(p,p-k) \\
&\quad + \Gamma^{\alpha\rho\sigma}(p'-k,p')\,\Delta_{\rho\eta}(p'-k)\,D_{\sigma\tau}(k)\,[\Delta^{-1}(p'-k)-\Delta^{-1}(p-k)]^{\eta\zeta}\times \\
&\qquad \Delta_{\zeta\xi}(p-k)\,\Gamma^{\xi\beta\tau}(p,p-k)\Big)\;\chi^*_\alpha\chi_\beta \\
&= e\Big(\Gamma^{\alpha\rho\sigma}(p'-k,p')\,\Delta_{\rho\eta}(p'-k)\,D_{\sigma\tau}(k)\,\Gamma^{\eta\beta\tau}(p,p-k) \\
&\quad - \Gamma^{\alpha\rho\sigma}(p'-k,p')\,\Delta_{\rho\eta}(p'-k)\,D_{\sigma\tau}(k)\,\Gamma^{\eta\beta\tau}(p',p'-k) \\
&\quad + \Gamma^{\alpha\zeta\sigma}(p-k,p)\,\Delta_{\zeta\xi}(p-k)\,D_{\sigma\tau}(k)\,\Gamma^{\xi\beta\tau}(p,p-k) \\
&\quad - \Gamma^{\alpha\zeta\sigma}(p'-k,p')\,\Delta_{\zeta\xi}(p-k)\,D_{\sigma\tau}(k)\,\Gamma^{\xi\beta\tau}(p,p-k) \\
&\quad + \Gamma^{\alpha\rho\sigma}(p'-k,p')\,D_{\sigma\tau}(k)\,\Delta_{\rho\xi}(p-k)\,\Gamma^{\xi\beta\tau}(p,p-k) \\
&\quad - \Gamma^{\alpha\rho\sigma}(p'-k,p')\,\Delta_{\rho\xi}(p'-k)\,D_{\sigma\tau}(k)\,\Gamma^{\xi\beta\tau}(p,p-k)\Big)\;\chi^*_\alpha\chi_\beta
\end{aligned}
$$

$$
\begin{aligned}
&= e \Big(\Gamma^{\alpha\rho\sigma}(p'-k,p')\,\Delta_{\rho\eta}(p'-k)\,D_{\sigma\tau}(k)\,\Gamma^{\eta\beta\tau}(p,p-k) \\
&\quad - \Gamma^{\alpha\rho\sigma}(p'-k,p')\,\Delta_{\rho\eta}(p'-k)\,D_{\sigma\tau}(k)\,\Gamma^{\eta\beta\tau}(p',p'-k) \\
&\quad + \Gamma^{\alpha\rho\sigma}(p-k,p)\,\Delta_{\rho\eta}(p-k)\,D_{\sigma\tau}(k)\,\Gamma^{\eta\beta\tau}(p,p-k) \\
&\quad - \Gamma^{\alpha\rho\sigma}(p'-k,p')\,\Delta_{\rho\eta}(p-k)\,D_{\sigma\tau}(k)\,\Gamma^{\eta\beta\tau}(p,p-k) \\
&\quad + \Gamma^{\alpha\rho\sigma}(p'-k,p')\,\Delta_{\rho\eta}(p-k)\,D_{\sigma\tau}(k)\,\Gamma^{\eta\beta\tau}(p,p-k) \\
&\quad - \Gamma^{\alpha\rho\sigma}(p'-k,p')\,\Delta_{\rho\eta}(p'-k)\,D_{\sigma\tau}(k)\,\Gamma^{\eta\beta\tau}(p,p-k) \Big)\ \chi^*_\alpha\chi_\beta \\
&= e \Big(-\Gamma^{\alpha\rho\sigma}(p'-k,p')\,\Delta_{\rho\eta}(p'-k)\,D_{\sigma\tau}(k)\,\Gamma^{\eta\beta\tau}(p',p'-k) \\
&\quad + \Gamma^{\alpha\rho\sigma}(p-k,p)\,\Delta_{\rho\eta}(p-k)\,D_{\sigma\tau}(k)\,\Gamma^{\eta\beta\tau}(p,p-k) \Big)\ \chi^*_\alpha\chi_\beta \\
&= e \Big(\Sigma^{\alpha\beta}(p) - \Sigma^{\alpha\beta}(p') \Big)\ \chi^*_\alpha\chi_\beta,
\end{aligned}
$$

with the self-energy

$$
\Sigma^{\alpha\beta} = \Gamma^{\alpha\rho\sigma}(p-k,p)\,\Delta_{\rho\eta}(p-k)\,D_{\sigma\tau}(k)\,\Gamma^{\eta\beta\tau}(p,p-k). \tag{5.37}
$$

In this section we proved the Ward-Takahashi identities, which link on the one hand the 3-point vertex and the massive spin-1 propagator and on the other hand the 4-point and 3-point vertices. Also, we proved that we have defined the propagator and its inverse in a matching way. We showed that the tadpole diagrams bild a current conserving set of diagrams. Finally, we saw that the sum of off-shell vertex modifications $\widetilde{\Gamma}^{\alpha\beta\mu}(p,p')$ (in the absense of the tadpole-vertex correction) is related to a difference of self-energies. Whereby the self-energies are propagator corrections to the massive vertex legs with momenta p and p'. This difference vanishes in the on-shell case, what indicates that the sum of vertex modifications bilds a current conserving set of diagrams, too.

CHAPTER 6

VERIFICATION OF THE SPIN-1 SUM RULES

Both sides of the sum rules should agree at every order of the perturbative expansion. In this chapter all the previously obtained results are gathered in order to verify the spin-1 sum rules at one-loop level.

6.1. Compton Scattering Amplitude

In the previous chapter, we have presented the analysis of the forward Compton scattering off massive vector bosons in spin-1 QED. Here we present the real parts of the scalar amplitudes for the one-loop diagrams. In all the following expressions the overall factor e^4 is omitted for brevity. Below we only give the results as a series expansion around $\nu = 0$. The exact results are given in the appendix B.

$$\begin{aligned}\operatorname{Re} F_0(\nu) = {} & \frac{-89 + 21L - 36\ln w}{72\pi^2} + \frac{5 + 24\ln\frac{2\nu}{M}}{18M^2\pi^2}\,\nu^2 \\ & + \frac{4\left(62 + 190\ln\frac{2\nu}{M}\right)}{75M^4\pi^2}\,\nu^4 + \frac{2\left(1223 + 5208\ln\frac{2\nu}{M}\right)}{147M^6\pi^2}\,\nu^6 + \mathcal{O}(\nu^7),\end{aligned} \tag{6.1a}$$

$$\begin{aligned}\operatorname{Re} F_1(\nu) = {} & \frac{41 + 60\ln\frac{2\nu}{M}}{18\pi^2M^3}\,\nu^2 + \frac{32\left(116 + 270\ln\frac{2\nu}{M}\right)}{225\pi^2M^5}\,\nu^4 \\ & + \frac{2\left(2533 + 7896\ln\frac{2\nu}{M}\right)}{49\pi^2M^7}\,\nu^6 + \mathcal{O}(\nu^7),\end{aligned} \tag{6.1b}$$

$$\begin{aligned}\operatorname{Re} F_2(\nu) = {} & \frac{83 - 39L}{72\pi^2}\frac{1}{\nu^2} + \frac{1}{M^2\pi^2} + \frac{7\left(11 + 20\ln\frac{2\nu}{M}\right)}{25\pi^2M^4}\,\nu^2 \\ & + \frac{4\left(2851 + 6552\ln\frac{2\nu}{M}\right)}{441\pi^2M^6}\,\nu^4 + \frac{4\left(29459 + 86760\ln\frac{2\nu}{M}\right)}{675\pi^2M^8}\,\nu^6 \\ & + \mathcal{O}(\nu^7),\end{aligned} \tag{6.1c}$$

$$\begin{aligned}\operatorname{Re} F(\nu) = {} & \frac{-101 - 15L - 108\ln w}{216\pi^2} + \frac{17 + 24\ln\frac{2\nu}{M}}{18\pi^2M^2}\,\nu^2 \\ & + \frac{2\left(201 + 520\ln\frac{2\nu}{M}\right)}{75\pi^2M^4}\,\nu^4 + \frac{2\left(22411 + 73080\ln\frac{2\nu}{M}\right)}{1323\pi^2M^6}\,\nu^6 \\ & + \mathcal{O}(\nu^7),\end{aligned} \tag{6.1d}$$

$$\operatorname{Re} G(\nu) = \frac{1}{3M^2\pi^2}\,\nu^2 + \frac{8(11+12\ln\frac{2\nu}{M})}{9\pi^2M^4}\,\nu^4 + \frac{4(59+120\ln\frac{2\nu}{M})}{3\pi^2M^6}\,\nu^6 + \mathcal{O}(\nu^7). \tag{6.1e}$$

The amplitudes contain ultra-violet divergences (L) and infra-red divergences ($\ln w$). Appendix D covers the dimensional regularization used to calculate the loop integrals and explains the origin of these divergences.

In the sum of amplitudes describing the Compton scattering process each s-channel diagram goes with a corresponding u-channel diagram. The sum of s- and u-channel diagrams is naturally invariant under photon 'crossing' ($\epsilon \leftrightarrow \epsilon^*$ and $\nu \leftrightarrow -\nu$) and the seagull diagrams are by themselves invariant under 'crossing', see eq. (C.8). From this 'crossing' symmetry one would expect the real parts of the scalar amplitudes to be even with respect to the photon energy ν and so they are.

6.2. Verification of the Optical Theorem

The integrands of the sum rules contain the tree-level cross-sections given in section 2.3 and the following cross-section combinations:

$$\begin{aligned}\Delta\sigma(\nu) &= \sigma_2(\nu) - \sigma_0(\nu) && \text{(6.2a)}\\ &= -\frac{15M^3+81M^2\nu+142M\nu^2+76\nu^3}{6\pi M\nu(M+2\nu)^3} + \frac{5M+2\nu}{4\pi M\nu^2}\ln\left[1+\frac{2\nu}{M}\right],\\ \sigma_Q(\nu) &= \sigma_0(\nu)+\sigma_2(\nu)-2\,\sigma_1(\nu) && \text{(6.2b)}\\ &= \frac{18M^5+99M^4\nu+183M^3\nu^2+132M^2\nu^3+52M\nu^4+24\nu^5}{6\pi M^2\nu^2(M+2\nu)^3}\\ &\quad - \frac{6M^2+3M\nu+2\nu^2}{4\pi M\nu^3}\ln\left[1+\frac{2\nu}{M}\right].\end{aligned}$$

With all QED results given one can easily check the optical theorem, see eqs. (4.4, 4.6, 4.7), by comparing the cross-sections with the results for the imaginary parts of the scalar amplitudes, see eqs. (B.2, B.4, B.6, B.8) in the appendix B.

6.3. No-Subtraction Hypothesis

In the dispersion relation derivation (section 2.4) we made the assumption that the scattering amplitudes $f(\nu)$ tend to zero for large energies, see eq. (2.50), and as a result the integration over the large semicircles vanishes. This assumption we called the no-subtraction hypothesis. As shown in [40] the no-subtraction hypothesis is warranted, for example, for quadratically integrable functions:

$$\int_{-\infty}^{\infty} |f(\nu)|^2 d\nu < C_1 \qquad \text{with constant } C_1. \tag{6.3}$$

In contrast, it is not sufficient that the function is bound:

$$|f(\nu)|^2 \le C_2 \qquad \text{with constant } C_2, \tag{6.4}$$

for completely determining $\operatorname{Re} f(\nu)$ as a function of $\operatorname{Im} f(\nu)$ by eq. (2.49). We therefore define then a quadratically integrable function

$$D(\nu) = \frac{f(\nu) - f(\hat{\nu})}{\nu - \hat{\nu}}, \tag{6.5}$$

whereby f should be bound and differentiable at $\hat{\nu}$. As one can show this function fulfills a dispersion relation:

$$D(\nu) = \frac{1}{i\pi} \fint_{-\infty}^{\infty} \frac{d\nu'}{\nu' - \nu} D(\nu'), \tag{6.6}$$

which equals:

$$f(\nu) = f(\hat{\nu}) + \frac{\nu - \hat{\nu}}{i\pi} \fint_{-\infty}^{\infty} \frac{d\nu'}{\nu' - \nu} \frac{f(\nu') - f(\hat{\nu})}{\nu' - \hat{\nu}}. \tag{6.7}$$

We call this a subtracted dispersion relation.

The dashed integrals denote Cauchy's principal value:

$$\fint_{-\infty}^{\infty} = \lim_{\epsilon \to 0^+} \left(\int_{-\infty}^{\nu-\epsilon} + \int_{\nu+\epsilon}^{\infty} \right). \tag{6.8}$$

At this point we want check if the large energy behaviour of our scattering amplitudes warrants the no-subtraction hypotheses. Therefore we calculate their limits $\nu \to \infty$, as explained in section 2.4:

$$\lim_{\nu\to\infty} F_0(\nu) = -\frac{77 - 21L + 36 \ln \frac{2\nu}{M} + 36 \ln w}{72\pi^2} + i\frac{1}{4\pi}, \tag{6.9a}$$

$$\lim_{\nu\to\infty} F_1(\nu) = 0, \tag{6.9b}$$

$$\lim_{\nu\to\infty} F_2(\nu) = -\frac{13L}{24\pi^2}\frac{1}{\nu^2}\Big|_{\nu\to\infty}, \tag{6.9c}$$

$$\lim_{\nu\to\infty} G(\nu) = -\frac{1}{6\pi^2}. \tag{6.9d}$$

The scalar amplitudes $F_0(\nu)$ and $F_2(\nu)$ contain divergences in the first terms of their energy expansion and for $G(\nu)$ the integration over the semicircles is non-vanishing and hence subtracted dispersion relations are needed. In these cases we choose $\hat{\nu} = 0$ to formulate subtracted dispersion relations analogously to eq. (6.7).

6.4. Verification of the Dispersion Relations

6.4.1. Real Parts

For F, G and F_0 we write down the following subtracted dispersion relation:

$$\operatorname{Re} \overline{F}(\nu) = \operatorname{Re} F(\nu) - \operatorname{Re} F(0) = \frac{2}{\pi} \int_0^{\infty} d\nu' \operatorname{Im} F(\nu') \frac{1}{\nu'^2 - \nu^2} \frac{\nu^2}{\nu'}. \tag{6.10}$$

For F_2 we have

$$\operatorname{Re} \overline{F}_2(\nu) = \operatorname{Re} F_2(\nu) - \frac{1}{\nu^2}\Big[\nu^2 \operatorname{Re} F_2(\nu)\Big]_{\nu=0} = \frac{2}{\pi} \int_0^{\infty} d\nu' \operatorname{Im} F_2(\nu') \frac{1}{\nu'^2 - \nu^2} \nu'. \tag{6.11}$$

Given the scalar amplitudes, eqs. (B.1, B.3, B.5, B.7), one can test that they indeed fulfill the expected dispersion relations.

6.4.2. Imaginary Parts

Reading the dispersion relation

$$\mathrm{Re}\, f_n(\nu) = \frac{2}{\pi}\int_0^\infty d\nu' \frac{\nu'}{\nu'^2 - \nu^2}\ \mathrm{Im}\, f_n(\nu') \tag{6.12}$$

one would expect that the solution of the integral is purely real, which is not true. Strictly one would have to write:

$$\mathrm{Re}\, f_n(\nu) = \mathrm{Re}\left[\frac{2}{\pi}\int_0^\infty d\nu' \frac{\nu'}{\nu'^2 - \nu^2 - i0^+}\ \mathrm{Im}\, f_n(\nu')\right], \tag{6.13}$$

which is refrained from for brevity. Even more

$$f_n(\nu) = \frac{2}{\pi}\int_0^\infty d\nu' \frac{\nu'}{\nu'^2 - \nu^2 - i0^+}\ \mathrm{Im}\, f_n(\nu') \tag{6.14}$$

would be correct. This becomes clear by looking back to section 2.4, where we have derived the dispersion relation. In the end we have performed the naive limit to the real axis. Using the Sokhotski-Plemelj theorem:

$$\lim_{\epsilon\to 0^+}\int_a^b \frac{f(x)}{x \pm i\epsilon}dx = \fint_a^b \frac{f(x)}{x}dx \mp i\pi f(0), \tag{6.15}$$

the limit would read

$$f(\nu) = \lim_{\eta\to 0^+} f(\nu_+) = \frac{1}{\pi}\int_{-\infty}^\infty d\nu' \frac{\mathrm{Im}\, f(\nu')}{\nu' - \nu - i0^+} = \frac{1}{\pi}\fint_{-\infty}^\infty d\nu' \frac{\mathrm{Im}\, f(\nu')}{\nu' - \nu} + i\,\mathrm{Im}\, f(\nu). \tag{6.16}$$

The dispersion relation provides a consistent contribution of the imaginary on both sides of the relation, which can easily be seen from the following:

$$\begin{aligned} f_n(\nu) &= \lim_{\epsilon\to 0^+}\frac{2}{\pi}\int_0^\infty d\nu' \frac{\nu'}{\nu'^2 - \nu^2 - i\epsilon}\ \mathrm{Im}\, f_n(\nu') \\ &= \lim_{\epsilon\to 0^+}\frac{2}{\pi}\int_0^\infty d\nu' \frac{\nu'(\nu'^2 - \nu^2 + i\epsilon)}{(\nu'^2 - \nu^2)^2 + \epsilon^2}\ \mathrm{Im}\, f_n(\nu') \\ \Rightarrow \mathrm{Im}\, f_n(\nu) &= \lim_{\epsilon\to 0^+}\frac{2\epsilon}{\pi}\int_0^\infty d\nu' \frac{\nu'}{(\nu'^2 - \nu^2)^2 + \epsilon^2}\ \mathrm{Im}\, f_n(\nu'). \end{aligned} \tag{6.17}$$

Now one can identify a nascent delta function:

$$\eta_\epsilon(x) = \frac{\epsilon}{\pi}\frac{1}{x^2 + \epsilon^2}, \tag{6.18}$$

which in the limiting case ($\epsilon \to 0^+$) becomes a Dirac delta function:

$$\delta(x) = \lim_{\epsilon\to 0^+}\eta_\epsilon(x). \tag{6.19}$$

Inserting this delta function in eq. (6.17) and using eq. (2.35) we obtain:

$$\begin{aligned}\operatorname{Im} f_n(\nu) &= \lim_{\epsilon\to 0^+} 2\int_0^\infty d\nu' \eta(\nu'^2-\nu^2)\ \nu'\ \operatorname{Im} f_n(\nu') \\ &= 2\int_0^\infty d\nu' \delta(\nu'^2-\nu^2)\ \nu'\ \operatorname{Im} f_n(\nu') \\ &= 2\int_0^\infty d\nu' \frac{1}{2\nu}\left[\delta(\nu'+\nu)+\delta(\nu'-\nu)\right]\ \nu'\ \operatorname{Im} f_n(\nu').\end{aligned} \tag{6.20}$$

Because the photon energy ν is positive, only one delta functions contributes, and hence the left- and right-hand-side coincide.

6.5. Verification of the GDH Sum Rule

The GDH sum rule can be easily verified at $\mathcal{O}(\alpha^2)$. The anomalous magnetic dipole moment κ is proportional to the fine-structure constant $\alpha = e^2/4\pi$ and the tree-level cross-sections are of order α^2. Hence the sum rule value on the lhs of the equation is vanishing up to $\mathcal{O}(\alpha^3)$. This means that the $\mathcal{O}(\alpha^2)$ integral on the rhs should also vanish, and so it does:

$$0+\mathcal{O}(\alpha^3) = \frac{e^2}{M^2}\kappa^2 = \frac{1}{\pi}\int_0^\infty d\nu\ \frac{\Delta\sigma(\nu)}{\nu} = 0+\mathcal{O}(\alpha^3). \tag{6.21}$$

6.6. Verification of Sum Rules and the Infra-red Cutoff

For the scalar Baldin sum rule eq. (3.19) we had to introduce an infra-red cutoff. In spin-1 QED we also find some coefficients of the low-energy expanded sum rules to be logarithmically divergent as ν goes to the QED production threshold 0. Just as for the scalar QED sum rule, we find that for the spin-1 sum rules the low-energy expansion of the rhs is quantitatively consistent with the expansion of the lhs when we introduce an infra-red cutoff equal to the photon energy ν. The following sum rules hold provided the cutoff is applied:

- F_0 sum rule

$$-\frac{e^2}{M^3}\kappa\,(\kappa+\mathcal{Q}) + \frac{\pi}{M}\left[a_1+b_1-\frac{2}{3}(a_2+b_2)\right] = \frac{1}{\pi}\int_\nu^\infty d\nu'\ \frac{\sigma_1(\nu')-\sigma(0)}{\nu'^2}, \tag{6.22}$$

- FSP sum rule

$$\frac{e^2}{4M^4}(\kappa+\mathcal{Q})^2 - \frac{2\pi}{M}(\gamma_E+\gamma_B) = \frac{1}{\pi}\int_\nu^\infty d\nu'\ \frac{\Delta\sigma(\nu')-\frac{2\nu'}{M}\sigma(0)}{\nu'^3}, \tag{6.23}$$

- Baldin sum rule

$$\frac{\pi}{M}(a_1+b_1) = \frac{1}{\pi}\int_\nu^\infty d\nu'\ \frac{\sigma(\nu')-\sigma(0)}{\nu'^2}, \tag{6.24}$$

6.7. Identification of the Polarizabilities

Because the anomalous e.m. moments of the W-boson are vanishing at tree-level and hence proportional to α, the anomalous e.m. moments contributions to the low-energy

theorem are always vanishing up to $\mathcal{O}(\alpha^3)$. So, the $\mathcal{O}(\alpha^2)$ contributions to low-energy part of the scattering amplitudes must be connected to polarizabilities. An investigation of the sum rule values read off from the scalar amplitudes and the way in which they appear as prefactors of polarization vector combinations in the scattering amplitude, see eq. (4.18), showed that at least four polarizabilities were necessary for our sum rules. From the proposed sum rules only the GDH sum rule is free of polarizability contributions.

The polarizability Lagrangian describes these multipole interactions:

$$\begin{aligned}\mathcal{L}_{\text{Pol.}} = -H =& 2\pi(a_1\vec{E}^2 + b_1\vec{B}^2 + a_2 E^i E^j X_{ij} + b_2 B^i B^j X_{ij} \\ &+ 2\gamma_E \dot{E}^i E^j X_{ij} + 2\gamma_B \dot{B}^i B^j X_{ij}),\end{aligned} \tag{6.25}$$

with $X_{ij} = \frac{4}{3}\delta_{ij} - \{S_i, S_j\}$ and the spin operators $\mathcal{S}$. From this we can identify the forward spin polarizability:

$$\gamma_0 = \frac{\alpha^2}{18\pi M^4}\left(41 + 60\ln\frac{2\nu}{M}\right), \tag{6.26}$$

the sum of electric and magnetic dipole polarizabilities:

$$\alpha_{E1} + \beta_{M1} = \frac{\alpha^2}{9\pi M^3}\left(17 + 24\ln\frac{2\nu}{M}\right), \tag{6.27}$$

and the electric and magnetic quadrupole polarizabilities:

$$\alpha_{E2} = \frac{8\,\alpha^2}{3\pi M^3}, \tag{6.28a}$$

$$\beta_{M2} = \frac{4\,\alpha^2}{3\pi M^3}. \tag{6.28b}$$

The extracted polarizabilities have the expected mass dimensions. The forward spin polarizability and the sum of electric and magnetic dipole polarizabilities are 'dynamical' and carry a residual dependence on the energy.

6.8. δSum Rules

To study the δsum rules we calculate the scattering amplitude and tree-level cross-sections including an additional anomalous magnetic dipole moment term from eq. (4.39). This anomalous magnetic moment term is sometimes referred to as the Corben-Schwinger term [34, 35].

The scalar amplitudes are given in the appendix B. It is striking that they contain divergences at higher orders in the ν expansion.

In what follows we give the spin-1 δsum rules and the pertinent derivatives of the cross-sections:

- δF_0 sum rule

$$-\frac{e^2}{M^3}(2\kappa + \mathcal{Q}) + \frac{\pi}{M}\left[a_1' + b_1' - \frac{2}{3}(a_2' + b_2')\right] = \frac{1}{\pi}\int_0^\infty \frac{d\nu}{\nu^2}\,\sigma_{1,\kappa_0}(\nu), \tag{6.29}$$

$$\text{with} \quad \sigma_{1,\kappa_0}(\nu) = -\frac{12M^3+39M^2\nu+22M\nu^2-13\nu^3}{6\pi M\nu^2(M+2\nu)^2} + \frac{4M^2+M\nu-\nu^2}{4\pi M\nu^3}\ln\left[1+\frac{2\nu}{M}\right]. \tag{6.30}$$

- δGDH sum rule

$$\frac{2\,e^2}{M^2}\kappa = \frac{1}{\pi}\int_0^\infty \frac{d\nu}{\nu}\,\Delta\sigma_{\kappa_0}(\nu), \tag{6.31}$$

- δFSP sum rule

$$\frac{e^2}{2M^4}(\kappa+\mathcal{Q}) - \frac{4\pi}{M}(\gamma'_E+\gamma'_B) = \frac{1}{\pi}\int_\nu^\infty d\nu'\,\frac{\Delta\sigma_{\kappa_0}(\nu') - \frac{2\nu'}{M}\sigma(0)}{\nu'^3}, \tag{6.32}$$

$$\text{with} \quad \Delta\sigma_{\kappa_0}(\nu) = -\frac{45M^3+237M^2\nu+396M\nu^2+188\nu^3}{6\pi M\nu(M+2\nu)^3} + \frac{15M+4\nu}{4\pi M\nu^2}\ln\left[1+\frac{2\nu}{M}\right]. \tag{6.33}$$

- δF_2 sum rule

$$\frac{3e^2}{M^3}(2\kappa+\mathcal{Q}) + \frac{2\pi}{M}(a'_2+b'_2) = \frac{1}{\pi}\int_0^\infty \frac{d\nu}{\nu^2}\,\sigma_{Q,\kappa_0}(\nu), \tag{6.34}$$

$$\text{with} \quad \sigma_{Q,\kappa_0}(\nu) = \frac{36M^5+189M^4\nu+333M^3\nu^2+258M^2\nu^3+184M\nu^4+96\nu^5}{6\pi M^2\nu^2(M+2\nu)^3} - \frac{12M^2+3M\nu+8\nu^2}{4\pi M\nu^3}\ln\left[1+\frac{2\nu}{M}\right]. \tag{6.35}$$

- δBaldin sum rule

$$\frac{\pi}{M}(a'_1+b'_1) = \frac{1}{\pi}\int_0^\infty \frac{d\nu}{\nu^2}\sigma_{\kappa_0}(\nu), \tag{6.36}$$

$$\text{with} \quad \sigma_{\kappa_0}(\nu) = \frac{33M^3+165M^2\nu+262M\nu^2+96\nu^3}{18\pi M^2(M+2\nu)^3} - \frac{11}{12\pi M\nu}\ln\left[1+\frac{2\nu}{M}\right]. \tag{6.37}$$

- δQSR sum rule

$$\frac{e^2}{M^3}(2\kappa+\mathcal{Q}) + \frac{\pi}{M}(a'_2-b'_2) = \frac{1}{\pi}\int_0^\infty \frac{d\nu}{\nu^2}\left[\sigma_{2\perp,\kappa_0}(\nu) - \sigma_{2\parallel,\kappa_0}(\nu)\right], \tag{6.38}$$

$$\text{with} \quad \sigma_{2\perp,\kappa_0}(\nu) - \sigma_{2||,\kappa_0}(\nu) = \frac{6M^4+27M^3\nu+35M^2\nu^2+20M\nu^3+36\nu^4}{6\pi M\nu^2(M+2\nu)^3} - \frac{2M^2-M\nu+2\nu^2}{4\pi M\nu^3}\ln\left[1+\frac{2\nu}{M}\right]. \tag{6.39}$$

We verified that the extended amplitudes fulfill subtracted dispersion relations and that they are connected to the cross-section derivatives by the optical theorem. Just as for the FSP sum rule, it was necessary to introduce an infra-red cutoff in the δFSP sum rule.

Making use of the δGDH in eq. (6.31) one reproduces the loop contribution to the anomalous magnetic dipole moment calculated in section 5.4:

$$\kappa = -\frac{5\alpha}{6\pi}. \tag{6.40}$$

The δsum rules provide no direct access to the anomalous electric quadrupole moment, because it is always shielded by polarizabilities. Since, as we obtained in eq. (5.24b), $\mathcal{Q} = 8\alpha/9\pi$, the derivatives of the polarizabilities are:

$$\gamma_0' = \frac{1}{2M}(\gamma_E' + \gamma_B') = \frac{\alpha^2}{\pi M^4}\left(\frac{413}{36} + \frac{208}{12}\ln\frac{2\nu}{M}\right), \tag{6.41a}$$

$$\alpha_{E1}' + \beta_{M1}' = \frac{a_1' + b_1'}{2M} = \frac{46\,\alpha^2}{9\pi M^3}, \tag{6.41b}$$

$$\alpha_{E2}' = \frac{a_2'}{2M} = \frac{11\,\alpha^2}{\pi M^3}, \tag{6.41c}$$

$$\beta_{M2}' = \frac{b_2'}{2M} = \frac{29\,\alpha^2}{3\pi M^3}, \tag{6.41d}$$

These derivatives were calculated from the energy-weighted integrals over the cross-sections. The derivative of the forward spin polarizability γ_0' is 'dynamical', i.e. depending on the energy.

CHAPTER 7

CONCLUSION AND OUTLOOK

In this thesis we have established Compton scattering sum rules for spin-1 targets, taking into account all of the anomalous e.m. moments as well as lowest-order polarizabilities. We than have verified them in a quantum field theory. All together we have obtained six sum rules, summarized in appendix A. The most notable are: the Gerasimov-Drell-Hearn (GDH), forward-spin polarizability (FSP), Baldin and quadrupole (QSR) sum rules.

The well-known GDH sum rule has the form analogous to the spin-1/2 case. An entirely new sum rule arises however when we consider the total-helicity-flip amplitude. We refer to it as the QSR sum rule. It relates the anomalous electric quadrupole moment to a difference of linearly polarized cross-sections. We show that several other sum rules (e.g., FSP) receive a contribution from the anomalous electric quadrupole moment, whose presence distinguishes spin-1 from spin-1/2 particles.

Furthermore, by taking the derivatives of these sum rule with respect to the anomalous magnetic moment, we have found the so-called δsum rules. From the δGDH we could reproduce the one-loop correction to the magnetic dipole moment, $\kappa = -5\alpha/6\pi$, correctly. The remaining sum rules do not give an independent evaluation of the anomalous electric quadrupole moment, because the latter is always shielded by polarizabilities.

We have calculated the forward Compton scattering amplitude in spin-1 QED at one-loop level and therewith verified that the scalar scattering amplitudes indeed fulfill (subtracted) dispersion relations. We checked the relation between the imaginary contribution of the forward scattering amplitude and the total Compton scattering cross-sections, which is given by the optical theorem. Both sides of the sum rule, i.e. the energy-weighted integrals over the tree-level photoabsorption cross-sections and the real parts of the one-loop forward Compton scattering amplitudes coincided at one-loop level.

The coefficients in the low-energy expansion of some sum rules are logarithmically divergent in the infra-red, eventhough the full expression is finite. This is because in QED the production threshold is at $\nu = 0$, since the photon is massless. In order to make the low-energy expansion of the rhs (of the F_0 sum rule, the FSP and δFSP sum rule, and the Baldin sum rule for spin-0 and spin-1) to be quantitatively consistent with the expansion of the lhs, we needed to introduce an infra-red cutoff equal to ν. In this way both sides of the sum rules gave the same results for the one-loop polarizabilities. Due to the cutoff, certain polarizabilities have a residual dependence on the energy and are therefore 'dynamical' rather than 'static' polarizabilities. Using the sum rules and

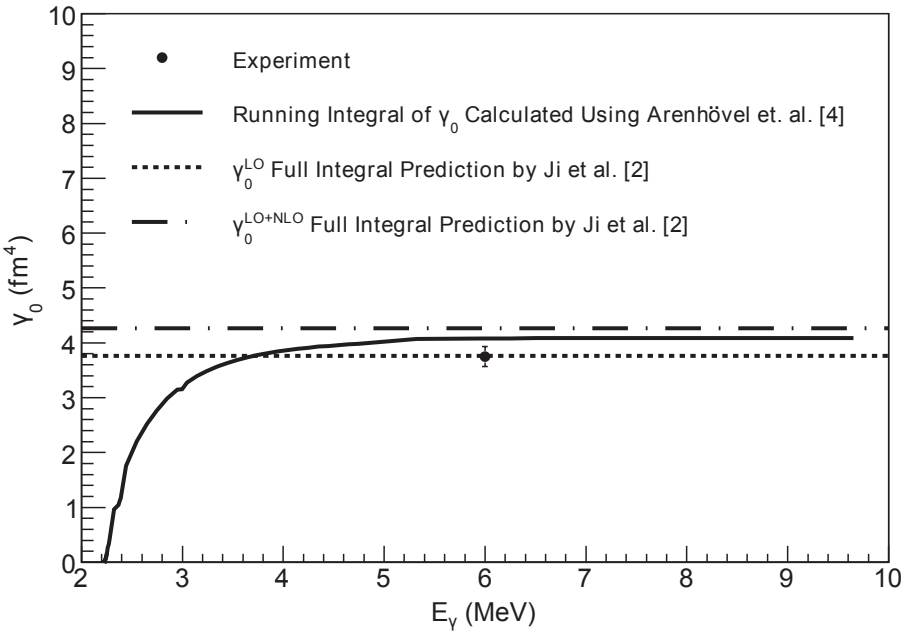

Figure 7.1.: Running integral of γ_0 (taken from [10]) [Arenhövel et al. [41], Ji et al. [11]]

δsum rules we obtain the polarizabilities and their derivatives from the integrals over the photoabsorption cross-sections.

As a first application of our results to a real physical system, we consider the FSP sum rule:

$$\frac{e^2}{4M^4}(\kappa+\mathcal{Q})^2-\frac{4\pi}{M}(\gamma_E+\gamma_B)=\frac{1}{\pi}\int_\nu^\infty\frac{d\nu'}{\nu'^3}\,\Delta\sigma(\nu'). \tag{7.1}$$

It is different from the one usually used in the literature: the first term is absent in the literature. How does this new term influence the forward-spin polarizability evaluation for the deuteron?

Using the empirical value for the deuteron mass [39]:

$$\begin{aligned} m_D &= 3.343\,583\,48(15)\times10^{-27}\,\mathrm{kg}, && (7.2a)\\ &= 1875.612\,859(41)\,\mathrm{MeV}, && (7.2b)\\ &= 9.505\,101\,314(4)\,\mathrm{fm}^{-1}. && (7.2c) \end{aligned}$$

we calculate the natural electromagnetic moments for a spin-1 particle with mass m_D:[1]

[1] For the fundamental constants we used [39]:

$$\begin{aligned} e &= 1.602\,176\,565(35)\times10^{-19}\,\mathrm{C},\\ \hbar &= 1.054\,571\,726(47)\times10^{-34}\,\mathrm{Js},\\ \alpha &= 7.297\,352\,5698(24)\times10^{-3}\approx1/137,\\ \hbar c &= 197.326\,9718(44)\,\mathrm{MeV\,fm}. \end{aligned}$$

$$\mu_{\text{nat.}} = \frac{e\hbar}{2m_D} = 2.526\,645\,612 \times 10^{-27}\,\text{JT}^{-1}, \tag{7.3a}$$

$$Q_{\text{nat.}} = -\frac{e}{m_D^2} = -0.011\,068\,44214(1)\,e\,\text{fm}^2. \tag{7.3b}$$

The deuteron magnetic dipole moment [39] is measured to be:

$$\mu_D = 0.433\,073\,489(10) \times 10^{-26}\,\text{JT}^{-1}, \tag{7.4}$$

which with our definition of the anomalous magnetic dipole moment leads to:[2]

$$\kappa_D = \frac{m_D}{e}\mu_D - 1 = -0.142\,987\,2728(2968). \tag{7.5}$$

The electric quadrupole moment of the deuteron was first observed by Kellogg, Rabi, Ramsey and Zacharias [42]. It is extracted from molecular-beam resonance experiments which measure the electric quadrupole interaction in diatomic molecules. The electric quadrupole interaction constant $e\,q\,Q/h$ is proportional to the quadrupole moment and the molecular electric field gradient q. This field gradient has to be estimated theoretically, which results in a large uncertainty of the measured electric quadrupole moment [43]:

$$Q_D = 0.2875(20)\,e\,\text{fm}^2. \tag{7.6}$$

The deviation of the deuteron quadrupole moment from its natural value is described by the anomalous electric quadrupole moment:

$$\mathcal{Q}_D = \frac{1}{2}\left(\frac{m_D^2}{e}Q_D + 1\right) = 13.49(9). \tag{7.7}$$

As expected, the anomalous e.m. moments of the deuteron which is composed of a proton and a neutron, are much larger than the anomalous e.m. moments for an elementary spin-1 particle, see eqs. (5.26).

The newly established factor in the FSP sum rule can now be evaluated for the deuteron:

$$\frac{e^2}{4m_D^4}(\kappa_D + \mathcal{Q}_D)^2 = 5.0 \times 10^{-4}\,\text{fm}^4. \tag{7.8}$$

Ahmed et al [10] used the former version of the FSP sum rule:

$$\gamma_0^{(D)} = -\frac{1}{8\pi^2}\int_{\nu_0}^{\infty}\frac{d\nu}{\nu^3}\Delta\sigma(\nu) \tag{7.9}$$

to obtain:

$$\gamma_0^{(D)} = 3.75 \pm 0.18\,\text{fm}^4, \tag{7.10}$$

from the energy-weighted cross-section integral between photodisintegration threshold and 6 MeV. The experimental result for the (running) FSP integral is indicated in fig. 7.1 along with predictions by [41] and [11]. Obviously, our correction to this value of γ_0, cf. eq. (7.8), is very small and falls well within the quoted experimental error.

We hope that the other sum rules derived and verified in this thesis will in near future become relevant to the experimental studies of the deuteron and other spin-1 particles.

[2] For the error estimate we have applied the Gaussian propagation of errors.

APPENDIX A

SUMMARY OF SPIN-1 SUM RULES

- F_0 sum rule

$$-\frac{e^2}{M^3}\kappa\,(\kappa+\mathcal{Q})+\frac{\pi}{M}\left[a_1+b_1-\frac{2}{3}(a_2+b_2)\right]=\frac{1}{\pi}\int_\nu^\infty d\nu'\,\frac{\sigma_1(\nu')-\sigma(0)}{\nu'^{\,2}}, \quad \text{(A.1)}$$

$$\text{with}\quad \sigma_1(\nu)=-\frac{9M^3+30M^2\nu+19M\nu^2-6\nu^3}{12\pi M\nu^2(M+2\nu)^2}+\frac{3M+\nu}{8\pi\nu^3}\ln\left[1+\frac{2\nu}{M}\right].$$

- GDH sum rule

$$\frac{e^2}{M^2}\kappa^2=\frac{1}{\pi}\int_0^\infty\frac{d\nu}{\nu}\,\Delta\sigma(\nu), \quad \text{(A.2)}$$

- FSP sum rule

$$\frac{e^2}{4M^4}(\kappa+\mathcal{Q})^2-\frac{4\pi}{M}(\gamma_E+\gamma_B)=\frac{1}{\pi}\int_\nu^\infty d\nu'\,\frac{\Delta\sigma(\nu')-\frac{2\nu'}{M}\sigma(0)}{\nu'^{\,3}}, \quad \text{(A.3)}$$

$$\text{with}\quad \Delta\sigma(\nu)=-\frac{15M^3+81M^2\nu+142M\nu^2+76\nu^3}{6\pi M\nu(M+2\nu)^3}+\frac{5M+2\nu}{4\pi M\nu^2}\ln\left[1+\frac{2\nu}{M}\right].$$

- F_2 sum rule

$$\frac{3e^2}{M^3}\kappa\,(\kappa+\mathcal{Q})+\frac{2\pi}{M}(a_2+b_2)=\frac{1}{\pi}\int_0^\infty\frac{d\nu}{\nu^2}\,\sigma_Q(\nu), \quad \text{(A.4)}$$

$$\text{with}\quad \sigma_Q(\nu)=\frac{18M^5+99M^4\nu+183M^3\nu^2+132M^2\nu^3+52M\nu^4+24\nu^5}{6\pi M^2\nu^2(M+2\nu)^3}-\frac{6M^2+3M\nu+2\nu^2}{4\pi M\nu^3}\ln\left[1+\frac{2\nu}{M}\right].$$

- Baldin sum rule

$$\frac{\pi}{M}(a_1+b_1)=\frac{1}{\pi}\int_\nu^\infty d\nu'\,\frac{\sigma(\nu')-\sigma(0)}{\nu'^2}, \tag{A.5}$$

$$\text{with}\quad \sigma(\nu)=\frac{9M^5+54M^4\nu+129M^3\nu^2+168M^2\nu^3+140M\nu^4+48\nu^5}{36\pi M^2\nu^2(M+2\nu)^3} + \frac{3M^2+3M\nu+4\nu^2}{24\pi M\nu^3}\ln\left[1+\frac{2\nu}{M}\right].$$

- QSR sum rule

$$\frac{e^2}{M^3}\kappa(\kappa+\mathcal{Q})+\frac{\pi}{M}(a_2-b_2)=\frac{1}{\pi}\int_0^\infty\frac{d\nu}{\nu^2}\left[\sigma_{2\perp}(\nu)-\sigma_{2\parallel}(\nu)\right], \tag{A.6}$$

$$\text{with}\quad \sigma_{2\perp}(\nu)-\sigma_{2||}(\nu)=\frac{3M^3+15M^2\nu+22M\nu^2+6\nu^3}{6\pi\nu^2(M+2\nu)^3}-\frac{M\ln\left[1+\frac{2\nu}{M}\right]}{4\pi\nu^3}.$$

APPENDIX B

FULL COMPTON SCATTERING AMPLITUDE

In all results the overall factor e^4 is omitted for brevity.

$$\begin{aligned}
\mathrm{Re}\, F_0(\nu) = {} & \frac{7L}{24\pi^2} - \frac{18M^4\pi^2 + 53M^2\nu^2 - 72M^2\pi^2\nu^2 - 308\nu^4}{72\pi^2\nu^2\left(M^2-4\nu^2\right)} - \frac{\ln w}{2\pi^2} \\
& - \frac{2\left(3M^4 - 19M^2\nu^2 + 12\nu^4\right)}{3\pi^2\left(M^2-4\nu^2\right)^2}\ln\frac{2\nu}{M} \\
& + \frac{M\left\{(3M+\nu)\,\mathrm{Re}\,\mathrm{Li}_2\left[1+\frac{2\nu}{M}\right] + (3M-\nu)\mathrm{Li}_2\left[1-\frac{2\nu}{M}\right]\right\}}{4\pi^2\nu^2}
\end{aligned} \tag{B.1}$$

$$\mathrm{Im}\, F_0(\nu) = -\frac{9M^3 + 30M^2\nu + 19M\nu^2 - 6\nu^3}{6\pi\nu(M+2\nu)^2} + \frac{M(3M+\nu)}{4\pi\nu^2}\ln\left[1+\frac{2\nu}{M}\right] \tag{B.2}$$

$$\begin{aligned}
\mathrm{Re}\, F_1(\nu) = {} & \frac{M\left(5\pi^2M^5 - 6M^2\nu^2 - 40\pi^2M^3\nu^2 + 56\nu^4 + 80\pi^2M\nu^4\right)}{12\pi^2\nu^2\left(M^2-4\nu^2\right)^2} \\
& + \frac{M\left(9M^4 - 76M^2\nu^2 + 224\nu^4\right)}{3\pi^2\left(M^2-4\nu^2\right)^3}\ln\frac{2\nu}{M} \\
& - \frac{(5M+2\nu)\,\mathrm{Re}\,\mathrm{Li}_2\left[1+\frac{2\nu}{M}\right] + (5M-2\nu)\mathrm{Li}_2\left[1-\frac{2\nu}{M}\right]}{4\pi^2\nu^2}
\end{aligned} \tag{B.3}$$

$$\mathrm{Im}\, F_1(\nu) = \frac{15M^3 + 81M^2\nu + 142M\nu^2 + 76\nu^3}{6\pi\nu(M+2\nu)^3} - \frac{5M+2\nu}{4\pi\nu^2}\ln\left[1+\frac{2\nu}{M}\right] \tag{B.4}$$

$$\begin{aligned}
\mathrm{Re}\, F_2(\nu) = {} & -\frac{13L}{24\pi^2\nu^2} + \frac{83M^4 - 784M^2\nu^2 + 2192\nu^4}{72\pi^2\nu^2\left(M^2-4\nu^2\right)^2} + \frac{3M^2+\nu^2}{6\nu^4} \\
& + \frac{9M^6 - 78M^4\nu^2 + 168M^2\nu^4 + 128\nu^6}{3\pi^2\nu^2\left(M^2-4\nu^2\right)^3}\ln\frac{2\nu}{M} \\
& - \frac{6M^2+3M\nu+2\nu^2}{4\pi^2\nu^4}\,\mathrm{Re}\,\mathrm{Li}_2\left[1+\frac{2\nu}{M}\right] \\
& - \frac{6M^2-3M\nu+2\nu^2}{4\pi^2\nu^4}\mathrm{Li}_2\left[1-\frac{2\nu}{M}\right]
\end{aligned} \tag{B.5}$$

$$\mathrm{Im}\, F_2(\nu) = \frac{18M^5 + 99M^4\nu + 183M^3\nu^2 + 132M^2\nu^3 + 52M\nu^4 + 24\nu^5}{6\pi M\nu^3(M+2\nu)^3} \tag{B.6}$$

$$
\begin{aligned}
&- \frac{6M^2+3M\nu+2\nu^2}{4\pi\nu^4}\ln\left[1+\frac{2\nu}{M}\right] \\
\operatorname{Re} G(\nu) = &\frac{\pi^2M^6-24M^4\nu^2-8\pi^2M^4\nu^2+176M^2\nu^4+16\pi^2M^2\nu^4-64\nu^6}{24\pi^2\nu^2\left(M^2-4\nu^2\right)^2} \\
&+ \frac{2M^2\left(3M^4-30M^2\nu^2+104\nu^4\right)}{3\pi^2\left(M^2-4\nu^2\right)^3}\ln\frac{2\nu}{M} - \frac{M^2\mathrm{Li}_2\left[1-\frac{4\nu^2}{M^2}\right]}{4\pi^2\nu^2}
\end{aligned} \tag{B.7}
$$

$$
\operatorname{Im} G(\nu) = \frac{M\left(3M^3+15M^2\nu+22M\nu^2+6\nu^3\right)}{3\pi\nu(M+2\nu)^3} - \frac{M^2}{2\pi\nu^2}\ln\left[1+\frac{2\nu}{M}\right] \tag{B.8}
$$

Extended Compton Scattering Amplitude

For the δsum rules we calculated the scalar amplitudes with an additional Corben-Schwinger interaction. Here only the portions proportional to κ_0 are given:

$$
\begin{aligned}
\operatorname{Re}\delta F_0(\nu) = &\frac{L\left(49M^2+2\nu^2\right)}{24\pi^2M^2} + \frac{1}{6} - \frac{2M^2}{3\nu^2} + \frac{-247M^4+1132M^2\nu^2+576\nu^4}{144\pi^2M^2\left(M^2-4\nu^2\right)} \\
&- \frac{2\left(9M^4-55M^2\nu^2+52\nu^4\right)}{3\pi^2(M-2\nu)^2(M+2\nu)^2}\ln\frac{2\nu}{M} \\
&+ \frac{4M^2+M\nu-\nu^2}{2\pi^2\nu^2}\operatorname{Re}\mathrm{Li}_2\left[1+\frac{2\nu}{M}\right] \\
&+ \frac{4M^2-M\nu-\nu^2}{2\pi^2\nu^2}\mathrm{Li}_2\left[1-\frac{2\nu}{M}\right]
\end{aligned} \tag{B.9}
$$

$$
\begin{aligned}
\operatorname{Im}\delta F_0(\nu) = &-\frac{12M^3+39M^2\nu+22M\nu^2-13\nu^3}{3\pi\nu(M+2\nu)^2} \\
&+ \frac{4M^2+M\nu-\nu^2}{2\pi\nu^2}\ln\left[1+\frac{2\nu}{M}\right]
\end{aligned} \tag{B.10}
$$

$$
\begin{aligned}
\operatorname{Re}\delta F_1(\nu) = &\frac{5M}{4\nu^2} - \frac{8\left(M^3-8M\nu^2\right)}{3\pi^2\left(M^2-4\nu^2\right)^2}\frac{M\left(33M^4-296M^2\nu^2+912\nu^4\right)}{3\pi^2\left(M^2-4\nu^2\right)^3}\ln\frac{2\nu}{M} \\
&- \frac{(15M+4\nu)\operatorname{Re}\mathrm{Li}_2\left[1+\frac{2\nu}{M}\right]+(15M-4\nu)\mathrm{Li}_2\left[1-\frac{2\nu}{M}\right]}{4\pi^2\nu^2}
\end{aligned} \tag{B.11}
$$

$$
\operatorname{Im}\delta F_1(\nu) = \frac{45M^3+237M^2\nu+396M\nu^2+188\nu^3}{6\pi\nu(M+2\nu)^3} - \frac{15M+4\nu}{4\pi\nu^2}\ln\left[1+\frac{2\nu}{M}\right] \tag{B.12}
$$

$$
\begin{aligned}
\operatorname{Re}\delta F_2(\nu) = &-\frac{L\left(18M^2+\nu^2\right)}{12\pi^2M^2\nu^2} + \frac{M^2}{\nu^4} + \frac{2}{3\nu^2} \\
&+ \frac{-29M^6+56M^4\nu^2+1072M^2\nu^4+768\nu^6}{48\pi^2M^2\nu^2\left(M^2-4\nu^2\right)^2} \\
&- \frac{27M^6-240M^4\nu^2+576M^2\nu^4+320\nu^6}{3\pi^2\nu^2\left(-M^2+4\nu^2\right)^3}\ln\frac{2\nu}{M} \\
&- \frac{12M^2+3M\nu+8\nu^2}{4\pi^2\nu^4}\operatorname{Re}\mathrm{Li}_2\left[1+\frac{2\nu}{M}\right] \\
&- \frac{12M^2-3M\nu+8\nu^2}{4\pi^2\nu^4}\mathrm{Li}_2\left[1-\frac{2\nu}{M}\right]
\end{aligned} \tag{B.13}
$$

$$\operatorname{Im}\delta F_2(\nu) = \frac{\left(36M^5 + 189M^4\nu + 333M^3\nu^2 + 258M^2\nu^3 + 184M\nu^4 + 96\nu^5\right)}{6\pi M\nu^3(M+2\nu)^3} \tag{B.14}$$
$$- \frac{12M^2 + 3M\nu + 8\nu^2}{4\pi\nu^4} \ln\left[1 + \frac{2\nu}{M}\right]$$

$$\operatorname{Re}\delta F(\nu) = \frac{L\left(75M^2 + 2\nu^2\right)}{72\pi^2M^2} - \frac{305M^6 - 2232M^4\nu^2 + 1808M^2\nu^4 + 768\nu^6}{144\pi^2M^2\left(M^2 - 4\nu^2\right)^2} \tag{B.15}$$
$$+ \frac{11}{18} + \frac{2\nu^2\left(33M^4 - 240M^2\nu^2 + 944\nu^4\right)}{9\pi^2\left(M^2 - 4\nu^2\right)^3} \ln\frac{2\nu}{M}$$
$$- \frac{11\left\{\operatorname{Re}\operatorname{Li}_2\left[1 + \frac{2\nu}{M}\right] + \operatorname{Li}_2\left[1 - \frac{2\nu}{M}\right]\right\}}{6\pi^2}$$

$$\operatorname{Im}\delta F(\nu) = \frac{\nu\left(33M^3 + 165M^2\nu + 262M\nu^2 + 96\nu^3\right)}{9\pi M(M+2\nu)^3} - \frac{11}{6\pi}\ln\left[1 + \frac{2\nu}{M}\right] \tag{B.16}$$

$$\operatorname{Re}\delta G(\nu) = \frac{13L}{12\pi^2} + \frac{M^2 + \nu^2}{3\nu^2} + \frac{-227M^4 + 1624M^2\nu^2 - 1328\nu^4}{36\pi^2\left(M^2 - 4\nu^2\right)^2} \tag{B.17}$$
$$+ \frac{2\left(9M^6 - 86M^4\nu^2 + 256M^2\nu^4 + 288\nu^6\right)}{3\pi^2\left(M^2 - 4\nu^2\right)^3} \ln\frac{2\nu}{M}$$
$$- \frac{2M^2 - M\nu + 2\nu^2}{2\pi^2\nu^2} \operatorname{Re}\operatorname{Li}_2\left[1 + \frac{2\nu}{M}\right]$$
$$- \frac{2M^2 + M\nu + 2\nu^2}{2\pi^2\nu^2}\operatorname{Li}_2\left[1 - \frac{2\nu}{M}\right]$$

$$\operatorname{Im}\delta G(\nu) = \frac{6M^4 + 27M^3\nu + 35M^2\nu^2 + 20M\nu^3 + 36\nu^4}{3\pi\nu(M+2\nu)^3} \tag{B.18}$$
$$- \frac{2M^2 - M\nu + 2\nu^2}{2\pi\nu^2}\ln\left[1 + \frac{2\nu}{M}\right]$$

Dilogarithm

The polylogarithm is defined as:

$$\operatorname{Li}_s[z] = \sum_{k=1}^{\infty} \frac{z^k}{k^s}, \tag{B.19}$$

for complex $|z| < 1$, and it is analytically continuable to other values.

The polylogarithms $\operatorname{Li}_s[z]$ are connected by a recursion formula:

$$\operatorname{Li}_{s+1}[z] = \int_0^z dt\, \frac{\operatorname{Li}_s[t]}{t} \qquad \text{with} \qquad \operatorname{Li}_0[z] = \frac{z}{1-z}. \tag{B.20}$$

Hence, the dilogarithm is connected to the logarithm in the following way:

$$\operatorname{Li}_2[z] = -\int_0^z dt\, \frac{\ln[1-t]}{t}. \tag{B.21}$$

From this definition one can see that for real z the dilogarithm becomes imaginary for $z > 1$ and it is

$$\operatorname{Li}_2[z] = \operatorname{Re}\operatorname{Li}_2[z] - i\pi\ln z. \tag{B.22}$$

APPENDIX C

FEYNMAN RULES

C.1. Scalar QED

- <u>propagators:</u>

  – scalar propagator: $\Delta(l) = \dfrac{1}{l^2 - M^2 + i0^+}$ (C.1)

  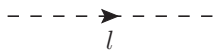

  – photon propagator (in Lorentz gauge): $D_{\rho\sigma}(k) = -\dfrac{g_{\rho\sigma}}{k^2 + i0^+}$ (C.2)

  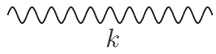

- <u>vertices:</u>

  – 3-point vertex: $-e(p + p')^\mu$ (C.3)

  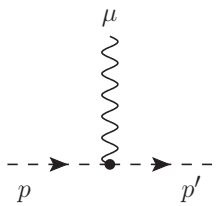

  – seagull vertex: $2e^2 g^{\mu\nu}$ (C.4)

  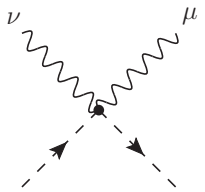

- external lines:
  - incoming photon: ε_ν,
  - outgoing photon: ε^*_μ.

C.2. Massive Yang-Mills QED and an Effective Spin-1 Theory

- propagators:
  - W-boson propagator: $\Delta_{\rho\sigma}(l) = -\frac{1}{l^2 - M^2 + i0^+}\left(g_{\rho\sigma} - \frac{l_\rho l_\sigma}{M^2}\right),$ (C.5)

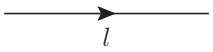

  - photon propagator (in Feynman gauge): $D_{\rho\sigma}(k) = -\frac{g_{\rho\sigma}}{k^2 + i0^+}.$ (C.6)

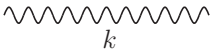

- vertices:
  - 3-point vertex: ($q = p' - p$ and $P = p + p'$)

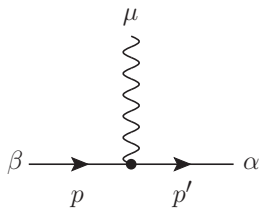

$$\begin{aligned}\Gamma^{\alpha\beta\mu}(p,p') = &-e\Big[P^\mu g^{\alpha\beta} - p'^\beta g^{\alpha\mu} - p^\alpha g^{\beta\mu} \\ &+ \ell_1(q^\alpha g^{\beta\mu} - q^\beta g^{\alpha\mu}) \\ &- \frac{\ell_2}{2M^2}\left(P^\mu q^\alpha q^\beta - p\cdot q\, q^\alpha g^{\beta\mu}\right. \\ &\left.- p'\cdot q\, q^\beta g^{\alpha\mu}\right)\Big],\end{aligned} \tag{C.7}$$

  - seagull vertex: (in the forward direction $q = q'$)

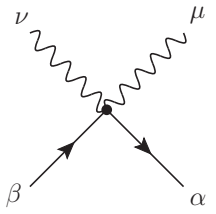

$$\begin{aligned}\Gamma^{\alpha\beta\mu\nu} = &\, e^2\Big[2g^{\alpha\beta}g^{\mu\nu} - g^{\alpha\mu}g^{\beta\nu} - g^{\alpha\nu}g^{\beta\mu} \\ &- \frac{\ell_2}{2M^2}\left(4g^{\mu\nu}q^\alpha q^\beta - q^\nu(q^\beta g^{\alpha\mu} + q^\alpha g^{\beta\mu})\right. \\ &\left.-q^\mu(q^\beta g^{\alpha\nu} + q^\alpha g^{\beta\nu})\right)\Big].\end{aligned} \tag{C.8}$$

  - WWWW-vertex:

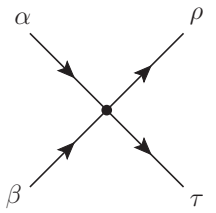

$$\Gamma^{\alpha\beta\rho\tau} = -e^2(2g^{\alpha\beta}g^{\rho\tau} - g^{\alpha\rho}g^{\beta\tau} - g^{\alpha\tau}g^{\beta\rho}) \tag{C.9}$$

- external lines:
  - incoming W-boson: χ_β,
  - outgoing W-boson: χ^*_α,
  - incoming photon: ε_ν,
  - outgoing photon: ε^*_μ.

C.3. Applying Feynman Rules

- multiply all parts of the diagram: polarization vectors, vertex functions and propagators
- integration over internal (propagator -) momenta: $\int d^4l \, \frac{1}{i\,(2\pi)^4}$
- conservation of energy and momentum at each vertex: $i\,(2\pi)^4\,\delta^{(4)}(k_1 + ... + k_n)$
- overall conservation of energy and momentum: $\frac{1}{i\,(2\pi)^4}\frac{1}{\delta^{(4)}(p+q-p'-q')}$

APPENDIX D

ONE-LOOP INTEGRALS

[1]

Calculation of Loop Integrals

At one-loop level the integration over internal momenta is not so trivial, because the number of delta functions is not sufficient to 'cancel' all momentum integrals. Therefore we want to go through the calculation of loop integrals and learn some important relations and tricks.

To outline the procedure one can say that the denominators of the propagators are combined to a quadratic polynomial in the integration momentum, which is then shifted in order to make the integral spherically symmetric. The remaining integral is solved by use of dimensional regularization.

Feynman Trick

The Feynman trick is helpful to rewrite a product of fractions. In our case it is used to combine the denominators of the propagators.

Feynman's formula reads as follows:

$$\frac{1}{A_1 A_2 \cdots A_n} = \int_0^1 dx_1 \cdots dx_n \, \delta\left(\sum\nolimits_i x_i - 1\right) \frac{(n-1)!}{(x_1 A_1 + x_2 A_2 + \cdots + x_n A_n)^n}, \tag{D.1}$$

it introduces auxiliary parameters x_i called Feynman parameters.

By differentiating one can find an even more general notation of Feynman's formula:

$$\begin{aligned} &\frac{1}{A_1^{m_1} A_2^{m_2} \cdots A_n^{m_n}} \\ &= \int_0^1 dx_1 \cdots dx_n \, \delta\left(\sum\nolimits_i x_i - 1\right) \frac{\prod_i x_i^{m_i - 1}}{\left(\sum_i x_i A_i\right)^{\sum_i m_i}} \frac{\Gamma(m_1 + \cdots + m_n)}{\Gamma(m_1) \cdots \Gamma(m_n)}. \end{aligned} \tag{D.2}$$

[1] In preparation of this chapter we used [44].

In our case it is enough to know the special cases with $n = 2, 3$ and 4, which can be examined by direct calculation.

$$\frac{1}{AB} = \int_0^1 dx \, \frac{1}{[Ax + B(1-x)]^2}, \tag{D.3a}$$

$$\frac{1}{A^2B} = \int_0^1 dx \, \frac{2x}{[Ax + B(1-x)]^3}, \tag{D.3b}$$

$$\begin{aligned} \frac{1}{ABC} &= \int_0^1 dx \int_0^{1-x} dy \, \frac{2}{[Ax + By + C(1-x-y)]^3} \\ &= \int_0^1 dx \int_0^x dy \, \frac{2}{[Ay + B(x-y) + C(1-x)]^3}, \end{aligned} \tag{D.3c}$$

$$\frac{1}{A^2BC} = \int_0^1 dx \int_0^x dy \, \frac{6(x-y)}{[A(x-y) + B(1-x) + Cy]^4}, \tag{D.3d}$$

$$\frac{1}{ABCD} = \int_0^1 dx \int_0^{1-x} dy \int_0^{1-x-y} dz \, \frac{6}{[Ax + By + Cz + D(1-x-y-z)]^4}. \tag{D.3e}$$

After applying the Feynman trick it is often possible to perform a momentum shift and obtain an denominator, which is quadratic in the integration momentum.

Dimensional Regularization

We will now introduce the dimensional regularization as a method to handle ultra-violet divergences.

After the momentum shifts the integrals are of these types:

$$\int d_D k \, \frac{1}{(k^2 - \mathcal{M})^n} = F_n, \tag{D.4a}$$

$$\int d_D k \, \frac{k_\alpha k_\beta}{(k^2 - \mathcal{M})^n} = g_{\alpha\beta} G_n, \tag{D.4b}$$

$$\int d_D k \, \frac{k_\alpha k_\beta k_\mu k_\nu}{(k^2 - \mathcal{M})^n} = g_{\alpha\beta\mu\nu} H_n, \tag{D.4c}$$

$$\int d_D k \, \frac{k_\alpha k_\beta k_\mu k_\nu k_\rho k_\sigma}{(k^2 - \mathcal{M})^n} = g_{\alpha\beta\mu\nu\rho\sigma} I_n. \tag{D.4d}$$

Here $\mathcal{M}$ is a reduced mass, which is actually proportional to M^2, and the g-functions with more than two indices represent the sum over all possible combinations of g-functions (Minkowski metric entries) with these indices, e.g.:

$$g_{\alpha\beta\mu\nu} = g_{\alpha\beta} g_{\mu\nu} + g_{\alpha\mu} g_{\beta\nu} + g_{\alpha\nu} g_{\beta\mu}. \tag{D.5}$$

To solve

$$F[\mathcal{M}, n, D] = \int_0^\infty d_D k \, \frac{1}{(k^2 - \mathcal{M} + i\epsilon)^n} \tag{D.6}$$

we perform a Wick rotation to imaginary times ($k_0 \to i k_0$ and $k^2 \to -k^2$) and use Euclidean, D-dimensional polar coordinates:

$$\int d_D k f(k) \tag{D.7}$$

$$= \int_0^\infty dr \int_0^\pi d\theta_{D-2} \int_0^\pi d\theta_{D-3} \cdots \int_0^{2\pi} d\theta_1 f(k)\, r^{D-1} \sin^{D-2}\theta_{D-1} \sin^{D-3}\theta_{D-2} \cdots ,$$

with

$$\int_0^\infty \sin^m \theta d\theta = \sqrt{\pi} \frac{\Gamma\left[\frac{m+1}{2}\right]}{\Gamma\left[\frac{m+2}{2}\right]}. \tag{D.8}$$

The Γ-functions from the angular integrations cancel each other except for $\Gamma[1] = 1$ and $\Gamma\left[\frac{D}{2}\right]$. So, one obtains:

$$F[\mathcal{M}, n, D] = \frac{2i\pi^{\frac{D}{2}}}{(-1)^n \Gamma\left[\frac{D}{2}\right]} \int_0^\infty dr\, r^{D-1} \frac{1}{(r^2 + \mathcal{M} - i\epsilon)^n} \tag{D.9}$$

The remaining integral is solved by the substitution $r^2 = \mathcal{M}t$, with $dr = \frac{1}{2}\sqrt{\mathcal{M}/t}dt$:

$$\begin{aligned} &\int_0^\infty dr\, r^{D-1} \frac{1}{(r^2 + \mathcal{M} - i\epsilon)^n} \\ &= \frac{1}{2}\mathcal{M}^{\frac{D}{2}-n} \int_0^\infty dt\, t^{\frac{D}{2}-1} \frac{1}{(t + 1 - i\frac{\epsilon}{\mathcal{M}})^n} \\ &= \frac{1}{2} \frac{\Gamma\left[\frac{D}{2}\right] \Gamma\left[n - \frac{D}{2}\right]}{\Gamma[n]\, \mathcal{M}^{n-\frac{D}{2}}}, \end{aligned} \tag{D.10}$$

where in the last step we used the definition of the Beta-function:

$$B(x, y) = \int_0^\infty dt\, \frac{t^{x-1}}{(1+t)^{x+y}} = \frac{\Gamma[x]\Gamma[y]}{\Gamma[x+y]}. \tag{D.11}$$

Altogether one has:

$$F[\mathcal{M}, n, D] = (-1)^n i\pi^{\frac{D}{2}} \frac{\Gamma\left[n - \frac{D}{2}\right]}{\Gamma[n]} \mathcal{M}^{\frac{D}{2}-n}. \tag{D.12}$$

Γ is only defined for positive integers. We will now investigate the crucial case, in which the argument of the $\Gamma\left[n - \frac{D}{2}\right]$-function tends to zero. For $n = 2$ and $D = 4 - 2\epsilon$ we have:

$$\Gamma[\epsilon] = \frac{1}{\epsilon} - \gamma + \mathcal{O}(\epsilon^2), \tag{D.13}$$

from the Laurent expansion in 1,

$$\mathcal{M}^{-\epsilon} = e^{-\epsilon \ln \mathcal{M}} = 1 - \epsilon \ln \mathcal{M} + \mathcal{O}(\epsilon^2), \tag{D.14}$$

and similar

$$\pi^{2-\epsilon} = \pi^2 \left(1 - \epsilon \ln \pi + \mathcal{O}(\epsilon^2)\right). \tag{D.15}$$

The overall result is:

$$F[\mathcal{M}, 2, 4 - 2\epsilon] = i\pi^2 \left(\frac{1}{\epsilon} - \gamma - \ln[\pi\mathcal{M}]\right). \tag{D.16}$$

The other integrals can be solved by differentiating this integral with respect to k. The results are listed below:

$$F_1 = -i\pi^2\mathcal{M}\left(\frac{2}{D-4} + \gamma - 1 + \ln\mathcal{M}\right), \tag{D.17a}$$

$$F_2 = -i\pi^2\left(\frac{2}{D-4} + \gamma + \ln\mathcal{M}\right), \tag{D.17b}$$

$$F_n = (-1)^n i\pi^2 \frac{\Gamma(n-2)}{\Gamma(n)}\mathcal{M}^{2-n}, \quad n \geq 3, \tag{D.17c}$$

$$G_1 = -i\frac{\pi^2}{4}\mathcal{M}^2\left(\frac{2}{D-4} + \gamma - \frac{3}{2} + \ln\mathcal{M}\right), \tag{D.17d}$$

$$G_n = \frac{1}{2(n-1)}F_{n-1}, \tag{D.17e}$$

$$H_1 = -i\frac{\pi^2}{24}\mathcal{M}^3\left(\frac{2}{D-4} + \gamma - \frac{11}{6} + \ln\mathcal{M}\right), \tag{D.17f}$$

$$H_n = \frac{1}{2(n-1)}G_{n-1}, \tag{D.17g}$$

$$I_1 = -i\frac{\pi^2}{192}\mathcal{M}^3\left(\frac{2}{D-4} + \gamma - \frac{25}{12} + \ln\mathcal{M}\right), \tag{D.17h}$$

$$I_n = \frac{1}{2(n-1)}H_{n-1}, \tag{D.17i}$$

with $D \to 4 - 2 \times 0^+$ being a fractional dimension and the Euler-Mascheroni constant γ, which is defined as:

$$\gamma = \lim_{n\to\infty}\left(\sum_{i=1}^{n}\frac{1}{i} - \ln n\right) \approx 0.57722. \tag{D.18}$$

In the later results we will combine some constants and define:

$$L = \frac{2}{D-4} + \gamma + \ln\left[\pi M^2\right]. \tag{D.19}$$

By looking closely at the F-functions, it strikes that F_1 and F_2 have so-called ultra-violet (UV) divergences for $0^+ = 0$, and F_n is singular for $\mathcal{M} = 0$, which is referred to as an infra-red (IR) singularity. In the scalar amplitudes the divergences emerge as L or $\ln w$. Integrals with odd powers of k in the nominator vanish due to symmetric reasons.

By contraction of the integrals (D.4a) with the g-functions one obtains the following replacement rules for the integrand nominators:

$$k_\alpha k_\beta \longrightarrow \frac{1}{D}k^2 g_{\alpha\beta} \tag{D.20a}$$

$$k_\alpha k_\beta k_\mu k_\nu \longrightarrow \frac{1}{D(D+2)}(k^2)^2 g_{\alpha\beta\mu\nu} \tag{D.20b}$$

$$k_\alpha k_\beta k_\mu k_\nu k_\rho k_\sigma \longrightarrow \frac{1}{D(D+2)(D+4)}(k^2)^3 g_{\alpha\beta\mu\nu\rho\sigma} \tag{D.20c}$$

After the dimensional regularization only the integration over the Feynman parameters x_i is left to perform. Thereby one has to remember that the propagators always have a small imaginary contribution. The denominators $(k^2 - \mathcal{M})^{-n}$ one would correctly write as $(k^2 - \mathcal{M} + i0^+)^{-n}$. Depending on the Feynman parameters, the reduced masses can

become negative. If the integrand contains the logarithm of the reduced mass, $\ln \mathcal{M}$, it is helpful to identify the domain where $\mathcal{M} < 0$. Then one can use the following property:

$$\ln z = \ln |z| + i\phi \qquad \text{with} \qquad z = |z|e^{i\phi} \in \mathbb{C} \quad \text{and} \quad -\pi \leq \phi \leq \pi, \tag{D.21}$$

to obtain:

$$\ln(\mathcal{M} \pm i0^{+}) = \ln(-\mathcal{M}) \pm i\pi, \qquad \text{for} \quad \mathcal{M} < 0. \tag{D.22}$$

APPENDIX E

ONE-LOOP CORRECTIONS

The amplitude for a full process to a particular order is made up of the sum of amplitudes of all topologically inequivalent connected diagrams. This is what was represented by the blob in the Compton scattering diagram, see fig. 2.1. Here we want to list the set of diagrams describing the spin-1 QED Compton scattering process at one-loop level. We will always give a description of the diagram in terms of propagators and vertex functions, a calculation which transforms the loop integral and the calculated scalar amplitudes for the combination of s- and u-channel diagram. Sometimes we combined diagrams, which give equal scalar amplitudes due to time reversal invariance.

1PR diagrams

During the calculation of the one-loop propagator and vertex modifications one has to keep in mind that some external legs are not on-shell. Hence, the corresponding polarization vectors take on a different form than in the on-shell case and no longer obey the transversality conditions.

The scalar amplitudes given here always refer to the complete one-loop Compton scattering diagrams including the described modification.

Propagator Modification

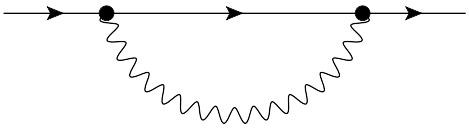

Figure E.1.: Self-energy correction (SC)

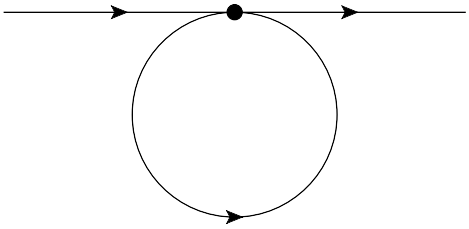

Figure E.2.: Tadpole-propagator correction

Tadpole-Propagator Correction

$$\mathcal{A}' = \chi^*_\alpha \Gamma^{\beta\rho\tau\alpha} \Delta_{\rho\tau}(l) \chi_\beta \tag{E.1}$$

$$\mathcal{A} = \int d^4l \, \frac{\mathcal{C}(l)}{l^2 - M^2 + i0^+} \tag{E.2}$$

$$F_0(\nu) = \frac{19 - 18L}{64\pi^2} \tag{E.3a}$$
$$F_1(\nu) = 0 \tag{E.3b}$$
$$F_2(\nu) = \frac{-19 + 18L}{64\pi^2} \frac{1}{\nu^2} \tag{E.3c}$$

Self-Energy Correction

$$\begin{aligned}\mathcal{A}' &= \chi^*_\alpha \, \Gamma^{\alpha\rho\sigma}(l, \tilde{p}) \, \Delta_{\rho\eta}(l) \, D_{\sigma\tau}(k) \, \Gamma^{\eta\beta\tau}(\tilde{p}, l) \, \chi_\beta \\ &= \chi^*_\alpha \, \Gamma^{\alpha\rho\sigma}(\tilde{p} - k, \tilde{p}) \, \Delta_{\rho\eta}(\tilde{p} - k) \, D_{\sigma\tau}(k) \, \Gamma^{\eta\beta\tau}(\tilde{p}, \tilde{p} - k) \, \chi_\beta\end{aligned} \tag{E.4}$$

$$\begin{aligned}\mathcal{A} &\propto \int d^4k \, \frac{\mathcal{C}(k)}{[(\tilde{p} - k)^2 - M^2 + i0^+](k^2 + i0^+)} \\ &\propto \int_0^1 dx \int d^4k \, \frac{\mathcal{C}(k)}{\{[(\tilde{p} - k)^2 - M^2 + i0^+]x + (k^2 + i0^+)(1 - x)\}^2} \\ &\propto \int_0^1 dx \int d^4K \, \frac{\mathcal{C}(K)}{\{K^2 - x^2\tilde{p}^2 + x(\tilde{p}^2 - M^2) + i0^+\}^2} \\ &\propto \int_0^1 dx \int d^4K \, \frac{\mathcal{C}(K)}{\{K^2 - \mathcal{M} + i0^+\}^2},\end{aligned} \tag{E.5}$$

here $K = k - x\tilde{p}$ and $\mathcal{M} = x^2\tilde{p}^2 - x(\tilde{p}^2 - M^2)$,
with $\tilde{p} = p \pm q$ in the one-loop self-energy diagrams

$$\begin{aligned}F_0(\nu) = {} & \frac{79M^2 - 40\nu^2}{96\pi^2 M^2} L + \frac{-835M^4 + 4028M^2\nu^2 - 1792\nu^4}{576\pi^2 M^2 \left(M^2 - 4\nu^2\right)} \\ & + \frac{-3M^4\nu^2 + 27M^2\nu^4 - 20\nu^6}{3\pi^2 M^2 \left(M^2 - 4\nu^2\right)^2} \ln \frac{2\nu}{M} \\ & - i \, \frac{\nu \left(3M^3 + 9M^2\nu + M\nu^2 - 5\nu^3\right)}{6\pi M^2 (M + 2\nu)^2}\end{aligned} \tag{E.6a}$$

$$\begin{aligned}F_1(\nu) = {} & \frac{5}{48\pi^2 M} L + \frac{29M^4 + 476M^2\nu^2 - 448\nu^4}{144\pi^2 M \left(M^2 - 4\nu^2\right)^2} \\ & + \frac{-3M^6 + 170M^4\nu^2 + 48M^2\nu^4 - 160\nu^6}{24\pi^2 M \left(M^2 - 4\nu^2\right)^3} \ln \frac{2\nu}{M} \\ & + i \, \frac{3M^3 + 36M^2\nu + 10M\nu^2 - 20\nu^3}{48\pi M (M + 2\nu)^3}\end{aligned} \tag{E.6b}$$

$$F_2(\nu) = \frac{40\nu^2 - 59M^2}{96\pi^2 M^2\nu^2} L + \frac{647M^6 - 4928M^4\nu^2 + 14992M^2\nu^4 - 7168\nu^6}{576\pi^2 M^2\nu^2 \left(M^2 - 4\nu^2\right)^2} \tag{E.6c}$$
$$+ \frac{21M^6 + 8M^4\nu^2 + 352M^2\nu^4 - 320\nu^6}{12\pi^2 M^2 \left(M^2 - 4\nu^2\right)^3} \ln\frac{2\nu}{M}$$
$$+ i\,\frac{21M^4 + 84M^3\nu + 142M^2\nu^2 - 4M\nu^3 - 80\nu^4}{48\pi M^2\nu(M + 2\nu)^3}$$

Vertex Modification

In the following notation we assume the incoming W- boson to be on-shell and we define:

$$p = \begin{pmatrix} M \\ 0 \\ 0 \\ 0 \end{pmatrix}, \qquad q = \begin{pmatrix} \nu \\ 0 \\ 0 \\ \nu \end{pmatrix}, \qquad p' = \begin{pmatrix} M + \nu \\ 0 \\ 0 \\ \nu \end{pmatrix}, \tag{E.7}$$

with $p + q = p'$.

Contact Correction

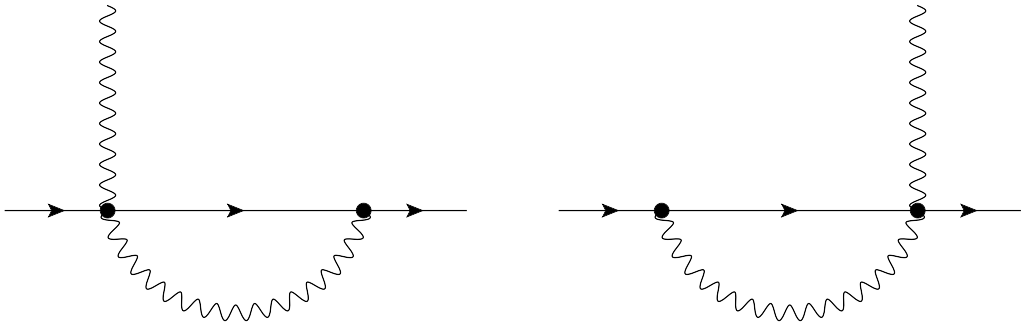

Figure E.3.: (a) left-sided (CCL) and (b) right-sided (CCR) contact correction

left-sided (CCL) contact correction

$$\mathcal{A}' = \chi_\alpha^*\,\Gamma^{\alpha\rho\sigma}(l, p')\,\Delta_{\rho\eta}(l)\,D_{\sigma\tau}(k)\,\Gamma^{\eta\beta\tau\nu}\,\varepsilon_\nu\,\chi_\beta \tag{E.8}$$
$$= \chi_\alpha^*\,\Gamma^{\alpha\rho\sigma}(l, p')\,\Delta_{\rho\eta}(l)\,D_{\sigma\tau}(p' - l)\,\Gamma^{\eta\beta\tau\nu}\,\varepsilon_\nu\,\chi_\beta$$
$$\mathcal{A} \propto \int d^4l\,\frac{\mathcal{C}(l)}{(l^2 - M^2 + i0^+)[(p' - l)^2 + i0^+]} \tag{E.9}$$
$$\propto \int_0^1 dx \int d^4l\,\frac{\mathcal{C}(l)}{\{(l^2 - M^2 + i0^+)x + [(p' - l)^2 + i0^+](1 - x)\}^2}$$
$$\propto \int_0^1 dx \int d^4L\,\frac{\mathcal{C}(L)}{\{L^2 + x(p'^2 - M^2) - x^2p'^2 + i0^+\}^2}$$
$$\propto \int_0^1 dx \int d^4L\,\frac{\mathcal{C}(L)}{\{L^2 - \mathcal{M} + i0^+\}^2},$$

here $L = l - (1 - x)p'$ and $\mathcal{M} = M^2\left[x^2 - 2\frac{\nu}{M}x(1 - x)\right]$

right-sided (CCR) contact correction

$$\begin{aligned}\mathcal{A}' &= \chi^*_\alpha\,\Gamma^{\alpha\rho\sigma\nu}\,\Delta_{\rho\eta}(l)\,D_{\sigma\tau}(k)\,\Gamma^{\eta\beta\tau}(p,l)\,\varepsilon_\nu\,\chi_\beta \qquad \text{(E.10)}\\ &= \chi^*_\alpha\,\Gamma^{\alpha\rho\sigma\nu}\,\Delta_{\rho\eta}(l)\,D_{\sigma\tau}(p-l)\,\Gamma^{\eta\beta\tau}(p,l)\,\varepsilon_\nu\,\chi_\beta\end{aligned}$$

$$\begin{aligned}\mathcal{A} &\propto \int d^4l\,\frac{\mathcal{C}(l)}{(l^2-M^2+i0^+)[(p-l)^2+i0^+]} \qquad \text{(E.11)}\\ &\propto \int_0^1 dx \int d^4l\,\frac{\mathcal{C}(l)}{\{(l^2-M^2+i0^+)x+[(p-l)^2+i0^+](1-x)\}^2}\\ &\propto \int_0^1 dx \int d^4L\,\frac{\mathcal{C}(L)}{\{L^2-x^2M^2+i0^+\}^2}\\ &\propto \int_0^1 dx \int d^4L\,\frac{\mathcal{C}(L)}{\{L^2-\mathcal{M}+i0^+\}^2},\end{aligned}$$

here $L = l-(1-x)p$ and $\mathcal{M} = x^2M^2$

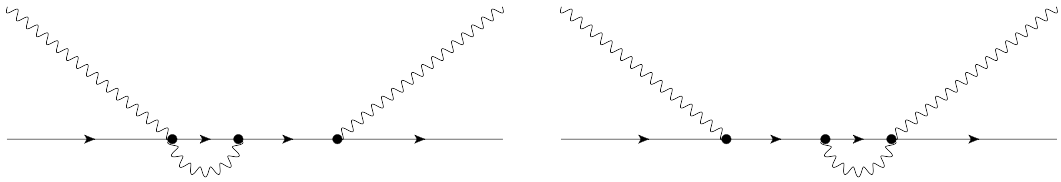

Figure E.4.: CCR correction to the right vertex + CCL correction to the left vertex

CCL correction to the left vertex + CCR correction to the right vertex:

$$\begin{aligned}F_0(\nu) &= \frac{7\nu^2}{16\pi^2M^2}L + \frac{-61M^4\nu^2+548M^2\nu^4-1280\nu^6}{96\pi^2M^2(M-2\nu)^2(M+2\nu)^2} \qquad \text{(E.12a)}\\ &\quad - \frac{\nu^2\left(3M^6-23M^4\nu^2+27M^2\nu^4+84\nu^6\right)}{3\pi^2M^2\left(M^2-4\nu^2\right)^3}\ln\frac{2\nu}{M}\\ &\quad + i\,\frac{\nu^2\left(6M^3+21M^2\nu+8M\nu^2-21\nu^3\right)}{12\pi M^2(M+2\nu)^3}\\ F_1(\nu) &= \frac{5}{96\pi^2M}L + \frac{-317M^4+1540M^2\nu^2-896\nu^4}{576\pi^2M(M-2\nu)^2(M+2\nu)^2} \qquad \text{(E.12b)}\\ &\quad + \frac{-6M^6+3M^4\nu^2+102M^2\nu^4-40\nu^6}{12\pi^2M\left(M^2-4\nu^2\right)^3}\ln\frac{2\nu}{M}\\ &\quad + i\,\frac{6M^3+12M^2\nu-3M\nu^2-5\nu^3}{24\pi M(M+2\nu)^3}\\ F_2(\nu) &= \frac{-28\nu^2+3M^2}{64\pi^2M^2\nu^2}L + \frac{-111M^6+792M^4\nu^2-2544M^2\nu^4+5120\nu^6}{384\pi^2M^2(M-2\nu)^2\nu^2(M+2\nu)^2} \qquad \text{(E.12c)}\\ &\quad + \frac{-12M^6+17M^4\nu^2+72M^2\nu^4+336\nu^6}{12\pi^2M^2\left(M^2-4\nu^2\right)^3}\ln\frac{2\nu}{M}\\ &\quad - i\,\frac{6M^4+24M^3\nu+39M^2\nu^2+11M\nu^3-42\nu^4}{24\pi M^2\nu(M+2\nu)^3}\end{aligned}$$

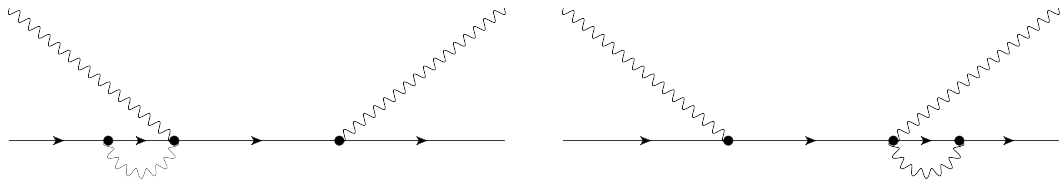

Figure E.5.: CCL correction to the right vertex + CCR correction to the left vertex

CCL correction to the right vertex + CCR correction to the left vertex:

$$F_0(\nu) = 0 \tag{E.13a}$$

$$F_1(\nu) = 0 \tag{E.13b}$$

$$F_2(\nu) = \frac{739 - 474L}{1152\pi^2}\frac{1}{\nu^2} \tag{E.13c}$$

Vertex Correction

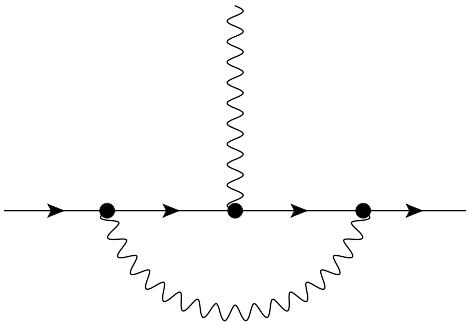

Figure E.6.: Vertex correction (VC)

$$\begin{aligned}\mathcal{A}' &= \chi^*_\alpha\,\Gamma^{\alpha\rho\sigma}(l_2,p')\,\Delta_{\rho\eta}(l_2)\,D_{\sigma\tau}(k)\,\Gamma^{\eta\zeta\nu}(l_1,l_2)\,\Delta_{\zeta\xi}(l_1)\,\Gamma^{\xi\beta\tau}(p,l_1)\,\varepsilon_\nu\,\chi_\beta \\ &= \chi^*_\alpha\,\Gamma^{\alpha\rho\sigma}(p'-k,p')\,\Delta_{\rho\eta}(p'-k)\,D_{\sigma\tau}(k)\,\Gamma^{\eta\zeta\nu}(p-k,p'-k)\times \\ &\quad \Delta_{\zeta\xi}(p-k)\,\Gamma^{\xi\beta\tau}(p,p-k)\,\varepsilon_\nu\,\chi_\beta\end{aligned} \tag{E.14}$$

$$\begin{aligned}\mathcal{A} &\propto \int d^4k\,\frac{\mathcal{C}(k)}{(k^2+i0^+)[(p-k)^2-M^2+i0^+][(p'-k)^2-M^2+i0^+]} \\ &\propto \int_0^1 dx\int_0^x dy\int d^4k\times \\ &\quad \frac{2\,\mathcal{C}(k)}{\{(k^2+i0^+)(1-x)+[(p-k)^2-M^2+i0^+](x-y)+[(p'-k)^2-M^2+i0^+]y\}^3} \\ &\propto \int_0^1 dx\int_0^x dy\int d^4K\,\frac{2\,\mathcal{C}(K)}{\{K^2-x^2M^2+(p'^2-M^2)y(1-x)+i0^+\}^3} \\ &\propto \int_0^1 dx\int_0^x dy\int d^4K\,\frac{2\,\mathcal{C}(K)}{\{K^2-\mathcal{M}+i0^+\}^3},\end{aligned} \tag{E.15}$$

here $K = k-(x-y)p-yp'$ and $\mathcal{M} = M^2\left[x^2 - 2\frac{\nu}{M}y(1-x)\right]$

$$
\begin{aligned}
F_0(\nu) = {} & \frac{19\nu^2}{48\pi^2 M^2} L + \frac{1}{8} + \frac{576M^6 - 4681M^4\nu^2 + 10388M^2\nu^4 - 3328\nu^6}{288\pi^2 M^2 (M-2\nu)^2 (M+2\nu)^2} \\
& + \frac{-12M^8 + 149M^6\nu^2 - 602M^4\nu^4 + 838M^2\nu^6 - 152\nu^8}{6\pi^2 M^2 \left(M^2 - 4\nu^2\right)^3} \ln\frac{2\nu}{M} \\
& + \frac{4M^2 - 3M\nu + 2\nu^2}{8\pi^2 M\nu} \mathrm{Li}_2\left[1 - \frac{2\nu}{M}\right] - \frac{4M^2 + 3M\nu + 2\nu^2}{8\pi^2 M\nu} \mathrm{Li}_2\left[1 + \frac{2\nu}{M}\right] \\
& + i\, \frac{12M^5 + 81M^4\nu + 193M^3\nu^2 + 185M^2\nu^3 + 44M\nu^4 - 19\nu^5}{12\pi M^2 (M+2\nu)^3} \\
& - \frac{i\left(4M^2 + 3M\nu + 2\nu^2\right)}{4\pi M\nu} \ln\left[1 + \frac{2\nu}{M}\right]
\end{aligned} \tag{E.16a}
$$

$$
\begin{aligned}
F_1(\nu) = {} & -\frac{25}{96\pi^2 M} L + \frac{M}{32\nu^2} + \frac{-11M^4 - 1460M^2\nu^2 + 4288\nu^4}{576\pi^2 M (M-2\nu)^2 (M+2\nu)^2} \\
& + \frac{24M^6 - 235M^4\nu^2 + 434M^2\nu^4 + 200\nu^6}{12\pi^2 M \left(M^2 - 4\nu^2\right)^3} \ln\frac{2\nu}{M} \\
& - \frac{3(M-\nu)}{32\pi^2\nu^2} \mathrm{Li}_2\left[1 + \frac{2\nu}{M}\right] - \frac{3(M+\nu)}{32\pi^2\nu^2} \mathrm{Li}_2\left[1 - \frac{2\nu}{M}\right] \\
& + i\, \frac{9M^4 + 6M^3\nu - 97M^2\nu^2 - 112M\nu^3 + 50\nu^4}{48\pi M\nu (M+2\nu)^3} \\
& - \frac{3i(M-\nu)}{16\pi\nu^2} \ln\left[1 + \frac{2\nu}{M}\right]
\end{aligned} \tag{E.16b}
$$

$$
\begin{aligned}
F_2(\nu) = {} & -\frac{38\nu^2 + 5M^2}{96\pi^2 M^2\nu^2} L - \frac{3}{32\nu^2} \\
& + \frac{-1195M^6 + 9040M^4\nu^2 - 19664M^2\nu^4 + 6656\nu^6}{576\pi^2 M^2 (M-2\nu)^2 \nu^2 (M+2\nu)^2} \\
& + \frac{57M^8 - 621M^6\nu^2 + 1918M^4\nu^4 - 1856M^2\nu^6 + 608\nu^8}{24\pi^2 M^2\nu^2 \left(M^2 - 4\nu^2\right)^3} \ln\frac{2\nu}{M} \\
& - \frac{19M^2 - 9M\nu + 8\nu^2}{32\pi^2 M\nu^3} \mathrm{Li}_2\left[1 - \frac{2\nu}{M}\right] + \frac{19M^2 + 9M\nu + 8\nu^2}{32\pi^2 M\nu^3} \mathrm{Li}_2\left[1 + \frac{2\nu}{M}\right] \\
& - i\, \frac{57M^5 + 330M^4\nu + 675M^3\nu^2 + 628M^2\nu^3 + 226M\nu^4 - 76\nu^5}{48\pi M^2\nu^2 (M+2\nu)^3} \\
& + \frac{i\left(19M^2 + 9M\nu + 8\nu^2\right)}{16\pi M\nu^3} \ln\left[1 + \frac{2\nu}{M}\right]
\end{aligned} \tag{E.16c}
$$

Tadpole-Vertex Correction

$$
\begin{aligned}
\mathcal{A}' &= \chi_\alpha^* \, \Gamma^{\beta\sigma\rho\alpha} \, \Delta_{\rho\eta}(l_2) \, \Gamma^{\tau\eta\mu}(l_2, l_1) \, \Delta_{\sigma\tau}(l_1) \, \chi_\beta \\
&= \chi_\alpha^* \, \Gamma^{\beta\sigma\rho\alpha} \, \Delta_{\rho\eta}(l_1 - q) \, \Gamma^{\tau\eta\mu}(l_1 - q, l_1) \, \Delta_{\sigma\tau}(l_1) \, \chi_\beta
\end{aligned} \tag{E.17}
$$

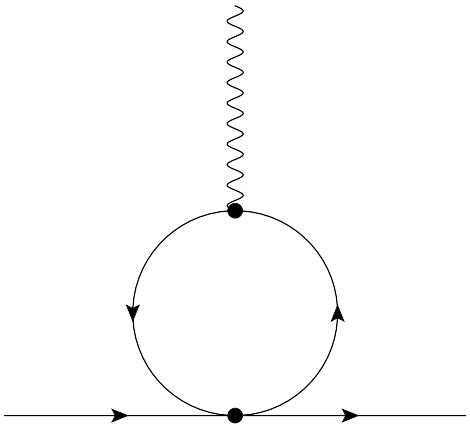

Figure E.7.: Tadpole correction (TC) to the 3-point vertex

$$\begin{aligned}\mathcal{A} &\propto \int d^4 l_1 \, \frac{\mathcal{C}(l_1)}{(l_1^2 - M^2 + i0^+)[(l_1 - q)^2 - M^2 + i0^+]} \\ &\propto \int_0^1 dx \int d^4 l_1 \, \frac{\mathcal{C}(l_1)}{\{(l_1^2 - M^2 + i0^+)(1-x) + [(l_1 - q)^2 - M^2 + i0^+]x\}^2} \\ &\propto \int_0^1 dx \int d^4 L \, \frac{\mathcal{C}(L)}{\{L^2 - M^2 + i0^+\}^2},\end{aligned} \tag{E.18}$$

here $L = l_1 - xq$

The tadpole-vertex correction is the same regardless whether the W-bosons are on- or off-shell.

The tadpole corrected combinations of s- and u-channel diagrams cancel each other, so that these vertex modification gives no contribution to the scattering amplitude.

One-Loop Corrections to the Vertex

The general Lorentz structure for the half-off-shell vertex function (p' off-shell) reads:

$$\begin{aligned}\widetilde{\Gamma}^{\alpha\beta\mu} =& \pi^2 \, e^3 \Big\{ B_1(\nu) \left[g^{\alpha\beta} p^\mu - g^{\alpha\mu} q^\beta + g^{\beta\mu} q^\alpha \right] + B_2(\nu) \left[g^{\alpha\mu} q^\beta - g^{\beta\mu} q^\alpha \right] \\ &+ B_3(\nu) \, \frac{1}{M^2} \, q^\alpha q^\beta p^\mu + B_4(\nu) \, g^{\beta\mu} p^\alpha + B_5(\nu) \, p^\alpha q^\beta p^\mu + B_6(\nu) \, g^{\beta\mu} q^\alpha \Big\},\end{aligned} \tag{E.19}$$

with:

$$\begin{aligned}B_1(\nu) =& \frac{2}{3} L \left(6 - \frac{5\nu}{M} \right) - \frac{2\left(30M^2 + 17M\nu - 56\nu^2\right)}{9M(M+2\nu)} \\ &+ \frac{8\left(3M^3 + 9M^2\nu + M\nu^2 - 5\nu^3\right)}{3M(M+2\nu)^2} \ln \frac{2\nu}{M} \\ &+ \frac{2i}{e^2\pi^2} - \frac{8i\pi\left(3M^3 + 9M^2\nu + M\nu^2 - 5\nu^3\right)}{3M(M+2\nu)^2},\end{aligned} \tag{E.20a}$$

$$
\begin{aligned}
B_2(\nu) =& 9L + \frac{24M^2 + 43M\nu + 8\nu^2}{3M\nu + 6\nu^2} + \frac{\pi^2\left(4M^2 + 3M\nu + 2\nu^2\right)}{6\nu^2} \\
&- \frac{2\left(12M^3 + 45M^2\nu + 49M\nu^2 + 32\nu^3\right)}{3\nu(M+2\nu)^2}\ln\frac{2\nu}{M} \\
&- \frac{4M^2 + 3M\nu + 2\nu^2}{\nu^2}\mathrm{Li}_2\left[1 + \frac{2\nu}{M}\right] \\
&+ \frac{2i\pi\left(12M^3 + 45M^2\nu + 49M\nu^2 + 32\nu^3\right)}{3\nu(M+2\nu)^2} \\
&- \frac{2i\pi\left(4M^2 + 3M\nu + 2\nu^2\right)}{\nu^2}\ln\left[1 + \frac{2\nu}{M}\right],
\end{aligned} \tag{E.20b}
$$

$$
\begin{aligned}
B_3(\nu) =& \frac{-48M^4 - 171M^3\nu - 120M^2\nu^2 + 25M\nu^3 + 2\nu^4}{3\nu^2(M+2\nu)^2} \\
&- \frac{M\pi^2\left(16M^2 + M\nu + \nu^2\right)}{12\nu^3} \\
&+ \frac{M\left(48M^4 + 243M^3\nu + 382M^2\nu^2 + 155M\nu^3 + 30\nu^4\right)}{3\nu^2(M+2\nu)^3}\ln\frac{2\nu}{M} \\
&+ \frac{M\left(16M^2 + M\nu + \nu^2\right)}{2\nu^3}\mathrm{Li}_2\left[1 + \frac{2\nu}{M}\right] \\
&- \frac{i\pi M\left(48M^4 + 243M^3\nu + 382M^2\nu^2 + 155M\nu^3 + 30\nu^4\right)}{3\nu^2(M+2\nu)^3} \\
&+ \frac{i\pi M\left(16M^2 + M\nu + \nu^2\right)}{\nu^3}\ln\left[1 + \frac{2\nu}{M}\right],
\end{aligned} \tag{E.20c}
$$

$$
\begin{aligned}
B_4(\nu) =& \frac{5L(-2M+\nu)}{3M} - \frac{\pi^2(M-\nu)}{4\nu} + \frac{20M^3 + 121M^2\nu + 97M\nu^2 - 106\nu^3}{9M(M+2\nu)^2} \\
&+ \frac{9M^4 + 18M^3\nu - 73M^2\nu^2 - 118M\nu^3 + 40\nu^4}{3M(M+2\nu)^3}\ln\frac{2\nu}{M} \\
&+ \frac{3(M-\nu)}{2\nu}\mathrm{Li}_2\left[1 + \frac{2\nu}{M}\right] \\
&- \frac{i}{e^2\pi^2} - \frac{i\pi\left(9M^4 + 18M^3\nu - 73M^2\nu^2 - 118M\nu^3 + 40\nu^4\right)}{3M(M+2\nu)^3} \\
&+ \frac{3i\pi(M-\nu)}{\nu}\ln\left[1 + \frac{2\nu}{M}\right],
\end{aligned} \tag{E.20d}
$$

$$
\begin{aligned}
B_5(\nu) =& \frac{\pi^2(M-\nu)}{4M\nu^2} + \frac{9M^3 + 32M^2\nu - 9M\nu^2 - 2\nu^3}{3M^2\nu(M+2\nu)^2} \\
&- \frac{9M^3 + 24M^2\nu - M\nu^2 - 98\nu^3}{3M\nu(M+2\nu)^3}\ln\frac{2\nu}{M} - \frac{3(M-\nu)}{2M\nu^2}\mathrm{Li}_2\left[1 + \frac{2\nu}{M}\right] \\
&+ \frac{i\pi\left(9M^3 + 24M^2\nu - M\nu^2 - 98\nu^3\right)}{3M\nu(M+2\nu)^3} - \frac{3i\pi(M-\nu)}{M\nu^2}\ln\left[1 + \frac{2\nu}{M}\right],
\end{aligned} \tag{E.20e}
$$

$$
\begin{aligned}
B_6(\nu) =& \frac{5L(-2M+\nu)}{3M} + \frac{\pi^2\left(16M^2+M\nu+\nu^2\right)}{12\nu^2} \\
&+ \frac{144M^4+560M^3\nu+577M^2\nu^2-5M\nu^3-118\nu^4}{9M\nu(M+2\nu)^2} \\
&- \frac{48M^5+243M^4\nu+388M^3\nu^2+227M^2\nu^3+50M\nu^4-40\nu^5}{3M\nu(M+2\nu)^3}\ln\frac{2\nu}{M} \\
&- \frac{16M^2+M\nu+\nu^2}{2\nu^2}\mathrm{Li}_2\left[1+\frac{2\nu}{M}\right] - \frac{i}{e^2\pi^2} \\
&+ \frac{i\pi\left(48M^5+243M^4\nu+388M^3\nu^2+227M^2\nu^3+50M\nu^4-40\nu^5\right)}{3M\nu(M+2\nu)^3} \\
&- \frac{i\pi\left(16M^2+M\nu+\nu^2\right)}{\nu^2}\ln\left[1+\frac{2\nu}{M}\right].
\end{aligned}
\tag{E.20f}
$$

One-Loop Corrections to the Propagator

The general Lorentz structure of this correction reads:

$$
\widetilde{\Delta}_{\rho\sigma}(l) = \pi^2\, e^2\big[P_1(\nu)\, l_\rho l_\sigma + P_2(\nu)\, g_{\rho\sigma}\big], \tag{E.21}
$$

with:

$$
\begin{aligned}
P_1(\nu) =& \frac{L\left(53M^2-82M\nu+12\nu^2\right)}{24M^4\nu^2} \\
&+ \frac{-503M^4-1246M^3\nu+1124M^2\nu^2+1960M\nu^3-576\nu^4}{144M^4\nu^2(M+2\nu)^2} \\
&+ \frac{2\left(3M^4+9M^3\nu-8M^2\nu^2-5M\nu^3+6\nu^4\right)}{3M^4\nu(M+2\nu)^3}\ln\frac{2\nu}{M}, \\
&- \frac{i}{2e^2\pi^2M^3\nu} - \frac{2i\pi\left(3M^4+9M^3\nu-8M^2\nu^2-5M\nu^3+6\nu^4\right)}{3M^4\nu(M+2\nu)^3}
\end{aligned}
\tag{E.22a}
$$

$$
\begin{aligned}
P_2(\nu) =& -\frac{L\left(53M^2+24M\nu-20\nu^2\right)}{24M^2\nu^2} - \frac{2\left(3M^3+9M^2\nu+M\nu^2-5\nu^3\right)}{3M^2\nu(M+2\nu)^2}\ln\frac{2\nu}{M} \\
&+ \frac{503M^3+1246M^2\nu+136M\nu^2-448\nu^3}{144M^2\nu^2(M+2\nu)} \\
&+ \frac{i}{2e^2\pi^2M\nu} + \frac{2i\pi\left(3M^3+9M^2\nu+M\nu^2-5\nu^3\right)}{3M^2\nu(M+2\nu)^2}.
\end{aligned}
\tag{E.22b}
$$

Irreducible Diagrams

1PI diagram type 1:

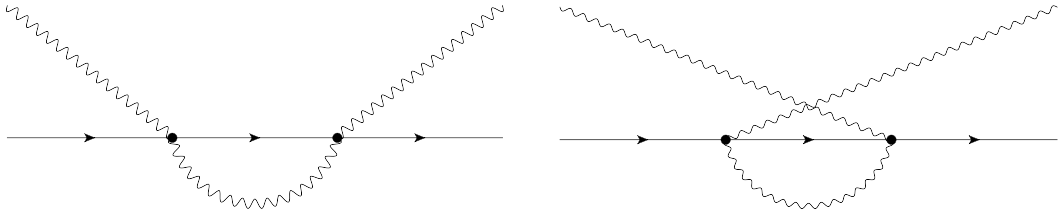

Figure E.8.: s- and u-channel contact corrections (CCL and CCR)

$$\mathcal{A}' = \chi^*_\alpha \, \varepsilon^*_\mu \, \Gamma^{\alpha\rho\mu\zeta} \, \Delta_{\rho\eta}(l_1) D_{\zeta\xi}(k_1) \, \Gamma^{\eta\beta\xi\nu} \, \varepsilon_\nu \, \chi_\beta \tag{E.23}$$

$$\begin{aligned}
\mathcal{A} &\propto \int d^4k_1 \, \frac{\mathcal{C}(k_1)}{[(p+q-k_1)^2 - M^2 + i0^+](k_1^2 + i0^+)} \\
&\propto \int_0^1 dx \int d^4k_1 \, \frac{\mathcal{C}(k_1)}{\{[(p+q-k_1)^2 - M^2 + i0^+]x + (k_1^2 + i0^+)(1-x)\}^2} \\
&\propto \int_0^1 dx \int d^4K_1 \, \frac{\mathcal{C}(K_1)}{\{K_1^2 - x^2M^2 + 2pqx(1-x) + i0^+\}^2} \\
&\propto \int_0^1 dx \int d^4K_1 \, \frac{\mathcal{C}(K_1)}{\{K_1^2 - \mathcal{M} + i0^+\}^2},
\end{aligned} \tag{E.24}$$

here $K_1 = k_1 - x(p+q)$ and $\mathcal{M} = M^2 \left[x^2 - 2\frac{\nu}{M}x(1-x)\right]$

$$\begin{aligned}
F_0(\nu) = &-\frac{L\left(25M^2 + 8\nu^2\right)}{48\pi^2 M^2} + \frac{155M^6 - 1122M^4\nu^2 + 1992M^2\nu^4 + 832\nu^6}{144\pi^2 M^2 (M-2\nu)^2 (M+2\nu)^2} \\
&+ \frac{15M^6\nu^2 - 86M^4\nu^4 + 152M^2\nu^6 + 64\nu^8}{6\pi^2 M^2 \left(M^2 - 4\nu^2\right)^3} \ln\frac{2\nu}{M} \\
&+ i\,\frac{\nu\left(15M^4 + 60M^3\nu + 77M^2\nu^2 + 34M\nu^3 + 16\nu^4\right)}{24\pi M^2 (M+2\nu)^3}
\end{aligned} \tag{E.25a}$$

$$\begin{aligned}
F_1(\nu) = &\frac{L}{48\pi^2 M} + \frac{-5M^2 + 32\nu^2}{144\pi^2\left(M^3 - 4M\nu^2\right)} + \frac{15M^4 - 58M^2\nu^2 + 8\nu^4}{24\pi^2 M (M-2\nu)^2 (M+2\nu)^2} \ln\frac{2\nu}{M} \\
&- i\,\frac{15M^2 + 30M\nu + 2\nu^2}{48\pi M (M+2\nu)^2}
\end{aligned} \tag{E.25b}$$

$$\begin{aligned}
F_2(\nu) = &\frac{L\left(4\nu^2 + 3M^2\right)}{24\pi^2 M^2\nu^2} - \frac{39M^6 - 206M^4\nu^2 + 184M^2\nu^4 + 832\nu^6}{144\pi^2 M^2 (M-2\nu)^2 \nu^2 (M+2\nu)^2} \\
&+ \frac{-9M^6 + 12M^4\nu^2 - 128\nu^6}{12\pi^2 M^2 \left(M^2 - 4\nu^2\right)^3} \ln\frac{2\nu}{M} \\
&- i\,\frac{9M^4 + 36M^3\nu + 66M^2\nu^2 + 60M\nu^3 + 32\nu^4}{48\pi M^2 \nu (M+2\nu)^3}
\end{aligned} \tag{E.25c}$$

1PI diagram type 2:

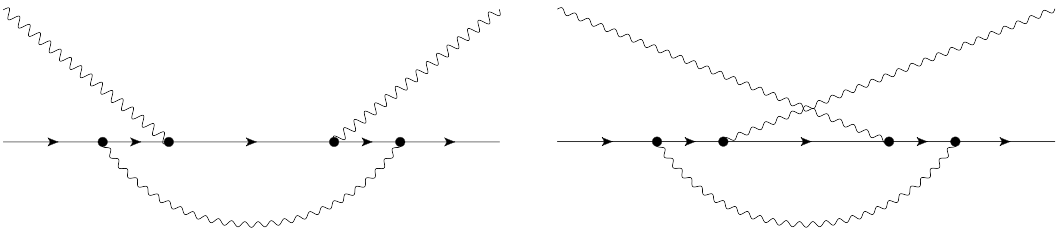

Figure E.9.: s- and u-channel vertex correction (VC)

$$\mathcal{A}' = \chi^*_\alpha\, \varepsilon^*_\mu\, \Gamma^{\alpha\rho\kappa}(l_4, p')\, \Delta_{\rho\eta}(l_4) D_{\kappa\iota}(k_2)\, \Gamma^{\eta\sigma\mu}(l_3, l_4)\, \Delta_{\sigma\tau}(l_3) \times \tag{E.26}$$
$$\Gamma^{\tau\zeta\nu}(l_2, l_3)\, \Delta_{\zeta\xi}(l_2)\, \Gamma^{\xi\beta\iota}(p, l_2)\, \varepsilon_\nu\, \chi_\beta$$

$$\mathcal{A} \propto \int d^4k_2 \times \tag{E.27}$$
$$\frac{\mathcal{C}(k_2)}{[(p-k_2)^2 - M^2 + i0^+][(p+q-k_2)^2 - M^2 + i0^+][(p'-k_2)^2 - M^2 + i0^+](k_2^2 + i0^+)}$$
$$\overset{p=p'}{\propto} \int_0^1 dx \int_0^x dy \int d^4k_2 \times$$
$$\frac{6(x-y)\,\mathcal{C}(k_2)}{\{[(p+q-k_2)^2 - M^2]y + [(p-k_2)^2 - M^2](x-y) + k_2^2(1-x) + i0^+\}^4}$$
$$\propto \int_0^1 dx \int_0^x dy \int d^4k_2\, \frac{6(x-y)\,\mathcal{C}(k_2)}{\{K_2^2 - x^2M^2 + 2y(1-x)pq\}^4}$$
$$\propto \int_0^1 dx \int_0^x dy \int d^4K_2\, \frac{6(x-y)\,\mathcal{C}(K_3)}{\{K_2^2 - \mathcal{M} + i0^+\}^4},$$
here $K_2 = k_2 - xp - yq$ and $\mathcal{M} = M^2\left[x^2 - 2\frac{\nu}{M}y(1-x)\right]$

$$F_0(\nu) = -\frac{1}{24} - \frac{M^2}{4\nu^2} - \frac{L\left(53M^2 + 24\nu^2\right)}{192\pi^2M^2} \tag{E.28a}$$
$$+ \frac{-2395M^6 + 19476M^4\nu^2 - 38112M^2\nu^4 + 1024\nu^6}{1152\pi^2M^2(M-2\nu)^2(M+2\nu)^2}$$
$$+ \frac{3M^8 - 76M^6\nu^2 + 510M^4\nu^4 - 900M^2\nu^6 + 112\nu^8}{12\pi^2M^2\left(M^2 - 4\nu^2\right)^3} \ln\frac{2\nu}{M}$$
$$+ \frac{12M^3 - 13M^2\nu + 2M\nu^2 - 4\nu^3}{16\pi^2M\nu^2} \mathrm{Li}_2\left[1 - \frac{2\nu}{M}\right]$$
$$+ \frac{12M^3 + 13M^2\nu + 2M\nu^2 + 4\nu^3}{16\pi^2M\nu^2} \mathrm{Li}_2\left[1 + \frac{2\nu}{M}\right]$$
$$- i\,\frac{36M^6 + 219M^5\nu + 478M^4\nu^2 + 452M^3\nu^3 + 189M^2\nu^4 + 44M\nu^5 - 14\nu^6}{24\pi M^2\nu(M+2\nu)^3}$$
$$+ \frac{i\left(12M^3 + 13M^2\nu + 2M\nu^2 + 4\nu^3\right)}{8\pi M\nu^2} \ln\left[1 + \frac{2\nu}{M}\right]$$

$$
\begin{aligned}
F_1(\nu) = {} & \frac{3L}{16\pi^2 M} + \frac{-23M^2+80\nu^2}{48\pi^2\left(M^3-4M\nu^2\right)} + \frac{37M}{96\nu^2} \\
& + \frac{M^4-14M^2\nu^2+24\nu^4}{8\pi^2 M(M-2\nu)^2(M+2\nu)^2}\ln\frac{2\nu}{M} \\
& + \frac{-37M+32\nu}{32\pi^2\nu^2}\mathrm{Li}_2\left[1-\frac{2\nu}{M}\right] - \frac{37M+32\nu}{32\pi^2\nu^2}\mathrm{Li}_2\left[1+\frac{2\nu}{M}\right] \\
& + i\,\frac{37M^3+147M^2\nu+142M\nu^2-6\nu^3}{16\pi M\nu(M+2\nu)^2} - \frac{i(37M+32\nu)}{16\pi\nu^2}\ln\left[1+\frac{2\nu}{M}\right]
\end{aligned}
\tag{E.28b}
$$

$$
\begin{aligned}
F_2(\nu) = {} & \frac{L\left(\frac{24}{M^2}-\frac{5}{\nu^2}\right)}{192\pi^2} - \frac{\ln[w]}{4\pi^2\nu^2} + \frac{4M^2+\nu^2}{8\nu^4} \\
& + \frac{3521M^6-28532M^4\nu^2+56320M^2\nu^4-1024\nu^6}{1152\pi^2M^2(M-2\nu)^2\nu^2(M+2\nu)^2} \\
& + \frac{-6M^8+111M^6\nu^2-650M^4\nu^4+1092M^2\nu^6-112\nu^8}{12\pi^2M^2\nu^2\left(M^2-4\nu^2\right)^3}\ln\frac{2\nu}{M} \\
& + \frac{-12M^3+13M^2\nu-3M\nu^2+2\nu^3}{8\pi^2M\nu^4}\mathrm{Li}_2\left[1-\frac{2\nu}{M}\right] \\
& - \frac{12M^3+13M^2\nu+3M\nu^2+2\nu^3}{8\pi^2M\nu^4}\mathrm{Li}_2\left[1+\frac{2\nu}{M}\right] \\
& + i\,\frac{72M^6+438M^5\nu+942M^4\nu^2+861M^3\nu^3+384M^2\nu^4+158M\nu^5-14\nu^6}{24\pi M^2\nu^3(M+2\nu)^3} \\
& - \frac{i\left(12M^3+13M^2\nu+3M\nu^2+2\nu^3\right)}{4\pi M\nu^4}\ln\left[1+\frac{2\nu}{M}\right]
\end{aligned}
\tag{E.28c}
$$

1PI diagram type 3:

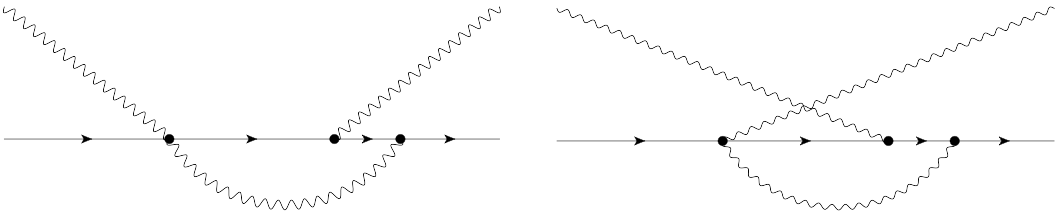

Figure E.10.: s- and u-channel vertex correction (VC) and contact correction (CCL)

$$
\mathcal{A}' = \chi^*_\alpha\,\varepsilon^*_\mu\,\Gamma^{\alpha\rho\kappa}(l_6,p')\,\Delta_{\rho\eta}(l_6)D_{\kappa\iota}(k_3)\,\Gamma^{\eta\sigma\mu}(l_5,l_6)\,\Delta_{\sigma\tau}(l_5)\,\Gamma^{\tau\beta\iota\nu}\,\varepsilon_\nu\,\chi_\beta \tag{E.29}
$$

$$\mathcal{A} \propto \int d^4k_3 \, \frac{\mathcal{C}(k_3)}{[(p+q-k_3)^2 - M^2 + i0^+][(p'-k_3)^2 - M^2 + i0^+](k_3^2 + i0^+)} \tag{E.30}$$
$$\propto \int_0^1 dx \int_0^x dy \int d^4k_3 \times$$
$$\frac{2\,\mathcal{C}(k_3)}{\{[(p+q-k_3)^2 - M^2]y + [(p'-k_3)^2 - M^2](x-y) + k_3^2(1-x) + i0^+\}^3}$$
$$\overset{p=p'}{\propto} \int_0^1 dx \int_0^x dy \int d^4k_3 \, \frac{2\,\mathcal{C}(k_3)}{\{K_3^2 - x^2M^2 + 2y(1-x)pq\}^3}$$
$$\propto \int_0^1 dx \int_0^x dy \int d^4K_3 \, \frac{2\,\mathcal{C}(K_3)}{\{K_3^2 - \mathcal{M} + i0^+\}^3},$$
here $K_3 = k_3 - xp - yq$ and $\mathcal{M} = M^2\left[x^2 - 2\frac{\nu}{M}y(1-x)\right]$

1PI diagram type 4:

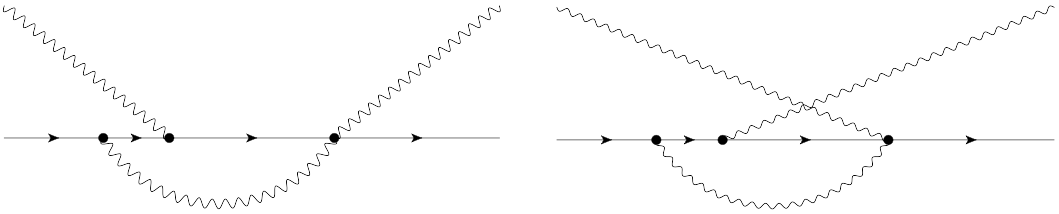

Figure E.11.: s- and u-channel vertex correction (VC) and contact correction (CCR)

$$\mathcal{A}' = \chi_\alpha^* \, \varepsilon_\mu^* \, \Gamma^{\alpha\rho\mu\kappa} \, \Delta_{\rho\eta}(l_8) D_{\kappa\iota}(k_4) \, \Gamma^{\eta\sigma\nu}(l_7, l_8) \, \Delta_{\sigma\tau}(l_7) \, \Gamma^{\tau\beta\iota}(p, l_7) \, \varepsilon_\nu \, \chi_\beta \tag{E.31}$$
$$\mathcal{A} \propto \int d^4k_4 \, \frac{\mathcal{C}(k_4)}{[(p+q-k_4)^2 - M^2 + i0^+][(p-k_4)^2 - M^2 + i0^+](k_4^2 + i0^+)} \tag{E.32}$$
$$\overset{p=p'}{\propto} \int_0^1 dx \int_0^x dy \int d^4K_4 \, \frac{2\,\mathcal{C}(K_4)}{\{K_4^2 - \mathcal{M} + i0^+\}^3},$$
here $K_4 = k_4 - xp - yq$ and $\mathcal{M} = M^2\left[x^2 - 2\frac{\nu}{M}y(1-x)\right]$

1PI diagram type 3+4:

$$F_0(\nu) = \frac{L\left(11M^2 - 10\nu^2\right)}{96\pi^2M^2} - \frac{1}{12} - \frac{11M^6 + 94M^4\nu^2 + 1336M^2\nu^4 - 1024\nu^6}{576\pi^2M^2(M-2\nu)^2(M+2\nu)^2} \tag{E.33a}$$
$$+ \frac{-3M^8 + 20M^6\nu^2 - 86M^4\nu^4 - 76M^2\nu^6 + 80\nu^8}{12\pi^2M^2\left(M^2 - 4\nu^2\right)^3} \ln\frac{2\nu}{M}$$
$$+ \frac{M+4\nu}{16\pi^2\nu}\mathrm{Li}_2\left[1 - \frac{2\nu}{M}\right] - \frac{M-4\nu}{16\pi^2\nu}\mathrm{Li}_2\left[1 + \frac{2\nu}{M}\right]$$
$$- i\,\frac{-3M^5 + 3M^4\nu + 74M^3\nu^2 + 176M^2\nu^3 + 106M\nu^4 - 10\nu^5}{24\pi M^2(M+2\nu)^3}$$
$$- \frac{i(M-4\nu)}{8\pi\nu}\ln\left[1 + \frac{2\nu}{M}\right]$$

$$
\begin{aligned}
F_1(\nu) = &-\frac{5L}{48\pi^2 M} + \frac{55M^2 - 172\nu^2}{144\pi^2\left(M^3 - 4M\nu^2\right)} \\
&+ \frac{21M^4 - 58M^2\nu^2 - 40\nu^4}{24\pi^2 M(M-2\nu)^2(M+2\nu)^2}\ln\frac{2\nu}{M} \\
&- \frac{13}{32\pi^2\nu}\mathrm{Li}_2\left[1-\frac{2\nu}{M}\right] + \frac{13}{32\pi^2\nu}\mathrm{Li}_2\left[1+\frac{2\nu}{M}\right] \\
&+ \frac{13i}{16\pi\nu}\ln\left[1+\frac{2\nu}{M}\right] + i\,\frac{-21M^2 - 33M\nu + 10\nu^2}{48\pi M(M+2\nu)^2}
\end{aligned}
\tag{E.33b}
$$

$$
\begin{aligned}
F_2(\nu) = &\frac{L\left(10\nu^2 + 11M^2\right)}{96\pi^2 M^2\nu^2} + \frac{13}{96\nu^2} \\
&- \frac{539M^6 - 4518M^4\nu^2 + 7560M^2\nu^4 + 1024\nu^6}{576\pi^2 M^2(M-2\nu)^2\nu^2(M+2\nu)^2} \\
&+ \frac{27M^8 - 225M^6\nu^2 + 652M^4\nu^4 - 152M^2\nu^6 - 160\nu^8}{24\pi^2 M^2\nu^2\left(M^2-4\nu^2\right)^3}\ln\frac{2\nu}{M} \\
&+ \frac{9M - 13\nu}{32\pi^2\nu^3}\mathrm{Li}_2\left[1+\frac{2\nu}{M}\right] - \frac{9M+13\nu}{32\pi^2\nu^3}\mathrm{Li}_2\left[1-\frac{2\nu}{M}\right] \\
&+ i\,\frac{-27M^5 - 90M^4\nu + 9M^3\nu^2 + 278M^2\nu^3 + 188M\nu^4 - 20\nu^5}{48\pi M^2\nu^2(M+2\nu)^3} \\
&+ \frac{i(9M-13\nu)}{16\pi\nu^3}\ln\left[1+\frac{2\nu}{M}\right]
\end{aligned}
\tag{E.33c}
$$

1PI diagram type 5:

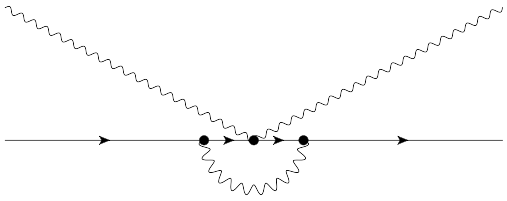

Figure E.12.: Seagull-vertex vertex correction (VC)

$$
\mathcal{A}' = \chi^*_\alpha\,\varepsilon^*_\mu\,\Gamma^{\alpha\rho\kappa}(l_{10},p')\,\Delta_{\rho\eta}(l_{10})D_{\kappa\iota}(k_5)\,\Gamma^{\eta\sigma\mu\nu}\,\Delta_{\sigma\tau}(l_9)\,\Gamma^{\tau\beta\iota}(p,l_9)\,\varepsilon_\nu\,\chi_\beta \tag{E.34}
$$

$$
\begin{aligned}
\mathcal{A} &\propto \int d^4k_5\,\frac{\mathcal{C}(k_5)}{[(p'-k_5)^2 - M^2 + i0^+][(p-k_5)^2 - M^2 + i0^+](k_5^2 + i0^+)} \\
&\propto \int_0^1 dx \int_0^x dy \int d^4k_5 \times \\
&\qquad \frac{2\,\mathcal{C}(k_5)}{\{[(p'-k_5)^2 - M^2]y + [(p-k_5)^2 - M^2](x-y) + k_5^2(1-x) + i0^+\}^3} \\
&\overset{p=p'}{\propto} \int_0^1 dx \int_0^x dy \int d^4K_5\,\frac{2\,\mathcal{C}(K_5)}{\{K_5^2 - x^2M^2 + i0^+\}^3} \\
&\propto \int_0^1 dx \int_0^x dy \int d^4K_5\,\frac{2\,\mathcal{C}(K_5)}{\{K_5^2 - \mathcal{M} + i0^+\}^3},
\end{aligned}
\tag{E.35}
$$

here $K_5 = k_5 - xp$ and $\mathcal{M} = x^2M^2$

$$F_0(\nu) = -\frac{647 - 498L + 576\ln w}{1152\pi^2} \tag{E.36a}$$

$$F_1(\nu) = 0 \tag{E.36b}$$

$$F_2(\nu) = \frac{229 - 6L + 288\ln w}{1152\pi^2}\frac{1}{\nu^2} \tag{E.36c}$$

Tadpole Diagrams

tadpole s-channel:

$$\mathcal{A}' = \chi^*_\alpha\,\varepsilon^*_\mu\,\Gamma^{\beta\sigma\rho\alpha}\,\Delta_{\rho\eta}(l_3)\,\Gamma^{\zeta\eta\mu}(l_3,l_2)\,\Delta_{\zeta\xi}(l_2)\,\Gamma^{\tau\xi\nu}(l_2,l_1)\,\Delta_{\sigma\tau}(l_1)\,\varepsilon_\nu\,\chi_\beta \tag{E.37}$$

$$\begin{aligned}\mathcal{A} &\propto \int d^4l_2\,\frac{\mathcal{C}(l_2)}{[(l_2+q)^2-M^2+i0^+](l_2^2-M^2+i0^+)[(l_2+q')^2-M^2+i0^+]} \\ &\overset{q=q'}{\propto} \int_0^1 dx\int_0^{1-x} dy\int d^4l_2 \\ &\qquad \frac{2\,\mathcal{C}(l_2)}{\{[(l_2+q)^2-M^2+i0^+](x+y)+(l_2^2-M^2+i0^+)(1-x-y)\}^3} \\ &\propto \int_0^1 dx\int_0^{1-x} dy\int d^4L_2\,\frac{2\,\mathcal{C}(L_2)}{\{L_2^2-M^2+i0^+\}^3},\end{aligned} \tag{E.38}$$

here $L_2 = l_2 + (x+y)q$

tadpole u-channel:

$$\mathcal{A}' = \chi^*_\alpha\,\varepsilon^*_\mu\,\Gamma^{\beta\sigma\rho\alpha}\,\Delta_{\rho\eta}(l_6)\,\Gamma^{\zeta\eta\nu}(l_6,l_5)\,\Delta_{\zeta\xi}(l_5)\,\Gamma^{\tau\xi\mu}(l_5,l_4)\,\Delta_{\sigma\tau}(l_4)\,\varepsilon_\nu\,\chi_\beta \tag{E.39}$$

$$\begin{aligned}\mathcal{A} &\propto \int d^4l_5\,\frac{\mathcal{C}(l_5)}{[(l_5-q')^2-M^2+i0^+](l_5^2-M^2+i0^+)[(l_5-q)^2-M^2+i0^+]} \\ &\overset{q=q'}{\propto} \int_0^1 dx\int_0^{1-x} dy\int d^4l_5 \\ &\qquad \frac{2\,\mathcal{C}(l_5)}{\{[(l_5-q)^2-M^2+i0^+](x+y)+(l_5^2-M^2+i0^+)(1-x-y)\}^3} \\ &\propto \int_0^1 dx\int_0^{1-x} dy\int d^4L_5\,\frac{2\,\mathcal{C}(L_5)}{\{L_5^2-M^2+i0^+\}^3},\end{aligned} \tag{E.40}$$

here $L_5 = l_5 - (x+y)q$

tadpole seagull-channel:

$$\mathcal{A}' = \chi^*_\alpha\,\varepsilon^*_\mu\,\Gamma^{\beta\sigma\rho\alpha}\,\Delta_{\rho\eta}(l_8)\,\Delta_{\sigma\tau}(l_7)\,\Gamma^{\tau\eta\mu\nu}\,\varepsilon_\nu\,\chi_\beta \tag{E.41}$$

$$\begin{aligned}\mathcal{A} &\propto \int d^4l_8\,\frac{\mathcal{C}(l_8)}{[(l_8+p'-p)^2-M^2+i0^+](l_8^2-M^2+i0^+)} \\ &\overset{p=p'}{\propto} \int d^4l_8\,\frac{\mathcal{C}(l_8)}{\{l_8^2-M^2+i0^+\}^2}\end{aligned} \tag{E.42}$$

$$F_0(\nu) = -\frac{-12+L}{48M^2\pi^2}\,\nu^2, \qquad F_1(\nu) = 0, \qquad F_2(\nu) = \frac{-12+L}{48M^2\pi^2}. \tag{E.43}$$

BIBLIOGRAPHY

[1] V.A. Novikov, L.B. Okun, Mikhail A. Shifman, A.I. Vainshtein, M.B. Voloshin, et al. Charmonium and Gluons: Basic Experimental Facts and Theoretical Introduction. *Phys. Rept.*, 41:1–133, 1978.

[2] S. B. Gerasimov. A Sum Rule for Magnetic Moments and the Damping of the Nucleon Magnetic Moment in Nuclei. *Sov. J. Nucl. Phys.*, 2:430, 1966.

[3] S.D. Drell and Anthony C. Hearn. Exact Sum Rule for Nucleon Magnetic Moments. *Phys. Rev. Lett.*, 16:908–911, 1966.

[4] A.M. Baldin. Polarizability of Nucleons. *Nuclear Physics*, 18:310–317, 1960.

[5] D. Drechsel, B. Pasquini, and M. Vanderhaeghen. Dispersion Relations in Real and Virtual Compton Scattering. *Phys. Rept.*, 378:99–205, 2003.

[6] Klaus Helbing. The Gerasimov-Drell-Hearn Sum Rule. *Prog. Part. Nucl. Phys.*, 57:405–469, 2006.

[7] V. Olmos de Leon, F. Wissmann, P. Achenbach, J. Ahrens, H.J. Arends, et al. Low-energy Compton Scattering and the Polarizabilities of the Proton. *Eur. Phys. J.*, A10:207–215, 2001.

[8] M.I. Levchuk and A.I. L'vov. Deuteron Compton Scattering below Pion Photoproduction Threshold. *Nucl. Phys.*, A674:449–492, 2000.

[9] B. Pasquini, P. Pedroni, and D. Drechsel. Higher Order Forward Spin Polarizability. *Phys. Lett. B*, 687:160-166,2010, January 2010.

[10] M.W. Ahmed, M.A. Blackston, B.A. Perdue, W. Tornow, H.R. Weller, et al. Near-threshold Deuteron Photodisintegration: An Indirect Determination of the Gerasimov-Drell-Hearn Sum Rule and Forward Spin Polarizability for the Deuteron at Low Energies. *Phys. Rev.*, C77:044005, 2008.

[11] Xiang-dong Ji and Ying-chuan Li. Sum Rules and Spin Dependent Polarizabilities of the Deuteron in Effective Field Theory. *Phys. Lett.*, B591:76–82, 2004.

[12] Ansgar Denner and T. Hahn. Radiative Corrections to $W^+ W^- \to W^+ W^-$ in the Electroweak Standard Model. *Nucl. Phys.*, B525:27–50, 1998.

[13] J.A.M. Vermaseren. New Features of FORM. *e-Print: math-ph/0010025*, 2000.

[14] T. Hahn and M. Perez-Victoria. Automatized One Loop Calculations in Four-Dimensions and D-Dimensions. *Comput. Phys. Commun.*, 118:153–165, 1999.

[15] D. Binosi, J. Collins, C. Kaufhold, and L. Theussl. JaxoDraw: A Graphical User Interface for Drawing Feynman Diagrams. Version 2.0 Release Notes. *Comput. Phys. Commun.*, 180:1709–1715, 2009.

[16] Micheal E. Peskin and Daniel V. Schroeder. *An Introduction to Quantum Field Theory*. Sarat Book House, 2005.

[17] John A. Wheeler. On the Mathematical Description of Light Nuclei by the Method of Resonating Group Structure. *Phys. Rev.*, 52:1107–1122, 1937.

[18] W. Heisenberg. The 'Observable Quantities' in the Theory of Elementary Particles. 1943.

[19] Mark Srednicki. *Quantum Field Theory*. Cambridge University Press, 2007.

[20] David Griffiths. *Introduction to Elementary Particles*. Wiley-VCH, 2008.

[21] L. H. Ryder. *Quantum Field Theory*. Cambridge University Press, 1986.

[22] Hans J. Weber, Frank E. Harris, and George B. Arfken. *Essential Mathematical Methods for Physicists: and Engineers*. Academic Press, 2003.

[23] Walter E. Thirring. Radiative Corrections in the Nonrelativistic Limit. *Phil. Mag.*, 41:1193–1194, 1950.

[24] F.E. Low. Scattering of Light of Very Low Frequency by Systems of Spin 1/2. *Phys. Rev.*, 96:1428–1432, 1954.

[25] Murray Gell-Mann and M.L. Goldberger. Scattering of Low-energy Photons by Particles of Spin 1/2. *Phys. Rev.*, 96:1433–1438, 1954.

[26] V. Bernard, Norbert Kaiser, and Ulf-G. Meissner. Chiral Dynamics in Nucleons and Nuclei. *Int. J. Mod. Phys.*, E4:193–346, 1995.

[27] Stefan Dittmaier. Thirring's Low-energy Theorem and its Generalizations in the Electroweak Standard Model. *Phys. Lett. B*, 409:509–516, 1997.

[28] Armin Wachter and Henning Hoeber. *Repetitorium Theoretische Physik (Springer-Lehrbuch) (German Edition)*. Springer, 2004.

[29] Bogdan Povh, Klaus Rith, Christoph Scholz, and Frank Zetsche. *Teilchen und Kerne: Eine Einführung in die physikalischen Konzepte (Springer-Lehrbuch) (German Edition)*. Springer, 2009.

[30] Jan Pieczkowski. Compton Scattering Sum Rules for Massive Vector Bosons. Master's thesis, Johannes Gutenberg-Universität Mainz, 2009.

[31] Cedric Lorce. Electromagnetic Properties for Arbitrary Spin Particles: Natural Electromagnetic Moments from Light-cone Arguments. *Phys. Rev.*, D79:113011, 2009.

[32] H.W. Griesshammer, J.A. McGovern, D.R. Phillips, and G. Feldman. Using Effective Field Theory to Analyse Low-energy Compton Scattering Data from Protons and Light Nuclei. *Prog. Part. Nucl. Phys.*, 67:841–897, 2012.

[33] Vladimir Pascalutsa, Barry R. Holstein, and Marc Vanderhaeghen. A Derivative of the Gerasimov-Drell-Hearn Sum Rule. *Phys. Lett.*, B600:239–247, 2004.

[34] H. Aronson. Spin-1 Electrodynamics with an Electric Quadrupole Moment. *Phys. Rev.*, 186:1434–1441, 1969.

[35] H. Corben and Julian Schwinger. The Electromagnetic Properties of Mesotrons. *Phys. Rev.*, 58(11):953–968, 1940.

[36] William A. Bardeen, R. Gastmans, and B.E. Lautrup. Static Quantities in Weinberg's Model of Weak and Electromagnetic Interactions. *Nucl. Phys.*, B46:319–331, 1972.

[37] Joannis Papavassiliou. Standard Model Higher Order Corrections to the WWγ / WWZ vertex. 1995. Presented at Conference: C95-02-01 (Vector Boson Symp. 1995:98-109).

[38] Julian S. Schwinger. On Quantum electrodynamics and the Magnetic Moment of the Electron. *Phys. Rev.*, 73:416–417, 1948.

[39] Peter J. Mohr, Barry N. Taylor, and David B. Newell. CODATA Recommended Values of the Fundamental Physical Constants: 2010. *Rev. Mod. Phys.*, 84,:1527–1605, March 2012.

[40] H. M. Nussenzveig. *Causality and Dispersion Relations, Volume 95 (Mathematics in Science and Engineering)*. Academic Press, 1972.

[41] Hartmuth Arenhövel, Alexander Fix, and Michael Schwamb. Spin Asymmetry and Gerasimov-Drell-Hearn Sum Rule for the Deuteron. *Phys. Rev. Lett.*, 93:202301, 2004.

[42] J.M.B. Kellogg, I.I. Rabi, N.F. Ramsey, and J.R. Zacharias. An Electrical Quadrupole Moment of the Deuteron. *Phys. Rev.*, 55:318–319, 1939.

[43] R.V. Reid and M.L. Vaida. Quadrupole Moment of the Deuteron. *Phys. Rev. Lett.*, 29:494–496, 1972.

[44] M.J.G. Veltman. Diagrammatica: The Path to Feynman Rules. *Cambridge Lect. Notes Phys.*, 4:1–284, 1994.